

LA-UR-09-1338  
March 2009  
EP2009-0140

# Completion Report for Regional Aquifer Well R-46

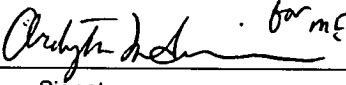
Prepared by the Environmental Programs Directorate

Los Alamos National Laboratory, operated by Los Alamos National Security, LLC, for the U.S. Department of Energy under Contract No. DE-AC52-06NA25396, has prepared this document pursuant to the Compliance Order on Consent, signed March 1, 2005. The Compliance Order on Consent contains requirements for the investigation and cleanup, including corrective action, of contamination at Los Alamos National Laboratory. The U.S. government has rights to use, reproduce, and distribute this document. The public may copy and use this document without charge, provided that this notice and any statement of authorship are reproduced on all copies.


# Completion Report for Regional Aquifer Well R-46

March 2009

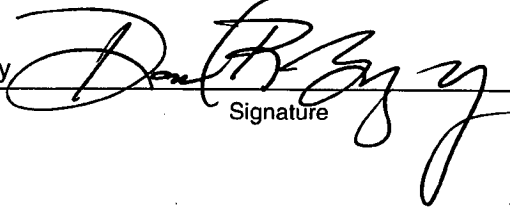
Responsible project leader:

Mark Everett		Project Leader	Environmental Programs	3-26-09
Printed Name	Signature	Title	Organization	Date

Responsible LANS representative:

Michael J. Graham		Associate Director	Environmental Programs	3/26/09
Printed Name	Signature	Title	Organization	Date

Responsible DOE representative:

David R. Gregory		Project Director	DOE-LASO	3/29/09
Printed Name	Signature	Title	Organization	Date

## EXECUTIVE SUMMARY

This well completion report describes the drilling, installation, development, and aquifer testing of Los Alamos National Laboratory's regional aquifer well R-46, which is located on Puye Road within Technical Area 63 (TA-63) in Los Alamos County, New Mexico. The well was installed at the direction of the New Mexico Environment Department (NMED), and this report was written in accordance with requirements in Section IV.A.3.e.iv of the March 1, 2005, Compliance Order on Consent. Well R-46 was drilled as a single-screen well in the regional aquifer to monitor groundwater quality in support of remedy selection for Material Disposal Area (MDA) C. Well R-46 is also used to assess the conceptual model for contaminant fate and transport from TA-50 and serves as a downgradient monitoring well for MDA C to safeguard the water supply well PM-5.

The R-46 borehole was drilled using dual-rotary and open-hole drilling. Fluid additives used during the drilling included potable water and foam. Foam-assisted drilling was used only in the vadose zone; no drilling-fluid additives, other than small amounts of potable water added to the air, were used within the regional aquifer. Additive-free drilling provides minimal impacts to the groundwater and aquifer materials. The R-46 borehole was successfully completed to total depth using casing-advance and open-hole drilling methods.

A retractable 18-in. casing was advanced through the Tshirege Member of the Bandelier Tuff using dual-rotary method and open-hole drilling to 291.4 ft below ground surface (bgs). A 16-in. retractable casing was advanced using dual-rotary methods through the Cerro Toledo interval, Otowi Member of the Bandelier Tuff, and Guaje Pumice Bed to 692.2 ft bgs. Open-hole drilling commenced with a 15-in. hammer bit through the unassigned dacitic lavas and top of the Puye Formation to 1070 ft bgs. A 12-in. casing was then advanced using dual-rotary methods through the Puye Formation and Miocene pumiceous sediments to a total depth of 1415 ft bgs. Well R-46 was completed with a screen near the top of the regional aquifer in the Puye Formation.

The well was completed in accordance with an NMED-approved well design. The well was thoroughly developed and all target water-quality parameters were achieved. A dedicated submersible pump sampling system will be installed in the R-46 well, and groundwater sampling will be performed as part of the facility-wide groundwater-monitoring program.

## CONTENTS

<b>1.0</b>	<b>INTRODUCTION</b> .....	<b>1</b>
<b>2.0</b>	<b>PRELIMINARY ACTIVITIES</b> .....	<b>1</b>
2.1	Administrative Preparation .....	1
2.2	Site Preparation .....	2
<b>3.0</b>	<b>DRILLING ACTIVITIES</b> .....	<b>2</b>
3.1	Drilling Approach .....	2
3.2	Chronological Drilling Activities .....	2
<b>4.0</b>	<b>SAMPLING ACTIVITIES</b> .....	<b>4</b>
4.1	Cuttings Sampling .....	5
4.2	Water and Sediment Sampling .....	5
<b>5.0</b>	<b>GEOLOGY AND HYDROGEOLOGY</b> .....	<b>6</b>
5.1	Stratigraphy .....	6
5.2	Groundwater .....	8
<b>6.0</b>	<b>BOREHOLE LOGGING</b> .....	<b>8</b>
6.1	Video Logging .....	8
6.2	Geophysical Logging .....	9
<b>7.0</b>	<b>WELL INSTALLATION</b> .....	<b>9</b>
7.1	Well Design .....	9
7.2	Well Construction R-46 .....	9
<b>8.0</b>	<b>POSTINSTALLATION ACTIVITIES</b> .....	<b>10</b>
8.1	Well Development .....	10
8.1.1	Field Parameters .....	10
8.2	Aquifer Testing .....	11
8.3	Dedicated Sampling System Installation .....	11
8.4	Wellhead Completion .....	11
8.5	Geodetic Survey .....	12
8.6	Waste Management and Site Restoration .....	12
<b>9.0</b>	<b>DEVIATIONS FROM PLANNED ACTIVITIES</b> .....	<b>13</b>
9.1	NMED-Approved Modifications to the Work Plan .....	13
<b>10.0</b>	<b>ACKNOWLEDGMENTS</b> .....	<b>13</b>
<b>11.0</b>	<b>REFERENCES</b> .....	<b>13</b>

### Figures

Figure 1.0-1	Regional aquifer well R-46 .....	15
Figure 5.1-1	R-46 borehole stratigraphy .....	16
Figure 7.2-1	R-46 as-built well construction diagram .....	17
Figure 8.3-1a	As-built schematic for regional well R-46 .....	19
Figure 8.3-1b	As-built technical notes for R-46 .....	20

## Tables

Table 3.1-1	Fluid Quantities Used during Drilling and Well Construction .....	21
Table 4.2-1	Summary of Groundwater and Sediment Screening Samples Collected during Drilling, Well Development, and Aquifer Testing of Well R-46.....	22
Table 6.0-1	R-46 Video and Geophysical Logging Runs.....	24
Table 7.2-1	R-46 Annular Fill Materials.....	24
Table 8.5-1	R-46 Survey Coordinates.....	25
Table 8.6-1	Summary of Waste Samples Collected during Drilling and Development of R-46.....	25

## Appendixes

Appendix A	Borehole R-46 Lithologic Log
Appendix B	Groundwater and Sediment Analytical Results
Appendix C	Aquifer Testing Report
Appendix D	Borehole Video Logging (on DVDs included with this document)
Appendix E	Jet West Geophysical Logs and Schlumberger Geophysical Logging Report (on CD included with this document)
Appendix F	Screen-Interval Selection

## Acronyms and Abbreviations

µS/cm	microsiemens per centimeter
amsl	above mean sea level
API	American Petroleum Institute
APS	Accelerator Porosity Sonde
bgs	below ground surface
CN	Compensated Neutron Log
Consent Order	Compliance Order on Consent
cu	capture unit
DO	dissolved oxygen
ECS	Elemental Capture Sonde
EES-14	Earth and Environmental Sciences Group
ENV-MAQ	Environmental Division–Meteorology and Air Quality Group
EP	Environmental Programs
gAPI	American Petroleum Institute gamma ray
GR	gamma ray
HNGS	Hostile Natural Gamma Spectroscopy
ID	identification

I.D.	inside diameter
ICPMS	inductively coupled (argon) plasma mass spectrometry
ICPOES	inductively coupled (argon) plasma optical emission spectroscopy
LANL	Los Alamos National Laboratory
MDA	material disposal area
mV	millivolt
NMED	New Mexico Environment Department
NTU	nephelometric turbidity unit
O.D.	outside diameter
ORP	oxidation-reduction potential
PVC	polyvinyl chloride
RPF	Records Processing Facility
SOP	standard operating procedure
SVOC	semivolatile organic compound
TA	technical area
TD	total depth
TLD	Triple Detector Litho-Density
TOC	total organic carbon
VOC	volatile organic compound
WCSF	waste characterization strategy form

## 1.0 INTRODUCTION

This completion report summarizes the site preparation, drilling, well construction, well development, and aquifer testing for regional aquifer well R-46. The report is written in accordance with the requirements in Section IV.A.3.e.iv of the March 1, 2005, Compliance Order on Consent (the Consent Order). Well R-46 was drilled from December 17, 2008, to February 5, 2009, and the well was completed from February 8, 2008, to February 26, 2009, at Los Alamos National Laboratory (LANL or the Laboratory) for the Environmental Programs (EP) Directorate Water Stewardship Project.

The R-46 project site is located on Puye Road within Technical Area 63 (TA-63) in Los Alamos County, New Mexico (Figure 1.0-1). The purposes of the R-46 monitoring well are to monitor potential releases of contaminants from Material Disposal Area (MDA) C to groundwater as part of the corrective measures evaluation for MDA C, assess the conceptual model for contaminant fate and transport from TA-50, monitor water levels within the regional aquifer, and measure pumping effects from wells in the vicinity.

The primary objective of the drilling activities was to drill and install a single-screened regional aquifer monitoring well in the upper portion of the regional aquifer. Secondary objectives were to collect drill-cutting samples, conduct borehole geophysical logging, and investigate potential perched groundwater zones.

The R-46 borehole was successfully drilled to a total depth (TD) of 1415 ft below ground surface (bgs). A monitoring well was installed with a screened interval between 1340.0 and 1360.7 ft bgs. Depth to water in the well following well development was 1327.9 ft bgs on March 7, 2009. Cuttings samples were collected at 5-ft intervals in the borehole from ground surface to TD. Postinstallation activities included well development, aquifer testing, and geodetic surveying. A dedicated sampling system comprising a 4-in. Grundfos submersible pump and 1-in. stainless-steel drop pipe will be installed in the well. Ongoing activities include waste management and site restoration.

The information presented in this report was compiled from field reports and daily activity summaries. Records, including field reports, field logs, and survey information, will be on file at the Records Processing Facility (RPF). This report contains brief descriptions of activities and supporting figures, tables, and appendixes completed to date associated with the R-46 project.

## 2.0 PRELIMINARY ACTIVITIES

Preliminary activities included preparing administrative planning documents and preparing the drill site and drill pad. All preparatory activities were completed in accordance with Laboratory policies and procedures.

### 2.1 Administrative Preparation

The following documents helped guide the implementation of the scope of work for well R-46: "Final Drilling Plan for Regional Aquifer Well R-46" (TerranearPMC 2008, 103941); "Integrated Work Document for Regional and Intermediate Aquifer Well Drilling" (LANL 2007, 100972); "Storm Water Pollution Prevention Plan" (LANL 2006, 092600); and "Waste Characterization Strategy Form for the R-38, R-41, R-44, R-45, and R-46 Regional Groundwater Well Installation and Corehole Drilling" (LANL 2008, 103916).



## 2.2 Site Preparation

Site preparation was performed between December 12 and December 17, 2008, and included mobilizing the drill rig, drilling pipe, air compressors, trailers, and support vehicles to the drill site and staging alternative drilling tools and construction materials at the Pajarito Road lay down yard.

Office supply trailers, generators, and general field equipment were moved on-site after mobilization of drilling equipment. Potable water was obtained from the Puye Road fire hydrant. Safety barriers and signs were installed around the borehole-cuttings containment pit and along the perimeter of the work area.

## 3.0 DRILLING ACTIVITIES

This section describes the drilling approach and provides a chronological summary of field activities conducted at monitoring well R-46.

### 3.1 Drilling Approach

The drilling methodology and selection of equipment and drill-casing sizes for R-46 were designed to retain the ability to case off perched groundwater and reach TD with sufficiently sized casing to meet the required 2-in. minimum annular thickness of the filter pack around a 5.50-in. outside-diameter (O.D.) well. Further, it was anticipated that if perched groundwater was encountered at R-46, the perched zone would be isolated and sealed off either with casing or by cementing to avoid commingling perched groundwater with the regional aquifer.

Dual-rotary air-drilling techniques and a Foremost DR-24HD drill rig were employed to drill the R-46 borehole. Dual-rotary drilling has the advantage of simultaneously advancing and casing the borehole. The Foremost DR-24HD drill rig was equipped with conventional direct circulation drilling rods, tricone bits, hammer bits, underreaming hammer bits, one deck-mounted 900 ft<sup>3</sup>/min air compressor, and general drilling equipment. Auxiliary equipment on-site included two Wagner/Sullair 1150 ft<sup>3</sup>/min trailer-mounted air compressors, water/pipe trucks, and welder/generators. Three sizes of A53 grade B flush-welded mild carbon-steel casing (18-in., 16-in., and 12-in.) were used for the R-46 project. The 18-in. casing was placed from ground surface to the top of the Cerros Toledo interval. The 16-in. casing was utilized in softer stable conditions to approximately the top of the dacite lavas at 692 ft bgs. Open-hole drilling commenced with a 15-in. hammer bit and progressed to a depth of 1070 ft bgs. The 12-in. casing was utilized to reach a TD of 1415 ft bgs in the Miocene pumiceous sediments in the Puye Formation.

Drilling fluids, other than air, used in the vadose zone included municipal water and a mixture of municipal water with Baroid AQF-2 foaming agent. The fluids were used to cool the bit and help lift cuttings from the borehole. Use of foaming agents was terminated at 1070 ft bgs, approximately 100 ft above the predicted regional aquifer water table. No additives other than municipal water were used for drilling within the regional aquifer. A cumulative total of drilling fluids introduced into the borehole and those recovered are recorded and presented in Table 3.1-1.

### 3.2 Chronological Drilling Activities

Mobilization of drilling equipment and supplies to the R-46 site began on December 12, 2008, and continued through December 17, 2008. All Laboratory operations were shut down during the afternoon of December 15, 2008, and remained closed the next day due to inclement weather (snow).

The borehole was initiated on December 17, 2008, using dual-rotary methods with 18-in. drill casing and a 16-in. tricone long-tooth bit. Initial drilling was slower than expected in the upper densely welded tuff units. This required switching to open-hole drilling at 125 ft bgs, still using a 16-in. tricone bit, the morning of December 19, 2008. Drilling progressed more quickly below 177 ft bgs. Because of problems with hole-stability at 221 ft bgs, dual-rotary drilling was resumed; a 19-in. reaming bit was placed immediately above the 16-in. tricone bit. The 18-in. drill casing was advanced in this fashion to a depth of 142 ft bgs. On December 21, 2008, the reaming bit was removed from the drill string after the existing open-hole section was reamed to 202 ft bgs where the formation tuff was less welded. By shift end on December 22, 2008, drilling then progressed smoothly to a depth of 291.2 ft, at which time activity was suspended in accordance with the Laboratory holiday shutdown.

Drilling activities resumed on January 5, 2009. The 18-in. casing was very tight in the hole after sitting over the break so it was landed at 291.4 ft bgs. Dual-rotary drilling methods then switched to 16-in. drill casing and a 15-in. tricone bit on January 7, 2009. Drilling abruptly slowed, and resistance to rotation increased on the 16-in. casing at 683.5 ft bgs on January 9, 2009. As a result, only about 10 ft more were advanced, and the 16-in. casing was landed at 692.2 ft bgs, just above the dacitic lavas, on January 11, 2009.

On January 13, 2009, open-hole drilling commenced using a 15-in. hammer bit. Drilling progressed smoothly to a depth of 1070 ft bgs, at which time the decision was made to stop open-hole drilling. The decision was made because of the requirement not to use drill fluid additives (foaming agents) within 100 ft of the top of the regional aquifer. At this time, the top of the aquifer was predicted to be encountered at or near 1150 ft bgs. The driller could not reliably lift cuttings from this depth in an open hole without foam. The drill string was tripped out in preparation for open-hole video/geophysical logging. An increased rate of penetration and the presence of sandy clasts of material had been noted at 949 ft bgs, both indicating likely entry into the semiconsolidated Puye Formation. Jet West Geophysical ran a video and a combined natural gamma ray/induction log in the borehole on January 14, 2009. The video log showed no water entering the open hole. The log also revealed several short brecciated sections within the dacitic interval that were likely the reasons for short losses of circulation. After logging concluded, the 16-in. drive shoe was cut off at 682.0 ft bgs on the morning of January 15, 2009. Installing the welded 12-in. drill casing string in the borehole was also started that day.

Dual-rotary drilling resumed on January 19, 2009, using 12-in. casing and a 12-in. tricone bit. The next day the tricone bit was exchanged for a 12-in. underreaming hammer bit due to cobbles and boulders in the formation. After changing to the underreaming hammer bit, there were problems maintaining circulation inside the 12-in. casing. Typically, when advancing casing with the dual-rotary method, there is a natural seal between the outside diameter of the casing and inside surface of the borehole. However, the underreaming hammer bit created a larger diameter than the outside diameter of the casing, thus resulting in a loss of the natural seal. A total of 9.5 ft<sup>3</sup> of ¼-in. hydrated coated bentonite pellets was added to the 12- × 16-in. annulus from ground surface, producing a calculated 21-ft long seal on January 22, 2009. Drilling resumed that day and groundwater was observed and sampled at a depth of 1115 ft bgs. Unfortunately, the annular seal started leaking 8 ft later at 1123 ft bgs. The next day, more bentonite (9.3 ft<sup>3</sup> of ¼-in. pellets plus 6.7 ft<sup>3</sup> of granular bentonite casing seal) was added from ground surface to reseal the 12- × 16-in. annulus. The calculated volume of bentonite was added to seal the annulus from 1036 to 1123 ft bgs. Drilling recommenced on January 23, 2009, with somewhat spotty circulation and with indications of variable rates of water production. That evening, 24-h operations also began at R-46. After a brief drilling shutdown for groundwater observation, water was recorded at a depth of 1108.5–1109 ft bgs on January 24, 2009.

By the morning of January 25, 2009, drilling progressed to a TD of 1230 ft bgs when the drill string was tripped out of the hole in preparation for multi-tool geophysical logging by Schlumberger, which was completed later the same day. A slight organic odor had been noticed in the drill cuttings. To investigate further, several bailed water samples were collected. A sand bailer was employed to collect bottom-hole formation samples. Attempts to retrieve sediment from the bottom of the hole with the bailer were unsuccessful because there was not enough sediment at the bottom of the hole. Two samples of drill cuttings collected from the 1210- to 1215-ft depth interval were submitted for volatile organic compound (VOC) analysis. Multiple photoionization detector readings were also taken of the ambient air around the drill site and water and cuttings samples that were brought to the surface. Monitoring for volatile organic vapors continued as a precaution during further drilling at R-46; no significant readings were observed. Depth to water in the borehole was monitored on January 26, 2009, and appeared to be fairly stable at 1118.6 ft bgs. The drill rods were run back into the hole later that day with a 12-in. tricone bit and the standing water circulated out of the borehole. The water level was then monitored inside the hanging drill rods for 22 h and stabilized at 1147–1148 ft bgs. Early in the morning of January 28, 2009, the hole was cleaned to a depth of 1231 ft bgs and several formation samples were obtained. No water was encountered in the bottom of the hole while measurements were taken through the drill rods, with the bottom of the tool string at 1229.6 ft bgs. One drill rod was removed, and air-only circulation was started in an effort to ensure the bit was not plugged. This put the bottom of the tool string at 1215 ft bgs and still no water was detected at that depth over the next 10 h. The drill string was tripped out, and the 12-in. casing was retracted to 1160 ft bgs early in the morning of January 29. A water level was recorded at approximately 1212 ft bgs; the water level appeared fairly constant. Jet West Geophysical ran a video and a combined natural gamma ray/induction log that morning. The video showed little water entering the borehole, and the geophysical tool reached a bottom depth of 1217.7 ft bgs. After the logging tools were out of the borehole, the 12-in. casing was further retracted to 1074.5 ft bgs (approximately 86 ft of 12-in. casing retracted) and the video camera was run again. The video showed a water level at 1210.5 ft bgs and several clay stringers in the borehole wall. The natural gamma ray and induction tools were also rerun.

Because of the lack of consistent and/or robust water in an apparent perched water zone (at the current drilling depth), the decision was made to place a 10-ft bentonite seal (10.7 ft<sup>3</sup> of ¾-in. bentonite chips) to seal off any water and continue advancing the 12-in. drill casing using a 12-in. underreaming hammer bit. TD was measured at 1207 ft bgs, and drilling from that depth began again early on the morning of January 31. The casing was inadvertently lowered onto the underreamer. Tapping the underreamer with the 12-in. drill casing resulted in minor damage to the rig's top head and the underreamer, both of which required repair. Drilling again started at midnight on February 2; by 0600 h on February 5, a depth of 1400 ft bgs was reached. Several hours were spent monitoring the depth to water, which was fairly stable at 1334 ft bgs. The borehole was drilled a final 15 ft TD (1415 ft bgs) and was reached at 1235 h on February 5, 2009; the drill string was pulled out of the hole.

Schlumberger returned to the drill site and logged the lower portion of the borehole using four geophysical tools: Accelerator Porosity Sonde (APS), Triple Detector Litho-Density (TLD), Elemental Capture Sonde (ECS), and natural gamma ray (GR) during two runs on the morning of February 6. Water levels were monitored over 24 h and reached 1342.4 ft bgs, with the water level continuing to slightly rise on February 7. Before moving the rig off-site the next day, the 12-in. drive shoe was cut off at 1386.8 ft bgs

#### 4.0 SAMPLING ACTIVITIES

This section describes the cuttings and groundwater-sampling activities at well R-46. All sampling activities were conducted in accordance with applicable quality procedures.

#### 4.1 Cuttings Sampling

Cuttings samples were collected from the R-46 borehole at 5-ft intervals from ground surface to the TD of 1415 ft bgs. Approximately 500 mL of bulk cuttings were collected every 5 ft from the discharge hose, sealed in resealable plastic bags, labeled, and archived in core boxes. Sieved fractions (>#10 and >#35 mesh) were processed from the bulk sample and placed in chip trays along with unsieved (whole rock) cuttings. Radiation control technicians screened all cuttings before they were removed from the site. The core boxes and chip trays were delivered to the Laboratory's archive at the conclusion of drilling activities.

Drilling and sample collection methods used at R-46 did not retain a majority of the fine fraction (silt and clay) of the drill cuttings, and much of the fine material throughout the borehole stratigraphy was lost. This effect was particularly evident with increasing depth and in the unconsolidated sedimentary units. The foaming agent helped to retain the fines and acquire more representative samples in the intervals where it was used. The volume of compressed air and water required for circulation made catching samples difficult, and fines were selectively lost during sample collection. Site geologists manually collected samples with a wire mesh basket directly from the discharge hose, but discharge velocities commonly forced the fine fraction of samples through the basket. Recovery of the coarser fraction of the cuttings samples was excellent in nearly 100% of the borehole. The R-46 stratigraphy is summarized in section 5.1 and detailed in Appendix A.

#### 4.2 Water and Sediment Sampling

Groundwater-screening samples were collected from the drilling discharge hose at approximate 20-ft intervals from the top of regional aquifer to the TD of 1415 ft bgs in the R-46 borehole. Typically, upon reaching the bottom of a 20-ft run of casing, the driller would stop water circulation (if injecting water) and circulate air to clean out the borehole. As the discharge cleared, a water sample was collected directly from the discharge hose. Not all depth intervals below the top of the regional groundwater table could be captured at the end of each casing run. Alternatively, some water samples were collected upon start-up of the next casing run, allowing groundwater to reenter the borehole. See Table 4.2-1 for a summary of groundwater- and sediment-screening samples collected.

Twelve regional groundwater-screening samples, from depths of 1115 to 1415 ft bgs, were collected during drilling operations by air-lifting water samples through the drill string. Four regional groundwater screening samples from the well's screen interval (1340–1360.7 ft bgs) were collected at regular durations (approximately one sample per 2 h) during well development. Drilling and development screening samples were analyzed for dissolved anions and metals.

Six regional groundwater-screening samples from the well's screen interval (1340–1360.7 ft bgs) were collected at regular durations (approximately one sample per 4 h) during aquifer testing. The groundwater samples were collected from the discharge port of the submersible development pump. Aquifer-testing screening samples were analyzed for dissolved anions, metals, and total organic carbon (TOC).

An additional 15 regional groundwater screening samples, from depths of 1115 to 1415 ft bgs, were collected during drilling operations and analyzed for VOCs, semivolatile organic compounds (SVOCs), and tritium. Two sediment samples were collected from the bottom of the borehole at 1210–1215 ft bgs and analyzed for VOCs. These samples were collected to evaluate the potential presence of organic contamination after organic odors were detected in drill cuttings (as discussed in section 3.2 of this report). These groundwater and sediment analytical results will be reported in the MDA C investigation report.

Groundwater characterization samples will be collected from the completed well in accordance with the Consent Order. The samples will be analyzed for the full suite of constituents, including radioactive elements; anions/cations; general inorganic chemicals; VOCs and SVOCs; and stable isotopes of hydrogen, nitrogen, and oxygen. These groundwater analytical results will be reported in the annual update to the "Interim Facility-Wide Groundwater Monitoring Plan."

## **5.0 GEOLOGY AND HYDROGEOLOGY**

A brief description of the geologic and hydrogeologic features encountered at R-46 is presented below. The Laboratory's geology task leader and site geologists examined cuttings and geophysical logs to determine geologic contacts and hydrogeologic conditions. Drilling observations, video logging, water-level measurements, and geophysical logs were used to characterize groundwater occurrences encountered at R-46.

### **5.1 Stratigraphy**

The stratigraphy for the R-46 borehole is presented below in order of youngest to oldest geologic units. Lithologic descriptions are based on cuttings samples collected from the discharge hose. Cuttings and borehole geophysical logs were used to identify geologic contacts. Figure 5.1-1 illustrates the stratigraphy at R-46. A detailed lithologic log based on analysis of drill cuttings is presented in Appendix A.

#### **Fill and Disturbed Soil (0–8 ft bgs)**

Quaternary alluvium occurs from 0 to 8 ft bgs and consists of a thin surficial layer of unconsolidated tuffaceous silty sand to sandy silt with pebble gravels containing quartz and sanidine crystals and volcanic lithic detritus. No evidence of alluvial groundwater was observed.

#### **Unit 3 of the Tshirege Member of the Bandelier Tuff, Qbt 3 (8–120 ft bgs)**

Unit 3 of the Tshirege Member of the Bandelier Tuff was encountered from 8 to 120 ft bgs, as interpreted from natural gamma geophysical log data. Unit 3 is a moderately welded ash-flow tuff that is crystal-rich, generally weakly pumiceous and lithic-poor and exhibits a matrix of fine vitric ash. The observed degree of welding varies somewhat within the section and locally ranges from strongly to poorly welded. Drill cuttings from unit 3 typically contain abundant fragments of welded tuff containing up to 25% by volume quartz and sanidine phenocrysts and minor volcanic lithics set in a matrix of fine volcanic ash.

#### **Unit 2 of the Tshirege Member of the Bandelier Tuff, Qbt 2 (120–210 ft bgs)**

Unit 2 of the Tshirege Member of the Bandelier Tuff was encountered from 120 to 210 ft bgs as interpreted from natural gamma geophysical log data. Unit 2 is a moderately to locally strongly welded ash-flow tuff that is crystal-rich, weakly pumiceous and generally lithic-poor. Drill cuttings from unit 2 typically contain a predominance of welded tuff fragments containing up to 30% by volume quartz and sanidine phenocrysts, up to 15% moderately flattened pumice lapilli, and minor volcanic lithics set in a matrix of fine volcanic ash.

#### **Unit 1v of the Tshirege Member of the Bandelier Tuff, Qbt 1v (210–253 ft bgs)**

Unit 1v of the Tshirege Member of the Bandelier Tuff was encountered from 210 to 253 ft bgs, as interpreted from natural gamma geophysical log data. Unit 1v is characterized by the presence of devitrified glass that occurs in the makeup of both pumice and ash matrix. As observed in R-46 drill cuttings, unit 1v is a poorly to moderately welded ash-flow tuff that is pumiceous, crystal-bearing and

lithic-poor. Fragments of the tuff typically contain up to 15% quartz and sanidine phenocrysts, pumices displaying sugary (i.e., granular, recrystallized) textures, and minor volcanic lithics in a matrix of devitrified volcanic ash.

**Unit 1g of the Tshirege Member of the Bandelier Tuff, Qbt 1g (253–290 ft bgs)**

Unit 1g of the Tshirege Member of the Bandelier Tuff was encountered from 253 to 290 ft bgs, as interpreted from natural gamma geophysical log data. Unit 1g is a moderately to poorly welded ash-flow tuff that is strongly pumiceous, generally crystal-bearing and lithic-poor, with abundant vitric ash matrix. The Qbt 1g section observed in R-46 contains abundant glassy pumice lapilli; minor, predominantly dacitic, volcanic lithics, and abundant quartz and sanidine phenocrysts.

**Cerro Toledo Interval, Qct (290–475 ft bgs)**

The Cerro Toledo interval, intersected from 290 to 475 ft bgs (as interpreted from natural gamma logging data), is apparently extraordinarily thick in the vicinity of R-46. This unit, consisting of poorly consolidated volcanoclastic sediments, stratigraphically separates the Tshirege and Otowi Members of the Bandelier Tuff. Locally, this unit consists of weakly consolidated silty fine to coarse sands and gravels made up of detrital volcanic materials (e.g., dacites, obsidian, flow-banded rhyodacite, and andesite), weathered to glassy pumice fragments, and abundant quartz and sanidine crystal grains.

**Otowi Member of the Bandelier Tuff, Qbo (475–684 ft bgs)**

The Otowi Member of the Bandelier Tuff is present in R-46 from 475 to 684 ft bgs, as interpreted from natural gamma geophysical log data. The Otowi Member is a poorly welded, pumiceous, locally lithic-rich, crystal-bearing ash-flow tuff. The Otowi Member contains abundant white to pale orange pumice lapilli that are glassy, fibrous-textured and quartz- and sanidine-phyric, and commonly abundant volcanic lithic fragments (i.e., xenoliths) enclosed in a matrix of vitric ash. Characteristically abundant lithic fragments (up to 25 mm in diameter) are subangular to subrounded and predominantly of intermediate volcanic composition (i.e., gray to pinkish gray hornblende- and/or biotite-phyric dacites, and some andesites).

**Guaje Pumice Bed of the Otowi Member of the Bandelier Tuff, Qbog (684–697 ft bgs)**

The Guaje Pumice Bed occurs in R-46 from 684 to 697 ft bgs on the basis of natural gamma log interpretation. Locally, the Guaje tuff unit is nonwelded, pumice-rich, lithic- and crystal-poor, and contains abundant (75%–95% by volume) pristine-appearing white vitric, phenocryst-poor pumice fragments and lapilli. Trace volumes of volcanic lithics, quartz and sanidine phenocrysts, and fine ash are present.

**Dacite Lava, Tt2 (697–921 bgs)**

A thick section of generally massive dacite lava(s) was encountered from 697 to 921 ft bgs. This volcanic unit has not yet been assigned a formal name or symbol. The upper 5 ft of the lava section is strongly vesicular to scoriaceous. However, below this zone, the dacite rapidly becomes dark gray, is massive (i.e., nonvesicular), and phenocryst-poor with an aphanitic groundmass. Phenocrysts of black opaque clinopyroxene and green-amber (possibly) opx, commonly in cumulophyric clusters, with or without plagioclase, make up no more than 1% of the total rock volume. The massive nature of the dacite is consistent throughout the section. Intervals of strong fracturing and jointing were observed in drill cuttings and a video log survey. The dacite groundmass is locally weakly altered.

### **Dacite Scoria and Breccia, Tt2 (921–955 bgs)**

The interval from 921 to 955 ft bgs contains abundant reddish brown, ferruginous, altered dacite that is vesicular to scoriaceous and partly glassy, suggesting a flow breccia forming the base of the overlying massive dacite lava. Angular dacite clasts are phenocryst-poor with an aphanitic groundmass.

### **Puye Formation, Tpf (955–1405 ft bgs)**

Puye Formation volcanoclastic sediments were encountered from 955 ft to 1405 ft bgs. These sedimentary rocks consist of texturally diverse, gray, grayish brown and pinkish tan, poorly sorted, fine to coarse gravels, gravelly sandstones, and silty sandstones with gravel. Significant intervals of silt-rich sediments, stacked, 5 to 25 ft thick, were observed in drill cuttings from 1115 to 1230 ft bgs. The interval from 955 to 980 ft contains phenocryst-poor dacite clasts similar to the overlying lava, scoria, and breccia; these phenocryst-poor dacite clasts are mixed with phenocryst-rich dacite clasts that are more typical of the Puye Formation. Below 980 ft, the detrital constituents that make up these sediments are generally subangular to subrounded and represent a range of volcanic lithologies, including massive pyroxene-phyric dacite, abundant biotite- and hornblende-phyric dacites (present as a major constituent in large volumes throughout the lower part of the section), reddish and black ferruginous vitrophyre, rhyodacite, weathered pumice, and scoria.

### **Miocene Pumiceous Sediments (not assigned) (1405–1415 ft bgs)**

The upper part of a section of pumice-rich volcanoclastic sediments was intersected from 1405 ft to the borehole TD at 1415 ft bgs. These deposits have not been formally assigned a name or symbol. They consist of fine- to coarse-grained sandstones with pebble gravels. Granules and small pebbles comprising these sediments are predominantly of gray, white, and reddish dacites and lesser (up to 15% by volume) white glassy, phenocryst-poor, weakly biotite-bearing, detrital pumices.

## **5.2 Groundwater**

Groundwater was first encountered at R-46 during drilling at approximately 1109 ft bgs in the Puye Formation on January 24, 2009. After the well was drilled to final depth of 1415 ft bgs, the water level was measured at approximately 1327.9 ft bgs in the borehole.

Groundwater-screening samples were collected during drilling, well development, and aquifer testing, as discussed in section 4.2. Groundwater chemistry and field water-quality parameters are discussed in Appendix B. Aquifer testing data and analysis are discussed in Appendix C.

## **6.0 BOREHOLE LOGGING**

Several video logs and a several suites of geophysical logs were collected during the R-46 drilling project. A summary of video and geophysical logging runs is presented in Table 6.0-1.

### **6.1 Video Logging**

Video logging of the R-46 borehole was conducted by Jet West and occurred on multiple occasions and aided both drilling and well construction activities (Table 6.0-1).

Video and natural gamma ray and induction logging were conducted on January 14, 2009, in the R-46 borehole, cased to 692.2 ft and open hole to bottom depth of 1064.7 ft bgs. The video log showed fractures with moisture from 735 to 833 ft bgs.

Video and natural gamma ray and induction logging were conducted on January 29, 2009, in the R-46 borehole with the 12-in. casing retracted to 1217.7 ft bgs, and no water was encountered. The 12-in. casing was further retracted to 1074.5 ft bgs, and a water level of 1210.5 ft bgs was observed along with several clay stringers in the borehole wall. Selected video logs from the borehole are presented on a digital video disc as part of Appendix D included with this document.

## 6.2 Geophysical Logging

Two suites of Jet West open-and cased-hole geophysical logs were collected at R-46. The first was on January 14 and the second was on January 29, 2009 (Appendix E).

Two suites of Schlumberger cased hole geophysical logs were collected in the R-46 borehole on January 25, 2009, and February 6, 2009. The first logging run was with the 12-in. casing at an intermediate depth of 1230 ft bgs. The geophysical suite included TLD, GR, ECS, and Hostile Natural Gamma Spectroscopy (HNGS) (Table 6.0-1). The second logging run was with the 12-in. casing at the TD of 1415 ft bgs. The geophysical suite included APS, TLD, ECS, and HNGS (Table 6.0-1). Interpretation and details of the Schlumberger logs are presented in the geophysical logging report on a CD as part of Appendix E.

## 7.0 WELL INSTALLATION

R-46 well casing and annular fill were installed between February 8, 2009, and February 26, 2009.

### 7.1 Well Design

The R-46 well was designed in accordance with the Consent Order. NMED approved the well design before installation. The well was designed with a single screened interval to monitor groundwater quality in the Puye Formation sediments within the uppermost productive zone of the regional aquifer. A discussion of the screen placement decision process is presented in Appendix F.

### 7.2 Well Construction R-46

The R-46 monitoring well was constructed of 5.0-in.-I.D./5.56-in.-O.D. schedule 40 type TP304/304L stainless-steel casing fabricated to American Society for Testing and Materials A312 standards. External couplings (also type A312/SA312 stainless steel) were used to connect individual casing and screen sections. The screen sections were 10.68 ft long with 10-ft lengths of 5.0-in.-I.D. rod-based 0.020-in. slot wire-wrapped well screen. The coupled unions between threaded sections were approximately 0.8 ft long. The casing and screen were factory-cleaned and steam-cleaned on-site before installation. A 2-in.-I.D. steel-threaded/coupled tremie pipe was used to deliver all backfill and annular fill materials during well construction.

A nominal 20-ft screened interval was used for R-46 with the top of the screen set at 1340 ft bgs. A 20.6-ft stainless-steel sump was placed below the well screen. The dual-rotary drill rig was removed from the site after the 12-in. casing drive shoe was cut off. A Pulstar work-over rig was used for all well construction activities. Figure 7.2-1 presents an as-built schematic showing construction details for the completed well.

After the well casing was assembled and lowered into the borehole, installation of annular backfill materials was started. This activity had two components: installing materials and retracting the drill casing. As the annular fill was emplaced, the drill casing was retracted and removed. The well-casing



string was hung under full tension throughout well construction. The well installation proceeded normally and few difficulties were encountered.

The bottom of the borehole was filled with 10/20 silica sand from 1371.7 to 1412.2 ft bgs. The lower bentonite seal of ¼-in. pellets was installed around the well sump from 1365.3 to 1371.7 ft bgs. A fine-grained transition-sand collar of 20/40 silica sand was placed from 1362.2 to 1365.3 ft bgs. The primary filter pack of 10/20 silica sand was placed across the screened interval from 1335.0 to 1362.2 ft bgs. R-46 is screened from 1340.0 to 1360.7 ft bgs. During and after installation of the primary filter pack, the work-over rig was used to surge the screened interval with a surge block to promote settling and compaction of the filter pack. A fine-grained transition-sand collar of 20/40 silica sand was placed above the primary filter pack from 1332.0 to 1335.0 ft bgs. After placement of the fine sand collar, a 3/8-in. bentonite chip seal was installed from 313.8 to 1332.0 ft bgs. The surface seal, composed of 98% cement and 2% bentonite, was installed from 3.0 to 313.8 ft bgs. Figure 7.2-1 depicts final depths and volumes used in each interval. Table 7.2-1 details volumes of materials used during well construction.

## 8.0 POSTINSTALLATION ACTIVITIES

Following well installation at R-46, the well was developed, aquifer pumping tests and a geodetic survey of the wellhead were performed, and the wellhead and surface pad was constructed. A dedicated submersible pump will be installed. Site restoration activities will be completed following the final disposition of contained drill cuttings and groundwater, per the NMED-approved waste-decision trees.

### 8.1 Well Development

Well development was conducted between February 26, 2009, and March 4, 2009. Initially, the screened interval was swabbed and bailed to remove suspended solids in the well and formation fines in the filter pack. Bailing and swabbing methods were used until returned water was clear, and then a submersible pump was utilized to complete development. The swabbing tool was a 4.75-in.-O.D. 1-in.-thick nylon disc attached to a steel rod. The swabbing tool was lowered by wireline and drawn repeatedly across the screened interval. After bailing and swabbing, a 5-hp, 4-in.-Berkeley submersible pump was lowered into the well for the final stage of well development.

During the pumping stage of well development, turbidity, temperature, pH, dissolved oxygen (DO), oxidation-reduction potential (ORP), and specific conductance parameters were collected. In addition, water samples for total organic carbon (TOC) analysis were collected. The required values for TOC and turbidity by the end of well development are less than 2.0 ppm and less than 5 nephelometric turbidity units (NTUs), respectively. TOC values were less than 1.0 ppm. Turbidity measurement at the end of well development was 4.5 NTUs.

Approximately 9498 gal. of groundwater was purged during development activities. A discussion of water removed during well development, water-quality parameters, and analytical results for samples collected during development is presented in Table B.1.2-1 of Appendix B.

#### 8.1.1 Field Parameters

Field parameters, including pH, temperature, DO, ORP, specific conductance, and turbidity, were measured at regular time intervals during well development and aquifer testing. Results are provided in Table B.1.2-1 of Appendix B. Field parameters were measured during well development at well R-46 by collecting aliquots of groundwater from the discharge pipe without the use of a flow-through cell, allowing the samples to be exposed to the atmosphere. This condition probably resulted in a slight variation of field

parameters during well development, most notably, temperature, pH, and DO. Measurements of pH and temperature varied from 8.0 to 8.07 and from 11.16°C to 18.54°C, respectively, at well R-46. Several of the low temperature measurements for groundwater samples were probably influenced by land surface-atmosphere conditions during sampling. Concentrations of DO varied from 10.99 to 12.30 mg/L. The maximum concentrations of DO are calculated at 8.87 and 7.29 mg/L at 11°C and 20°C, respectively, at 6000 ft, based on solubility calculations. ORP was not recorded at R-46 during well development because a groundwater-flow through cell was not used during sampling. Specific conductance ranged from 130 to 135 microsiemens per centimeter ( $\mu\text{S}/\text{cm}$ ). Values of turbidity measured at R-46 ranged from 4.5 to 5.2 NTUs for the nonfiltered groundwater samples.

Field parameters were measured during aquifer testing at well R-46 by collecting aliquots from the discharge port of the submersible development pump. This condition probably resulted in a slight variation of field parameters, most notably, temperature, pH, and DO. Measurements of pH and temperature varied from 7.94 to 8.05 and from 17.13°C to 23.31°C, respectively, at well R-46. Concentrations of DO and ORP ranged from 5.62 to 9.59 mg/L and from 29.5 to 76.7 millivolt (mV), respectively. Specific conductance ranged from 104 to 124  $\mu\text{S}/\text{cm}$ . Values of turbidity ranged from 3.6 to 11.6 NTUs for the nonfiltered groundwater samples.

## 8.2 Aquifer Testing

Aquifer pumping tests were conducted at R-46 between March 7 and March 12, 2009. Several short-duration tests with short-duration recovery periods were performed on March 8 before a 24-h constant rate test was conducted on March 10. The 24-h constant rate test was then followed by a 24-h recovery/background data collection period. A shrouded 10-hp Grundfos pump was used to perform the aquifer tests. Approximately 12,168 gal. of groundwater was purged during aquifer testing activities. The results of the R-46 aquifer test are presented in Appendix C.

## 8.3 Dedicated Sampling System Installation

A dedicated sampling system consisting of a 4-in. Grundfos submersible pump (environmentally retrofitted with Teflon with a 4-in., 3-phase, 460-V, viton-fitted Franklin submersible motor will be installed in the R-46 well. Observations made during well development and aquifer testing indicate that a 5-hp Grundfos model 10S50-58DS will be the most appropriate pump for permanent system installation.

All materials that contact the groundwater will be constructed of stainless steel, Teflon, or polyvinyl chloride (PVC). All components of the pump column will be new. The pump column will be constructed of 1 in. threaded/coupled stainless-steel pipe with check valves installed in the pipe string every 200 ft. A weep hole will be installed at the bottom of the uppermost pipe joint to protect the pump column from freezing. To measure water levels in the well, two 1-in. I.D. schedule 80 PVC pipes will be installed to sufficient depth to set a dedicated transducer below the measured static water level and to provide access for manual water-level measurements. The PVC transducer tubes will be equipped with a 6-in. section of 0.010 in. slot screen with a threaded end cap at the bottom of the tube. A weather-resistant pump control box will be installed next to the wellhead. A schematic of the proposed pump and surface equipment is shown in Figure 8.3-1a.

## 8.4 Wellhead Completion

A reinforced concrete surface pad, 10 ft  $\times$  10 ft  $\times$  6 in. thick, was installed at the R-46 well head on March 16, 2009. The pad will provide long-term structural integrity for the well. A brass survey monument imprinted with well identification information was placed in the northwest corner of the pad. A 10-in.-I.D.

steel protective casing with a locking lid was installed around the stainless-steel well riser. A weep hole was installed to prevent water buildup inside the protective casing. The concrete pad is slightly elevated above the ground surface to promote runoff. A total of four bollards, painted yellow for visibility, are set at the outside corners of the pad to protect the well from traffic. All of the four bollards are designed for easy removal to allow access to the well. Details of the wellhead completion are presented in Figure 8.3-1b.

### **8.5 Geodetic Survey**

A New Mexico licensed professional land surveyor conducted a geodetic survey on February 10, 2009, (Table 8.5-1). The survey data collected conforms to Laboratory Information Architecture project standards IA-CB02, "GIS Horizontal Spatial Reference System," and IA-D802, "Geospatial Positioning Accuracy Standard for A/E/C and Facility Management." All coordinates are expressed as New Mexico State Plane Coordinate System Central Zone (NAD 83); elevation is expressed in feet above mean sea level (amsl) using the National Geodetic Vertical Datum of 1929. Survey points include ground-surface elevation near the concrete pad, the top of the brass pin in the concrete pad, the top of the well casing, and the top of the protective casing.

### **8.6 Waste Management and Site Restoration**

Waste generated from the R-46 project includes contact waste, decontamination water, petroleum contaminated soil, drill cuttings, drilling fluids, cement slurry, and purged groundwater. A summary of the waste characterization samples collected from the R-46 well is presented in Table 8.6-1.

All waste streams produced during drilling and development activities were sampled in accordance with "Waste Characterization Strategy Form for the R-38, R-41, R-44, R-45, and R-46 Regional Groundwater Well Installation and Corehole Drilling" (LANL 2008, 103916).

Fluids produced during drilling and well development are expected to be land-applied after a review of associated analytical results per the waste characterization strategy form (WCSF) and the EP-Directorate Standard Operating Procedure (SOP) 010.0, Land Application of Groundwater. If it is determined that drilling fluids are nonhazardous but cannot meet the criterion for land application, the drilling fluids will be evaluated for treatment and disposal at one of the Laboratory's six wastewater treatment facilities. If analytical data indicate that the drilling fluids are hazardous/nonradioactive or mixed low-level waste, the drilling fluids will be disposed of at an authorized facility.

Cuttings produced during drilling are anticipated to be land-applied after a review of associated analytical results per the WCSF and ENV-RCRA SOP-011.0, Land Application of Drill Cuttings. If the drill cuttings do not meet the criterion for land application, they will be removed from the pit and disposed of at an authorized facility. The cement slurry waste stream will be managed as industrial nonhazardous waste, pending analytical review. Disposal of this cement slurry will take place at an authorized disposal facility. Characterization of contact waste will be based upon acceptable knowledge, pending analyses of the waste samples collected from the drill cuttings, purge water, and cement slurry. Petroleum-contaminated soil was managed (or is being managed) as a New Mexico Special Waste and disposed of (or will be disposed of) at an authorized facility. Decontamination fluid used for cleaning the drill rig and equipment is containerized. The fluid waste was sampled and will be disposed of at an authorized facility.

Site restoration activities will include removing drilling fluids and cuttings from the pit and managing the fluids and cuttings in accordance with SOP-010.06, removing the polyethylene liner, removing the containment area berms, and backfilling and regrading the containment area, as appropriate.

## 9.0 DEVIATIONS FROM PLANNED ACTIVITIES

Drilling, sampling, and well construction at R-46 were performed as specified in the "Final Drilling Plan for Regional Aquifer Well R-46" (TerranearPMC 2008, 105083).

### 9.1 NMED-Approved Modifications to the Work Plan

Drilling, sampling, and well construction at R-46 were performed as specified in the "Drilling Work Plan for Regional and Intermediate Wells at Technical Area 54" (LANL 2007, 099662).

## 10.0 ACKNOWLEDGMENTS

Pat Longmire wrote Appendix B, Groundwater Analytical Results.

Boart Longyear drilled the R-46 borehole and installed the well.

Jet West Geophysical ran downhole video equipment.

David C. Schafer designed, implemented and analyzed the aquifer testing.

Schlumberger Water Services performed the geophysical log processing and log interpretation.

Schlumberger Wireline Services performed the final geophysical logging of the borehole.

TerranearPMC provided oversight on all preparatory and field-related activities.

## 11.0 REFERENCES

*The following list includes all documents cited in this report. Parenthetical information following each reference provides the author(s), publication date, and ER ID number. This information is also included in text citations. ER ID numbers are assigned by the Environmental Programs Directorate's RPF and are used to locate the document at the RPF and, where applicable, in the master reference set.*

*Copies of the master reference set are maintained at the NMED Hazardous Waste Bureau and the Directorate. The set was developed to ensure that the administrative authority has all material needed to review this document, and it is updated with every document submitted to the administrative authority. Documents previously submitted to the administrative authority are not included.*

LANL (Los Alamos National Laboratory), March 2006. "Storm Water Pollution Prevention Plan for SWMUs and AOCs (Sites) and Storm Water Monitoring Plan," Los Alamos National Laboratory document LA-UR-06-1840, Los Alamos, New Mexico. (LANL 2006, 092600)

LANL (Los Alamos National Laboratory), October 4, 2007. "Integrated Work Document for Regional and Intermediate Aquifer Well Drilling (Mobilization, Site Preparation and Setup Stages)," Los Alamos National Laboratory, Los Alamos, New Mexico. (LANL 2007, 100972)

LANL (Los Alamos National Laboratory), November 2007. "Drilling Work Plan for Regional and Intermediate Wells at Technical Area 54," Los Alamos National Laboratory document LA-UR-07-7578, Los Alamos, New Mexico. (LANL 2007, 099662)

LANL (Los Alamos National Laboratory), October 2008. "Waste Characterization Strategy Form for the R-38, R-41, R-44, R-45, and R-46 Regional Groundwater Well Installation and Corehole Drilling," Los Alamos, New Mexico. (LANL 2008, 103916)

TerranearPMC, October 2008. "Final Drilling Plan for Regional Aquifer Well R-38," plan prepared for Los Alamos National Laboratory, Los Alamos, New Mexico. (TerranearPMC 2008, 103941)

TerranearPMC, December 2008. "Drilling Plan for Regional Aquifer Well R-46," plan prepared for Los Alamos National Laboratory, Los Alamos, New Mexico. (TerranearPMC 2008, 105083)

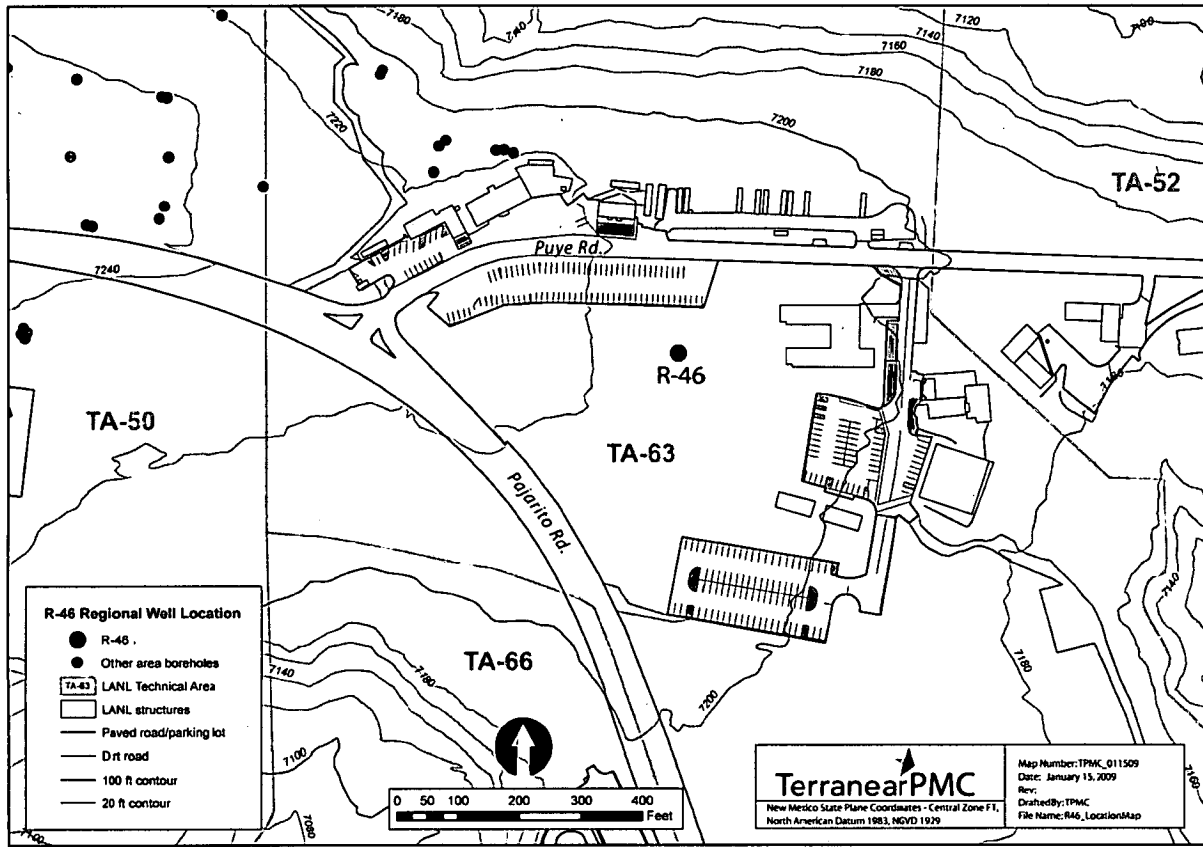


Figure 1.0-1 Regional aquifer well R-46

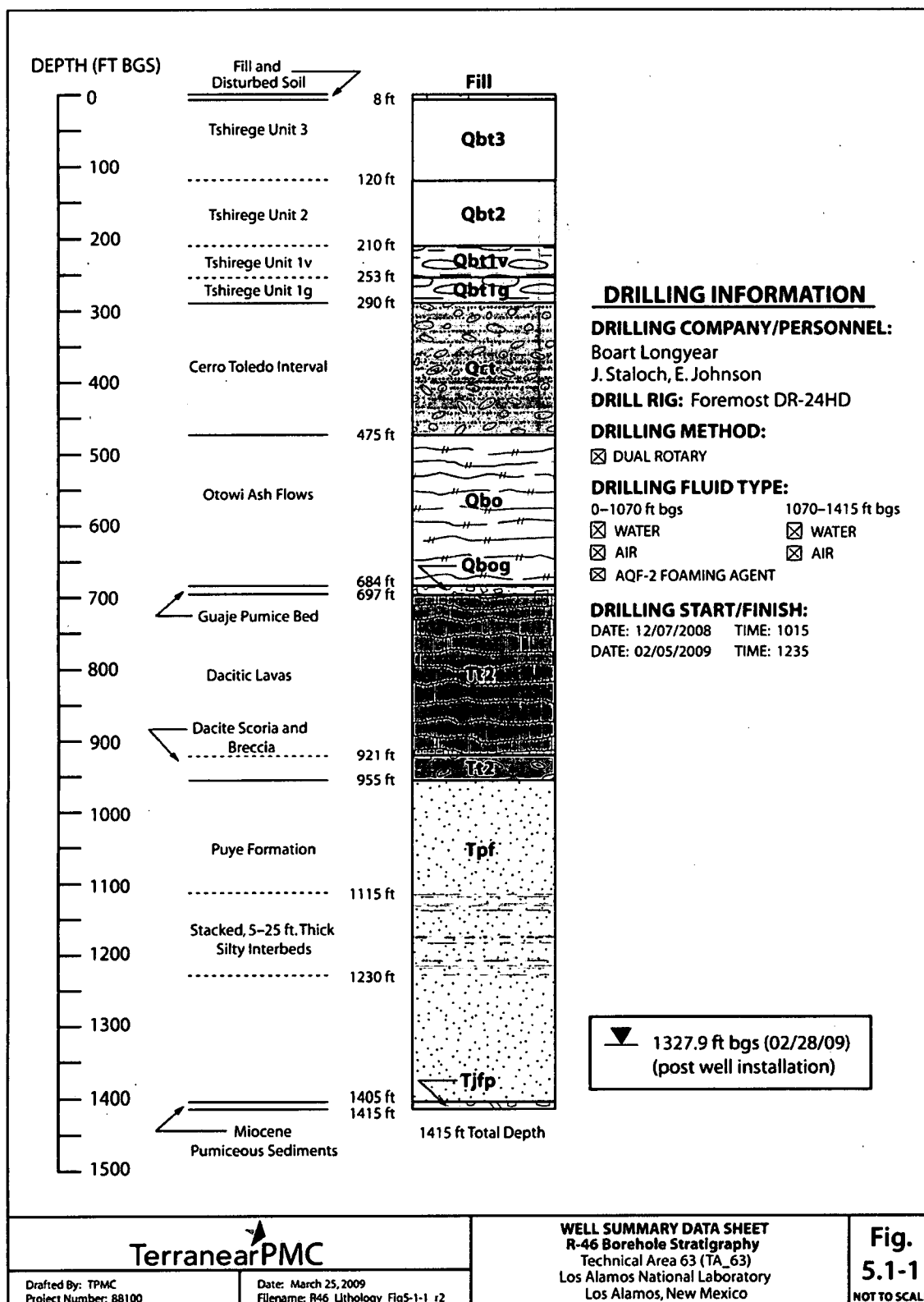


Figure 5.1-1 R-46 borehole stratigraphy

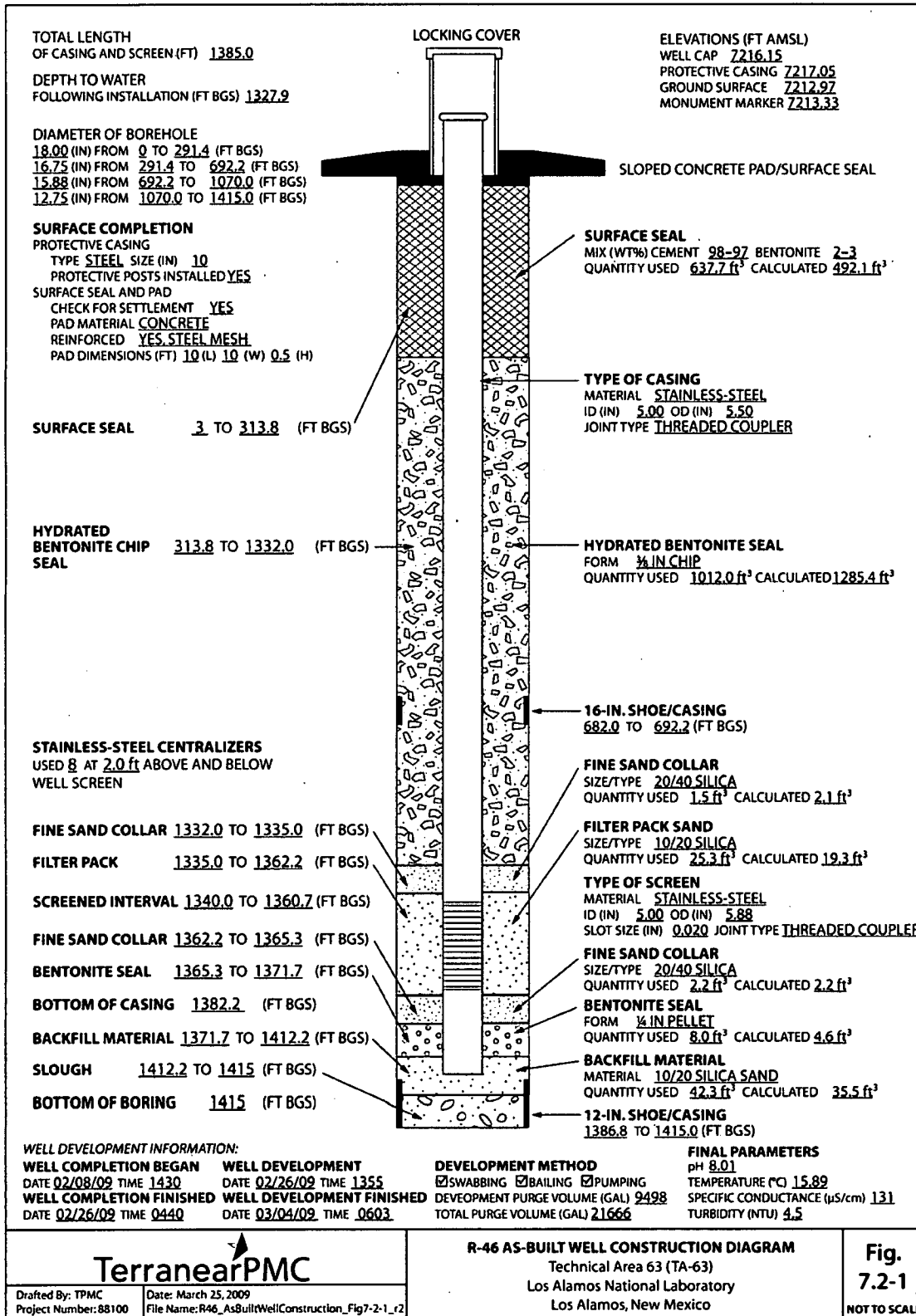


Figure 7.2-1 R-46 as-built well construction diagram





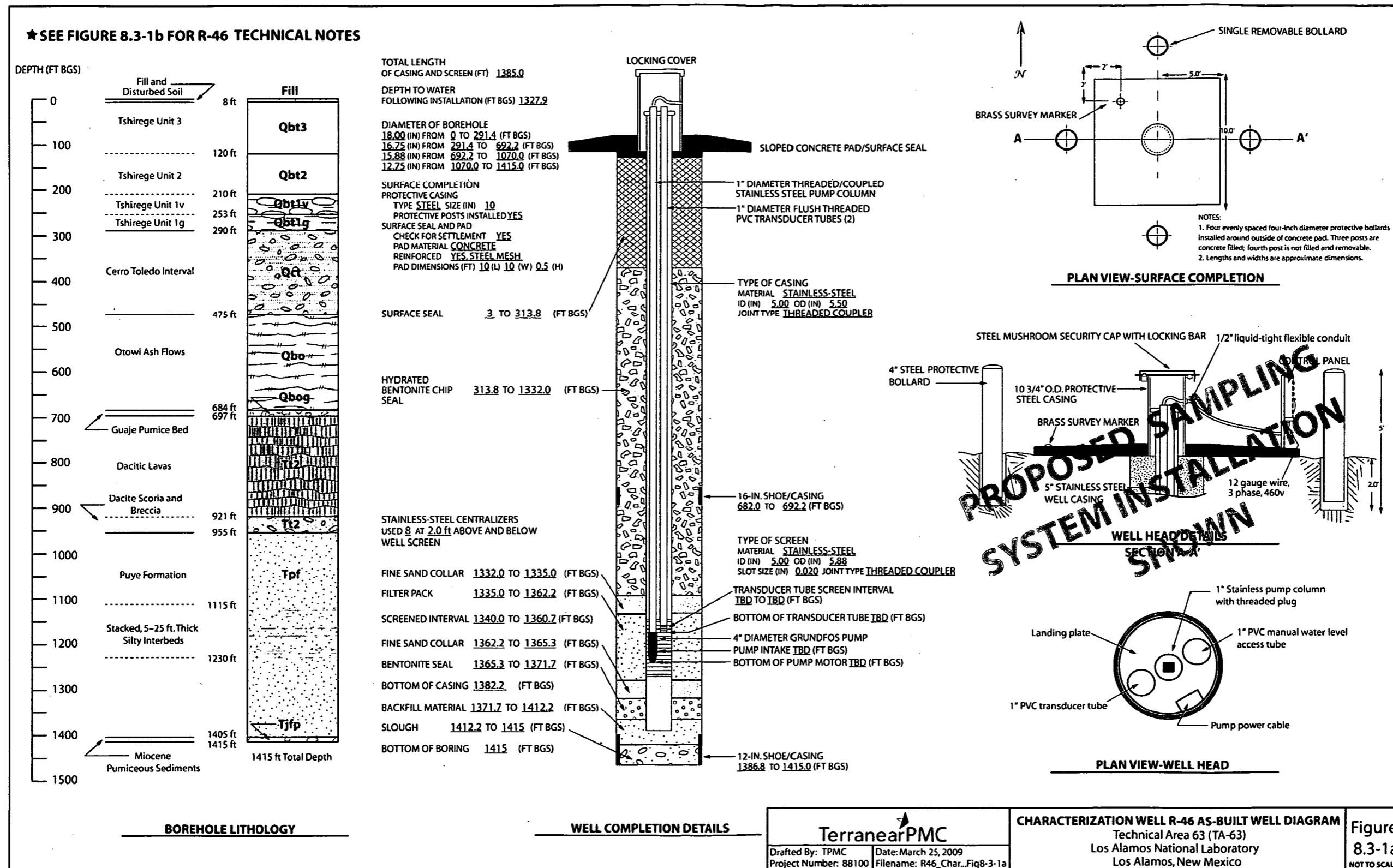


Figure 8.3-1a As-built schematic for regional well R-46


<b>R-46 TECHNICAL NOTES: 1</b>	
<p><b>SURVEY INFORMATION<sup>2</sup></b>  <b>Brass Marker</b>                      Northing: 1768183.02 ft                      Easting: 1627433.85 ft                      Elevation: 7213.33 ft AMSL</p> <p><b>Well Casing</b> (top of stainless steel)                      Northing: 1768178.26 ft                      Easting: 1627437.39 ft                      Elevation: 7216.15 ft AMSL</p> <p><b>BOREHOLE GEOPHYSICAL LOGS</b>                      Jet West Geophysical - video (3), gamma ray (3), induction (3)                      Schlumberger - CN, TLD (2), ECS (2), HNGS (2), APS</p> <p><b>DRILLING INFORMATION</b>  <b>Drilling Company</b>                      Boart Longyear</p> <p><b>Drill Rig</b>                      Foremost DR-24HD</p> <p><b>Drilling Methods</b>                      Dual Rotary                      Fluid-assisted air rotary, Foam-assisted air rotary</p> <p><b>Drilling Fluids</b>                      Air, potable water, AQF-2 Foam</p> <p><b>MILESTONE DATES</b>  <b>Drilling</b>                      Start: 12/07/2008                      Finished: 02/05/2009</p> <p><b>Well Completion</b>                      Start: 02/08/2009                      Finished: 02/26/2009</p> <p><b>Well Development</b>                      Start: 02/26/2009                      Finished: 03/04/2009</p> <p><b>WELL DEVELOPMENT</b>  <b>Development Methods</b>                      Performed swabbing, bailing, and pumping                      Total Volume Purged: 9498 gallons</p> <p><b>Parameter Measurements (Final)</b>                      pH: 8.01                      Temperature: 15.89°C                      Specific Conductance: 131 µS/cm                      Turbidity: 4.5 NTU</p> <p>NOTES:                      1) Additional information available in "Final Completion Report, Characterization Well R46, Los Alamos National Laboratory, Los Alamos, New Mexico, TBD 2009."                      2) Coordinates based on New Mexico State Plane Grid Coordinates, Central Zone (NAD83); Elevation expressed in feet above mean sea level using the National Geodetic Vertical Datum of 1929.</p>	<p><b>AQUIFER TESTING</b>                      Constant Rate Pumping Test  <b>Upper Screen</b>                      Water Produced: 12168 gallons                      Average Flow Rate: 9.1 gpm                      Performed on: 03/10/09</p> <p><b>DEDICATED SAMPLING SYSTEM</b>  <b>Pump</b>                      Type: TBD                      Model: TBD                      TBD U.S. gpm, intake at TBD ft bgs                      Environmental Retrofit</p> <p><b>Motor</b>                      Type: TBD                      Model: TBD</p> <p><b>Pump Column</b>                      TBD</p> <p><b>Transducer Tubes</b>                      TBD</p> <p><b>Transducer</b>                      Type: TBD                      Model: TBD                      S/N: TBD</p>
	<p><b>R-46 TECHNICAL NOTES</b>                      Technical Area 63 (TA-63)                      Los Alamos National Laboratory                      Los Alamos, New Mexico</p>
Drafted By: TPMC Project Number: 86000	Date: March 20, 2009 Filename: R46_TechnicalNotes_Fig8-3-1b_r1
<p><b>Figure 8.3-1b</b>                      NOT TO SCALE</p>	

Figure 8.3-1b As-built technical notes for R-46

**Table 3.1-1  
Fluid Quantities Used during Drilling and Well Construction**

Date	Water (gal.)	Cumulative Water (gal.)	AQF-2 Foam (gal.)	Cumulative AQF-2 Foam (gal.)
<b>Drilling</b>				
12/17/08	500	500	10	10
12/18/08	200	700	5	15
12/19/08	2700	3400	40	55
12/20/08	150	3550	0	55
12/21/08	400	3950	10	65
12/22/08	1100	5050	25	90
01/07/09	700	5750	10	100
01/08/09	2000	7750	25	125
01/09/09	300	8050	5	130
01/10/09	3000	11050	35	165
01/11/09	400	11450	5	170
01/12/09	5000	16450	40	210
01/13/09	3000	19450	55	265
01/15/09	100	19550	0	265
01/19/09	200	19750	0	265
01/21/09	3000	22750	0	265
01/22/09	1000	23750	0	265
01/23/09	2800	26550	0	265
01/24/09	2100	28650	0	265
01/30/09	1500	30150	0	265
01/31/09	400	30550	0	265
02/02/09	1500	32050	0	265
02/03/09	200	32250	0	265
02/04/09	1170	33420	0	265
<b>Well Construction</b>				
02/10/09	2500	35920	n/a*	n/a
02/11/09	1200	37120	n/a	n/a
02/12/09	2000	39120	n/a	n/a
02/13/09	1200	40320	n/a	n/a
02/14/09	3100	43420	n/a	n/a
02/15/09	5500	48920	n/a	n/a
02/16/09	5500	54420	n/a	n/a
02/17/09	4000	58420	n/a	n/a

Table 3.1-1 (continued)

Date	Water (gal.)	Cumulative Water (gal.)	AQF-2 Foam (gal.)	Cumulative AQF-2 Foam (gal.)
<b>Well Construction (cont.)</b>				
02/19/09	800	59220	n/a	n/a
02/20/09	2600	61820	n/a	n/a
02/24/09	4250	66070	n/a	n/a
02/25/09	336	66406	n/a	n/a

Note. Cumulative returns in the pit following drilling and well development are estimated to be approximately 33,420 gal.

\*n/a = Not applicable. Foam use terminated before completing drilling activities; none used during well construction.

**Table 4.2-1**  
**Summary of Groundwater and Sediment Screening Samples Collected**  
**during Drilling, Well Development, and Aquifer Testing of Well R-46**

Location ID	Sample ID	Date Collected	Collection Depth (ft bgs)	Sample Type	Analysis
<b>Drilling</b>					
R-46	GW46-09-1847	01/22/09	1115	Groundwater	Anions, metals
R-46	GW46-09-1848	01/23/09	1134	Groundwater	Anions, metals
R-46	GW46-09-1849	01/23/09	1155	Groundwater	Anions, metals
R-46	GW46-09-1850	01/24/09	1175	Groundwater	Anions, metals
R-46	GW46-09-1851	01/24/09	1195.5	Groundwater	Anions, metals
R-46	GW46-09-1852	01/24/09	1215	Groundwater	Anions, metals
R-46	GW46-09-1853	01/25/09	1230	Groundwater	Anions, metals
R-46	GW46-09-1854	01/26/09	1220	Groundwater	Anions, metals
R-46	GW46-09-1855	02/04/09	1340	Groundwater	Anions, metals
R-46	GW46-09-1856	02/04/09	1360	Groundwater	Anions, metals
R-46	GW46-09-1857	02/05/09	1395	Groundwater	Anions, metals
R-46	GW46-09-1858	02/05/09	1415	Groundwater	Anions, metals
<b>Well Development</b>					
R-46	GW46-09-1867	03/03/09	1340–1360.7	Groundwater	Anions, metals
R-46	GW46-09-1868	03/04/09	1340–1360.7	Groundwater	Anions, metals
R-46	GW46-09-1869	03/04/09	1340–1360.7	Groundwater	Anions, metals
R-46	GW46-09-1870	03/04/09	1340–1360.7	Groundwater	Anions, metals
<b>Aquifer Pump Test</b>					
R-46	GW46-09-1871	03/10/09	1340–1360.7	Groundwater	Anions, metals, TOC
R-46	GW46-09-1872	03/10/09	1340–1360.7	Groundwater	Anions, metals, TOC
R-46	GW46-09-1873	03/10/09	1340–1360.7	Groundwater	Anions, metals, TOC
R-46	GW46-09-1874	03/11/09	1340–1360.7	Groundwater	Anions, metals, TOC
R-46	GW46-09-1875	03/11/09	1340–1360.7	Groundwater	Anions, metals, TOC
R-46	GW46-09-1876	03/11/09	1340–1360.7	Groundwater	Anions, metals, TOC

Table 4.2-1 (continued)

Location ID	Sample ID	Date Collected	Collection Depth (ft bgs)	Sample Type	Analysis
<b>Aquifer Pump Test</b>					
R-46	GW46-09-1871	03/10/09	1340–1360.7	Groundwater	Anions, metals, TOC
R-46	GW46-09-1872	03/10/09	1340–1360.7	Groundwater	Anions, metals, TOC
R-46	GW46-09-1873	03/10/09	1340–1360.7	Groundwater	Anions, metals, TOC
R-46	GW46-09-1874	03/11/09	1340–1360.7	Groundwater	Anions, metals, TOC
R-46	GW46-09-1875	03/11/09	1340–1360.7	Groundwater	Anions, metals, TOC
R-46	GW46-09-1876	03/11/09	1340–1360.7	Groundwater	Anions, metals, TOC
<b>Additional Sampling for Organic Compounds</b>					
R-46	GW46-09-1842	1/22/09	1115	Groundwater	Tritium
R-46	GW46-09-1843	1/23/09	1134	Groundwater	Tritium
R-46	GW46-09-1844	1/23/09	1155	Groundwater	Tritium
R-46	GW46-09-1845	1/24/09	1175	Groundwater	Tritium
R-46	GW46-09-1846	1/24/09	1195	Groundwater	Tritium
R-46	GW46-09-2847	1/26/09	1220	Groundwater	VOCs, SVOCs
R-46	GW46-09-2848	1/26/09	1220	Groundwater	VOCs, SVOCs
R-46	GW46-09-2849	1/26/09	1210–1215	Solid-cuttings	VOCs
R-46	GW46-09-2850	1/26/09	1210–1215	Solid-cuttings	VOCs
R-46	GW46-09-2854	1/28/09	1216–1231	Solid-cuttings	VOCs, SVOCs
R-46	GW46-09-2855	1/28/09	1216–1231	Solid-cuttings	VOCs, SVOCs
R-46	GW46-09-2851	1/26/09	1210–1215	Groundwater	VOCs trip blank
R-46	GW46-09-2852	1/26/09	1220	Groundwater	VOCs trip blank
R-46	GW46-09-3249	2/04/09	1340	Groundwater	VOCs
R-46	GW46-09-3264	2/04/09	1340	Groundwater	Tritium
R-46	GW46-09-3265	2/04/09	1360	Groundwater	Tritium
R-46	GW46-09-3250	2/04/09	1360	Groundwater	VOCs
R-46	GW46-09-3251	2/05/09	1395	Groundwater	VOCs
R-46	GW46-09-3266	2/05/09	1395	Groundwater	Tritium
R-46	GW46-09-3252	2/05/09	1415	Groundwater	VOCs
R-46	GW46-09-3251	2/05/09	1395	Groundwater	VOCs

Note: Tritium, VOC, and SVOC samples were submitted for off-site analyses.

**Table 6.0-1  
R-46 Video and Geophysical Logging Runs**

Date	Depth (ft bgs)	Description
01/14/09	1064.7	Jet West Geophysical logged the cased and open-hole section with a video and combined natural gamma ray and induction tools. Little water was observed entering the borehole and several brecciated zones indicated in the long dacite volcanic interval.
01/25/09	1230	Schlumberger ran a suite of CN*-TLD, ECS-GR, and HNGS-GR in the 12-in. casing at intermediate depth.
01/29/09	1159.9–1217.7	Jet West Geophysical logged the lower portion of the borehole with video and combined natural gamma ray and induction tools while the 12-in. casing was retracted to 1217.7 ft bgs. Little water entering the borehole was noted.
01/29/09	1074.5–1217.7	Jet West Geophysical relogged the lower portion of the borehole with video and combined natural gamma ray and induction tools when the 12-in. casing was further retracted to 1074.5 ft bgs (see above). A water level of 1210.5 ft bgs was observed along with several clay stringers in the borehole wall.
02/06/09	Surf (for APS only)–1414	Schlumberger ran a suite of APS, TLD, ECS, and HNGS in the 12-in. casing at TD.

\*CN = Compensated Neutron Log.

**Table 7.2-1  
R-46 Annular Fill Materials**

Material	Volume
Surface seal: cement slurry	637.7 ft <sup>3</sup>
Upper seal: bentonite chips	1012.0 ft <sup>3</sup>
Upper fine sand collar: 20/40 silica sand	1.5 ft <sup>3</sup>
Filter pack: 10/20 silica sand	25.3 ft <sup>3</sup>
Lower fine sand collar: 20/40 silica sand	2.2 ft <sup>3</sup>
Lower seal: bentonite pellets	8.0 ft <sup>3</sup>
Backfill material: 10/20 silica sand	42.3 ft <sup>3</sup>
Potable water used in the regional aquifer (drilling and well construction)	66,406 gal.*

\*Volume comprises all water added to the borehole (including water used for bentonite and cement slurries and hydration of bentonite seal).

**Table 8.5-1  
R-46 Survey Coordinates**

North	East	Elevation (ft amsl)	Identification
1768183.02	1627433.85	7213.33	R-46 brass pin embedded in pad
1768184.36	1627435.16	7212.97	R-46 ground surface near pad
1768178.79	1627437.40	7217.05	R-46 top of 10-in. protective casing
1768178.26	1627437.39	7216.15	R-46 top of stainless-steel well casing

Note: All coordinates are expressed as New Mexico State Plane Coordinate System Central Zone (NAD 83); elevation is expressed in feet above mean sea level using the National Geodetic Vertical Datum of 1929.

**Table 8.6-1  
Summary of Waste Samples Collected during Drilling and Development of R-46**

Location ID	Sample ID	Date Collected	Description	Sample Type
R-46	RC46-09-3031	02/10/09	Decontamination water	liquid
R-46	RC46-09-3032	02/10/09	QA sample for RC46-09-3032	liquid
R-46	RC46-09-3033	02/10/09	Decontamination water, filtered	liquid
R-46	RC46-09-3034	02/10/09	Decontamination water	liquid
R-46	RC46-09-3035	2/25/09	Drilling pit fluid	liquid
R-46	RC46-09-3036	2/25/09	Drilling pit fluid	liquid
R-46	RC46-09-3037	2/25/09	Drilling pit fluid	liquid
R-46	RC46-09-3038	2/25/09	Drilling pit fluid	liquid
R-46	RC46-09-3039	2/25/09	Drilling pit cuttings	solid
R-46	RC46-09-3040	2/25/09	Drilling pit cuttings	solid
R-46	RC46-09-3455	3/17/09	Purge water	liquid
R-46	RC46-09-3456	3/17/09	Purge water	liquid
R-46	RC46-09-3457	3/17/09	Purge water	liquid
R-46	RC46-09-3458	3/17/09	Purge water	liquid





# **Appendix A**

---

## *Borehole R-46 Lithologic Log*

**Los Alamos National Laboratory  
Regional Hydrogeologic Characterization Project  
Borehole Lithologic Log**

<b>COREHOLD IDENTIFICATION (ID):</b> R-46		<b>Technical Area (TA):</b> 63	<b>PAGE:</b> 1 of 25
<b>DRILLING COMPANY:</b> Boart Longyear Company		<b>START DATE/TIME:</b> 12/13/08: 1215	<b>END DATE/TIME:</b> 02/05/09: 1235
<b>Drilling Method:</b> Dual Rotary		<b>MACHINE:</b> Foremost DR24 HD	<b>Sampling Method:</b> Grab
<b>Ground Elevation:</b>			<b>TOTAL DEPTH:</b> 1415 ft below ground surface (bgs)
<b>DRILLERS:</b> C. Johnson, J. Staloch		<b>SITE GEOLOGISTS:</b> C. Pigman, J.R. Lawrence	
Depth (ft bgs)	Lithology	Lithologic Symbol	Notes
0-8	<b>FILL AND DISTURBED SOIL:</b> Construction fill and tuffaceous sediments—pale pinkish brown (7.5YR 7/1) unconsolidated silty fine to coarse sand with minor pebble gravel; detrital grains/clasts of quartz and sanidine crystals, and volcanic lithics. Note: Presence of quartzite in upper few feet of the interval indicates material imported for drill pad construction.	Qal	Drill cuttings for microscopic and descriptive analysis were collected at 5-ft intervals from 0 ft to borehole total depth (TD) at 1415 ft bgs.  Quaternary alluvial sediments, from 0 to 8 ft bgs, are estimated to be 8 ft thick.  Qal-Qbt3 contact is placed at 8 ft bgs, as interpreted from cuttings and natural gamma log geophysical data.
8-20	<b>UNIT 3, TSHIREGE MEMBER OF THE BANDELIER TUFF:</b> Tuff—pinkish gray (5YR 7/1), weathered crystal tuff, moderately welded. 8-15 ft WR: abundant fine volcanic ash. +10F: small volume preserved; fragments of crystal tuff, free quartz and sanidine crystals. 15-20 ft: No cuttings returned; lost circulation.	Qbt 3	Unit 3, Tshirege Member of the Bandelier Tuff, encountered from 8 to 120 ft bgs, is estimated to be 112 ft thick.
20-35	Tuff—pale pinkish brown (5YR 6/3), moderately welded crystal tuff, lithic-bearing, weakly pumiceous. 20-35 ft WR: contains abundant reddish silty weathered volcanic ash. +10F: 90%–95% welded tuff fragments, phenocrysts (10%–20% by volume) of quartz and sanidine, minor pumice and lithics, matrix of fine ash; 5%–10% volcanic lithic fragments (up to 10 mm in diameter) composed of varieties of dacite, 2%–3% coarse quartz and sanidine crystals. +35F: 85%–90% quartz and sanidine crystals, 10%–15% fragments of welded tuff, 2%–3% volcanic lithics.	Qbt 3	

## Borehole Lithologic Log (continued)

Borehole ID: R-46		TA: 63	Page: 2 of 25
DEPTH (ft.bgs)	Lithology	Lithologic Symbol	Notes
35-50	Tuff—pale lavender gray (10R 6/1), moderately welded crystal tuff, lithic-bearing, weakly pumiceous. 35-50 ft +10F: 95%–97% welded tuff fragments, phenocrysts (10%–20% by volume) of quartz, sanidine, and minor ferromagnesian mineral, minor volcanic lithics, rare pumice (devitrified) and matrix of fine ash; 1%–2% coarse quartz and sanidine crystals; up to 1% dacite lithics. +35F: 75%–80% quartz and sanidine crystals, 15%–25% fragments of welded tuff, 1%–2% volcanic lithic fragments.	Qbt 3	
50-65	Tuff—white (5YR 8/1), moderately to poorly welded crystal tuff, crystal-rich, lithic-poor, pumice-poor. 50-55 ft +10F: 95% fragments of moderately to poorly welded crystal-rich tuff, phenocrysts (20%–30% by volume) of quartz and sanidine, friable matrix of fine ash; 5% coarse quartz and sanidine crystals. +35F: 98%–99% quartz and sanidine crystals, 1%–2% volcanic lithic fragments. 55-65 ft +10F: 30% welded tuff fragments, 60% coarse quartz and sanidine crystals, 10% volcanic lithics.	Qbt 3	
65-90	Tuff—pale lavender gray (10R 6/1), moderately to poorly welded crystal tuff, crystal-rich, lithic-bearing, pumice-poor. 65-75 ft +10F: 60%–70% welded tuff fragments, phenocrysts (20%–30% by volume) of quartz and sanidine, friable matrix of fine ash; 25%–30% volcanic lithic fragments including a variety of lithologies (gray porphyritic dacites, brown andesite, flow-banded rhyodacite); 5%–7% coarse quartz and sanidine crystals. +35F: more than 99% quartz and sanidine crystals, trace volcanic lithic fragments. 75-80 ft +10F: 30% welded tuff fragments (friable ash matrix appearing poorly welded), 70% coarse quartz and sanidine crystals. 80-90 ft +10F: similar to 65-70 ft.	Qbt 3	
90-100	Tuff—pale lavender gray (10R 6/1), moderately to poorly welded crystal tuff, crystal-rich, lithic-bearing, pumice-poor. 95-100 ft +10F: 15%–25% fragments of welded crystal tuff with friable matrix of fine ash; 20%–30% volcanic lithic, 50%–60% coarse quartz and sanidine crystals. +35F: more than 99% quartz and sanidine crystals, trace volcanic lithic fragments.	Qbt 3	

## Borehole Lithologic Log (continued)

Borehole ID: R-46		TA: 63	Page: 3 of 25
DEPTH (ft bgs)	Lithology	Lithologic Symbol	Notes
100-120	<p>Tuff—light brownish gray (10YR 7/1), moderately welded crystal-lithic tuff, pumice-poor.</p> <p>100-110 ft +10F: 20%–30% welded tuff fragments made up of phenocrysts (15%–20% by volume) of quartz and sanidine in a matrix of fine ash; 30%–40% coarse quartz and sanidine crystals; 20%–30% volcanic lithic fragments (hornblende-phyric dacite, andesite). +35F: 99% quartz and sanidine crystals, up to 1% volcanic lithic fragments.</p> <p>110-115 ft +10F: wide variety of volcanic lithic fragments (gray hbn-dacite, white cpx-dacite, brown andesite).</p> <p>115-120 ft +10F: predominantly fragments of welded tuff, trace volcanic lithics.</p>	Qbt 3	The Qbt 3–Qbt 2 contact is placed at 120 ft bgs, as interpreted from cuttings and natural gamma log geophysical data.
120-140	<p><b>UNIT 2, TSHIREGE MEMBER OF THE BANDELIER TUFF:</b></p> <p>Tuff—light lavender gray (10R 6/1), moderately to strongly welded crystal tuff, crystal-rich, lithic-poor, pumice-poor.</p> <p>120-140 ft +10F: 100% welded tuff fragments made up of phenocrysts (15%–20% by volume) of quartz and sanidine, trace pumices that are flattened/compressed, trace volcanic lithics; very fine welded ash matrix. +35F: 30%–40% welded tuff fragments, 60%–70% ash-coated quartz and sanidine crystals, trace volcanic lithic fragments.</p>	Qbt 2	Unit 2, Tshirege Member of the Bandelier Tuff, encountered from 120 to 210 ft bgs, is estimated to be 90 ft thick.
140-160	<p>Tuff—light lavender gray (10R 6/1), moderately to strongly welded tuff, crystal-rich, lithic-poor, pumice-poor.</p> <p>140-150 ft WR/+10F: 100% fragments of welded tuff, phenocrysts (15%–20% by volume) of quartz and sanidine, trace small pumices that are flattened/compressed; minor dacite lithics (up to 10 mm in diameter). +35F: 50%–60% welded tuff fragments, 40%–50% ash-coated quartz and sanidine crystals, trace volcanic lithic fragments.</p> <p>150-155 ft WR/+10F: similar to 140-145 ft, trace tan-colored clayey fine-grained volcaniclastic sandstone to claystone lithics(?).</p> <p>155-160 ft WR/+10F: similar to 140-145 ft.</p>	Qbt 2	

## Borehole Lithologic Log (continued)

Borehole ID: R-46		TA: 63	Page: 4 of 25
DEPTH (ft bgs)	Lithology	Lithologic Symbol	Notes
160–180	<p>Tuff—pale lavender gray (10R 6/1), moderately to strongly welded crystal tuff, crystal-rich, lithic-poor, pumice-poor.</p> <p>160–165 ft WR/+10F: 99%–100% fragments of welded tuff with phenocrysts (15%–20% by volume) of quartz and sanidine plus unidentified black ferromagnesian mineral, trace pumices that are moderately flattened/compressed and partly devitrified (i.e., recrystallized with fine sugary texture); trace dacite lithic fragments. +35F: 30%–40% welded tuff fragments, 60%–70% quartz and sanidine crystals, trace volcanic lithic fragments.</p> <p>160–165 ft WR/+10F: similar to 160–165 ft plus more abundant angular dacite lithics (up to 20 mm in diameter).</p> <p>160–165 ft WR/+10F: similar to 160–165 ft.</p>	Qbt 2	
180–200	<p>Tuff—pale lavender gray (10R 6/1), moderately to strongly welded crystal tuff (i.e., ignimbrite), crystal-rich, lithic-poor, pumice-poor.</p> <p>180–185 ft +10F: 100% fragments of welded tuff composed of phenocrysts (15%–25% by volume) of quartz and sanidine, pumices (10%–15% by volume and up to 15 mm in diameter) that appear flattened and display devitrified textures plus minor dactile lithics in a matrix of fine volcanic ash. +35F: 40%–50% quartz and sanidine crystals, 50%–60% welded tuff fragments and devitrified pumices.</p> <p>185–190 ft +10F: similar to 180–185 ft also more abundant lithic fragments (hbn-dacites).</p> <p>190–200 ft +10F: similar to 180–185 ft.</p>	Qbt 2	
200–210	<p>Tuff—pale pinkish gray (10R 7/1), moderately welded tuff, crystal-rich, lithic-poor, weakly pumiceous.</p> <p>200–210 ft +10F: 85%–90% indurated fragments of crystal-rich tuff with phenocrysts (20%–30% by volume) of quartz and sanidine, minor small devitrified pumices; rare volcanic lithics set in a matrix of granular (i.e., devitrified) volcanic ash; 10%–15% angular volcanic lithics (predominantly light gray porphyritic dacites). +35F: 60%–70% ash-coated quartz and sanidine crystals, 30%–40% welded tuff fragments and devitrified pumices; 3%–5% volcanic lithic fragments.</p>	Qbt 2	<p>The Qbt 2–Qbt 1v contact is placed at 210 ft bgs, as interpreted from cuttings and natural gamma log geophysical data.</p> <p>Likely top of Qbt 1v at approximately 200–205 ft, based on first appearance of poorly welded tuffs</p>

## Borehole Lithologic Log (continued)

Borehole ID: R-46		TA: 63	Page: 5 of 25
DEPTH (ft bgs)	Lithology	Lithologic Symbol	Notes
210-230	<p><b>UNIT 1V, TSHIREGE MEMBER OF THE BANDELIER TUFF:</b></p> <p>Tuff—light pinkish gray (10R 7/1), poorly welded, pumiceous, crystal-bearing, lithic-poor, presence of devitrified pumice.</p> <p>210-230 ft +10F: 80%–85% fragments of welded tuff with phenocrysts (10%–15% by volume) of quartz and sanidine, small pumices displaying granular (i.e., recrystallized/devitrified) textures, minor volcanic lithics set in a matrix of volcanic ash; 15%–20% angular volcanic lithic fragments (up to 20 mm in diameter), predominantly dacitic. +35F: 85%–90% ash-coated quartz and sanidine crystals, 10%–15% fragments of volcanic ash; trace volcanic lithics.</p>	Qbt 1v	Unit 1v, Tshirege Member of the Bandelier Tuff, encountered from 210 to 253 ft bgs, is estimated to be 43 ft thick.
230-253	<p>Tuff—varicolored pale tan (10R 8/1) to medium gray (GLE Y1 6/0), poorly welded, pumiceous, crystal-bearing, lithic-poor, presence of devitrified pumice.</p> <p>230-235 ft +10F: 80%–90% fragments of pumiceous welded tuff composed of phenocrysts (10%–15% by volume) of quartz and sanidine, small devitrified pumices (10%–20% by volume) and a matrix of fine volcanic ash; 10%–20% angular volcanic lithic fragments (light gray and white porphyritic dacites. +35F: 95%–98% ash-coated quartz and sanidine crystals, 2%–5% volcanic lithics.</p> <p>235-240 ft +10F: 65%–75% fragments of welded tuff with pinkish brown devitrified pumices (10%–20% by volume), phenocrysts (10%–15% by volume) of quartz and sanidine, minor volcanic lithics and a matrix of fine ash; 25%–35% dacitic lithic fragments.</p> <p>240-253 ft +10F: similar to 235-240 ft.</p>	Qbt 1v	The Qbt 1v–Qbt 1g contact is placed at 253 ft bgs, as interpreted from cuttings and natural gamma log geophysical data.

## Borehole Lithologic Log (continued)

Borehole ID: R-46		TA: 63	Page: 6 of 25
DEPTH (ft bgs)	Lithology	Lithologic Symbol	Notes
253-275	<p><b>UNIT 1g, TSHIREGE MEMBER OF THE BANDELIER TUFF:</b></p> <p>Tuff—very pale yellowish tan (10R 8/2) poorly welded ignimbrite tuff, pumiceous (generally glassy pumices), crystal-bearing, lithic-poor.</p> <p>253-265 ft WR/+10F: 50%–60% fragments of poorly welded tuff containing vitric pumice lapilli, phenocrysts (7%–10% by volume) of quartz and sanidine, conspicuous blebs of black obsidian and minor volcanic lithics in a matrix of pale tan volcanic ash; 30%–40% large (up to 30 mm in diameter) vitric quartz- and sanidine-phyric pumice lapilli; 5%–10% dacitic lithic fragments. +35F: 30%–40% fragments of tuff and glassy pumice; 60%–70% quartz and sanidine crystals commonly with fused dark gray glassy (i.e., obsidian) surfaces; 1%–2% volcanic lithics.</p> <p>265-275 ft +10F: compositionally similar to 253-265 ft. Note distinctive quartz and sanidine crystals enclosed in fibrous-textured vitric pumices that have dark gray glassy (i.e., obsidian) rinds, suggesting induced melting of pumiceous glass by hot phenocrysts.</p>	Qbt 1g	Unit 1g, Tshirege Member of the Bandelier Tuff, encountered from 253 to 290 ft bgs, is estimated to be 37 ft thick.
275-290	<p>Tuff—pale yellowish tan (10R 8/2) nonwelded tuff, pumiceous (with glassy pumices), crystal-bearing, lithic-poor.</p> <p>275-280 ft WR/+10F: 60%–70% vitric quartz- and sanidine-phyric pumices with blebs of dark gray glass surrounding some phenocrysts; 20%–30% volcanic lithics (hbn-dacites, vitrophyre). +35F: 40%–50% quartz and sanidine phenocrysts commonly with dark gray obsidian-fused surfaces; 30%–40% glassy pumices; 10%–15% volcanic lithic fragments.</p>	Qbt 1g	<p>Note disappearance of welded tuff fragments, suggesting diminishing degree of welding downward in this interval.</p> <p>The Qbt 1g–Qct contact is placed at 290 ft bgs, as interpreted from cuttings and natural gamma log geophysical data.</p>



## Borehole Lithologic Log (continued)

Borehole ID: R-46		TA: 63	Page: 7 of 25
DEPTH (ft bgs)	Lithology	Lithologic Symbol	Notes
290-305	<p><b>CERRO TOLEDO INTERVAL:</b> Tuffaceous sediments—pale tan (10R 8/2) to yellowish tan (10YR 7/8) poorly consolidated fine to medium gravels with coarse to fine sand and silty volcanic ash matrix; detritus of glassy pumice and mixed volcanic lithologies.</p> <p>290-295 ft WR: silty ash matrix. +10F: 60%–70% rounded vitric, quartz- and sanidine-phyric pumices; 30%–40% broken chips and subangular clasts (up to 20 mm in diameter) various volcanic lithologies (white and gray dacites, and andesite).</p> <p>295-300 ft WR: lacks silty ash matrix. +10F: similar composition to 290-295 ft.</p> <p>300-305 ft +10F: predominantly pumice clasts.</p>	Qct	<p>The Cerro Toledo interval, encountered from 290 to 475 ft bgs, is estimated to be 185 ft thick.</p> <p>Color change in this interval to yellow ochre, indicating weak Fe-oxide (limonite) alteration of pumices.</p>
305-335	<p>Tuffaceous sediments—white (10YR8/1) to pale tan (10R 8/3) weakly consolidated silty fine gravel with fine to coarse sand, fine ash to silty matrix; detritus predominantly of glassy pumice, minor volcanic lithologies.</p> <p>305-335 ft WR: silty ash matrix. +10F: 97%–99% fragments of subrounded glassy, quartz- and sanidine-phyric pumices; 3%–7% subangular dacitic lithics.</p>	Qct	
335-350	<p>Tuffaceous sediments—white (10YR8/1) to varicolored, unconsolidated coarse sand and pebble gravels, detritus predominantly pumice plus quartz and sanidine grains, minor dacite.</p> <p>335-335 ft+10F: 100% pumice fragments (up to 15 mm in diameter) that are white, quartz- and sanidine-phyric. +35F: 80%–85% quartz and sanidine crystals; 15%–20% white pumice fragments; &lt;1% grains of black obsidian.</p> <p>340-350 ft+10F: 90%–95% pumice fragments; 5%–10% subangular dacite clasts (up to 7 mm in diameter).</p>	Qct	
350-365	<p>Tuffaceous sediments—pale orange tan (10YR 7/6) unconsolidated pebble gravels and fine to coarse sand, detritus predominantly pumice and minor dacite.</p> <p>350-365 ft +10F: 97%–99% rounded to subrounded detrital granules (up to 10 mm in diameter) pale orange and white vitric pumices; 1%–3% detrital dacite clasts. +35F: 75%–80% pumice grains; 5%–10% grains of dacite and obsidian; 10%–15% quartz and sanidine crystals.</p>	Qct	

## Borehole Lithologic Log (continued)

Borehole ID: R-46		TA: 63	Page: 8 of 25
DEPTH (ft bgs)	Lithology	Lithologic Symbol	Notes
365-390	<p>Tuffaceous sediments—very pale orange tan (10YR 8/2) unconsolidated fine to medium gravels with fine to coarse sand, mixed pumice and volcanoclastic detritus.</p> <p>365-370 ft +10F: 20%-25% white vitric, quartz- and sanidine-phyric pumice clasts (up to 23 mm in diameter); 75%-80% broken and subangular volcanic clasts (up to 15 mm in diameter) composed of various volcanic lithologies (brown andesite, dacite, and flow-banded rhyodacite). +35F: 70%-80% pumice fragments; 10%-15% volcanoclastic grains; 10%-15% quartz and sanidine crystals.</p> <p>370-375 ft +10F: 40% pale yellowish pumices; 60% subangular clasts (up to 12 mm) of various volcanic lithologies (andesite, dacite).</p> <p>375-380 ft +10F: 95%-97% pinkish orange vitric pumice fragments; 3%-5% subangular volcanic (andesite, dacite) clasts.</p> <p>380-390 ft+10F: similar to 370-375 ft.</p>	Qct	
390-425	<p>Tuffaceous sediments—pale yellowish tan (10YR 8/3) unconsolidated silty fine gravels with fine to coarse sand, mixed pumice and volcanoclastic detritus.</p> <p>390-395 ft WR: matrix of silty volcanic ash. +10F: 70%-80% broken and subangular clasts of volcanic lithologies (andesite, dacite); 20%-30% pale orange vitric, quartz- and sanidine-phyric pumice fragments (up to 12 mm). +35F: 75%-80% quartz and sanidine crystal grains; 5%-10% pumice fragments; 10%-15% volcanic lithic grains.</p> <p>395-420 ft +10F: 50%-60% pale orange vitric pumices (up to 22 mm in diameter); 40%-50% subangular volcanic lithic clasts.</p> <p>420-425 ft +10F: 20%-30% pale orange to white glassy and weathered pumices; 70%-80% broken and subangular volcanic lithic clasts (up to 15 mm in diameter), including andesite, dacites and obsidian.</p>	Qct	

## Borehole Lithologic Log (continued)

Borehole ID: R-46		TA: 63	Page: 9 of 25
DEPTH (ft bgs)	Lithology	Lithologic Symbol	Notes
425-475	<p>Tuffaceous sediments—varicolored, pale orange (10YR 7/4) to medium brown (10YR 5/1) unconsolidated fine to medium gravels with fine to coarse sand, mixed pumice and volcanoclastic detritus.</p> <p>425-430 ft +10F: 80%–90% fragments of pale orange, mostly weathered, quartz- and sanidine-phyric pumices; 10%–20% subangular clasts of mixed volcanic lithologies (andesites, dacites). +35F: 60%–70% pumice fragments; 20%–25% quartz and sanidine crystal grains; 10%–15% volcanic lithic grains.</p> <p>430-440 ft +10F: 50%–60% broken and subangular clasts (up to 25 mm) of diverse volcanic rocks (biotite- and hornblende-dacites, fine-grained rhyolite?); 40%–50% pale orange pumices.</p>	Qct	The Qct-Qbo contact is placed at 475 ft bgs, as interpreted from cuttings and natural gamma log geophysical data.
475-490	<p><b>OTOWI ASH FLOW MEMBER OF THE BANDELIER TUFF:</b></p> <p>Tuff—medium gray (GLE Y1 7/0) to white (10YR 8/1) poorly welded, pumiceous, crystal-bearing, lithic-rich.</p> <p>475-490 ft +10F: 70%–80% broken chips and subangular lithic fragments composed of various volcanic lithologies (predominantly dacite); 20%–30% white glassy, quartz- and sanidine-phyric pumices. +35F: 30%–40% volcanic lithics, 30%–40% pumice fragments; 10%–20% quartz and sanidine crystals.</p>	Qbo	The Otowi Member of the Bandelier Tuff, encountered from 475 ft to 684 ft bgs, is estimated to be 209 ft thick.
490-510	<p>Tuff—varicolored, medium gray (GLE Y1 6/0) to very pale orange (10YR 8/1), poorly welded, lithic-rich, pumiceous, crystal-bearing.</p> <p>490-510 ft +10F: 90% broken (up to 25 mm in diameter) and subangular volcanic lithics (predominantly varieties of dacite); 10% white to pale orange glassy pumice.</p>	Qbo	
510-530	<p>Tuff—varicolored, white (10YR 8/1) to light gray (GLE Y1 7/0), poorly welded, lithic-rich, pumiceous, crystal-bearing.</p> <p>510-530 ft +10F: 40%–50% broken chips and subangular volcanic lithics (andesite, dacite); 50%–60% white glassy, quartz- and sanidine-phyric pumice fragments commonly with abundant small black Mn-, Fe-oxide spots. +35F: 40%–50% quartz and sanidine crystals; 20%–30% pumice fragments, 30%–40% volcanic lithic fragments.</p>	Qbo	

## Borehole Lithologic Log (continued)

Borehole ID: R-46		TA: 63	Page: 10 of 25
DEPTH (ft bgs)	Lithology	Lithologic Symbol	Notes
530-550	Tuff—varicolored, white (10YR 8/1) to medium gray (GLE Y1 6/0), poorly welded, lithic-rich, pumiceous, crystal-bearing. 530-550 ft +10F: 50%–60% angular volcanic lithics (up to 10 mm in diameter), including andesite and varieties of dacite; 40%–50% white glassy, quartz- and sanidine-phyric pumice lapilli/fragments (up to 15 mm in diameter) with locally abundant small black secondary Mn, Fe-oxide spots. +35F: 30% quartz and sanidine crystals; 30% pumice fragments, 40% volcanic lithic fragments.	Qbo	
550-555	Tuff—white (10YR 8/1) poorly welded, strongly pumiceous, lithic- and crystal-bearing. 550-555 ft +10F: 80%–95% white to very pale yellowish tan glassy, quartz- and sanidine-phyric pumice lapilli (up to 25 mm in diameter). 10% volcanic lithic fragments (andesite, hornblende-dacite).	Qbo	
555-570	Tuff—varicolored, white (10YR 8/1) to medium gray (GLE Y1 6/0), poorly welded, lithic-rich, pumiceous, crystal-bearing. 555-570 ft +10F: 60%–70% white glassy, quartz- and sanidine-phyric pumice fragments; 30%–40% volcanic lithics (up to 18 mm in diameter), including andesite and dacites; +35F: 15% quartz and sanidine crystals; 70% pumice fragments, 15% volcanic lithic fragments.	Qbo	
570-600	Tuff—varicolored, white (10YR 8/1) to medium gray (GLE Y1 6/0), poorly welded, lithic-rich, pumiceous, crystal-bearing. 555-570 ft WR/+10F: 70%–80% white glassy, porphyritic (quartz- and sanidine-phyric), fibrous-textured pumice lapilli/fragments (up to 16 mm in diameter); 20%–30% angular volcanic lithic fragments (up to 18 mm in diameter) composed of dacite, andesite and minor black porphyritic vitrophyre). +35F: 10% quartz and sanidine crystals; 75% pumice fragments, 15% volcanic lithic fragments.	Qbo	

## Borehole Lithologic Log (continued)

Borehole ID: R-46		TA: 63	Page: 11 of 25
DEPTH (ft bgs)	Lithology	Lithologic Symbol	Notes
600-610	<p>Tuff—varicolored, white (10YR 8/1) to grayish brown (10YR 5/1), poorly welded, lithic-bearing, pumiceous, crystal-poor.</p> <p>600-610 ft WR/+10F: 80%–85% white glassy; porphyritic (quartz- and sanidine-phyric) pumice lapilli/fragments (up to 25 mm), commonly with black spots of secondary black Mn-, Fe-oxides; 15%–20% angular volcanic lithic fragments (dacite, andesite). +35F: 5%–10% quartz and sanidine crystals; 75%–85% pumice fragments, 10%–15% volcanic lithic fragments.</p>	Qbo	
610-630	<p>Tuff—varicolored, white (10YR 8/1) and light gray (GLE Y1 7/0) poorly welded, lithic-rich, pumiceous, crystal-bearing.</p> <p>610-620 ft +10F: 70%–80% white vitric, porphyritic (quartz- and sanidine-phyric) pumices; 20%–30% volcanic lithics (dacite, minor flow-banded rhyodacite). +35F: 15%–20% quartz and sanidine crystals; 35%–45% pumice fragments, 30%–40% volcanic lithic fragments.</p> <p>620-625 ft+10F: similar to 610-615 ft. +35F: more abundant crystal interval (30%–35% quartz and sanidines).</p> <p>625-630 ft similar to 610-615 ft.</p>	Qbo	
630-665	<p>Tuff—varicolored, white (10YR 8/1) and light gray (GLE Y1 7/0) poorly welded, lithic-bearing, strongly pumiceous, crystal-bearing.</p> <p>630-645 ft WR/+10F: 97%–98% white to locally pale orange-tan vitric, fibrous-textured, quartz- and sanidine-phyric pumice lapilli/fragments; 2%–3% volcanic lithic fragments (dacites, minor rhyodacite, up to 10 mm in diameter). +35F: 5%–7% quartz and sanidine crystals; 80%–85% pumice fragments; 10%–15% volcanic lithic fragments.</p> <p>645-650 ft WR/+10F: similar in composition to 630-645 ft; lithic fragments (10%–20% by volume) of moderately welded tuff, minor black dacitic? vitrophyre.</p>	Qbo	

## Borehole Lithologic Log (continued)

Borehole ID: R-46		TA: 63	Page: 12 of 25
DEPTH (ft bgs)	Lithology	Lithologic Symbol	Notes
665-684	<p>Tuff—varicolored, white (10YR 8/1) and medium gray (GLE Y1 6/0) poorly welded, lithic-bearing, strongly pumiceous, crystal-bearing.</p> <p>665-675 ft +10F: 90%–98% white vitric, porphyritic (quartz- and sanidine-phyric) pumice lapilli/fragments, fibrous-textured; 2%–10% volcanic lithics (predominantly light gray dacites). +35F: 30%–40% quartz and sanidine crystals; 30%–35% pumice fragments; 20%–25% volcanic lithic fragments.</p> <p>675-684 ft +10F: 80%–85% white vitric pumices; 15%–20% volcanic lithics (fine-grained andesite, dacites).</p>	Qbo	The Qbo–Qbog contact is placed at 684 ft bgs, as interpreted from cuttings and natural gamma log geophysical data.
684-697	<p><b>GUAJE PUMICE BED:</b></p> <p>Tuff—varicolored, white (10YR 8/1) to medium brown (10YR 5/3), pumice-rich, lithic- and crystal-bearing, no apparent volcanic ash matrix.</p> <p>684-685 ft +10F: 90%–95% white vitric pumice lapilli/fragments, quartz- and sanidine-phyric; 5%–10% volcanic lithics (andesite, dacite). +35F: 75%–80% pumice fragments; 10%–15% quartz and sanidine crystals; 5%–10% volcanic lithic grains.</p> <p>685-690 ft +10F: 65%–75% white vitric pumice lapilli/fragments, quartz- and sanidine-phyric; 25%–35% volcanic lithics (andesite, dacite).</p> <p>690-697 ft +10F: similar to 685-690 ft +35F: 90% white vitric pumice fragments; 10% quartz and sanidine crystals; trace volcanic lithic grains.</p>	Qbog	<p>The Guaje Pumice Bed, from 684 to 697 ft bgs, is estimated to be 13 ft thick.</p> <p>The Qbog–dacite lava contact is placed at 697 ft bgs, as interpreted from cuttings and natural gamma log geophysical and video log data.</p>

## Borehole Lithologic Log (continued)

Borehole ID: R-46		TA: 63	Page: 13 of 25
DEPTH (ft bgs)	Lithology	Lithologic Symbol	Notes
697-705	<p><b>DACITE LAVAS:</b> Dacite lava-varicolored, dark gray (GLE Y1 3/0) to white (10YR 8/1) dark gray vesicular dacite</p> <p>697-700 ft WR/+10F: 90% large angular dark gray chips of vesicular to scoriaceous phenocryst-poor, dacite lava; 5%-10% fragments of light tan volcanoclastic siltstone; up to 5% white vitric pumice lapilli. +35F: 60% pumice fragments (probable mixed cuttings that include Banderliel Tuff); 40% dacite chips.</p> <p>700-705 ft WR/+10F: similar composition to 697-700 ft; dacitic lava becoming more massive (i.e., less vesicular) with depth. +35F: 85% dacitic lava; 15% pumice and siltstone.</p> <p>% white glassy phenocryst-poor pumice fragments that are locally Fe-oxide stained; 30-40% subangular dacite granules (up to 4 mm in diameter). 10-15% lapilli cinders of ferruginous scoria and black vitrophyric scoria</p>	Tt2	<p>The dacitic lava section, from 697 to 921 ft bgs, is estimated to be 243 ft thick.</p> <p>Highly vesicular dacite in 697-705-ft cuttings</p>
705-720	<p>Dacite lava-very dark gray (GLE Y1 3/0) massive (i.e., nonvesicular), phenocryst-poor, pyroxene-phyric, aphanitic groundmass.</p> <p>705-720 ft WR/+10F: 99% angular chips of dark gray massive dacite, phenocrysts (&lt;1% by volume) small (&lt;1 mm in diameter) black opaque clinopyroxene (cpx) and amber translucent orthopyroxene? (opx) that commonly occur in cumulophyric clusters; groundmass aphanitic, fresh; 1% fragments of pumice and siltstone.</p>	Tt2	
720-735	<p>Dacite lava-very dark gray (GLE Y1 3/0) to medium grey (GLE Y1 6/0) massive, phenocryst-poor with aphanitic groundmass, pyroxene-phyric.</p> <p>720-735 ft WR/+10F: 100% angular chips of gray massive dacite lava, phenocrysts (&lt;1% by volume) small (&lt;1 mm in diameter) black cpx and opx(?) that occur as cumulophyric intergrowths; groundmass fresh to weakly altered.</p>	Tt2	

## Borehole Lithologic Log (continued)

Borehole ID: R-46		TA: 63	Page: 14 of 25
DEPTH (ft bgs)	Lithology	Lithologic Symbol	Notes
735-755	<p>Dacite lava—light gray (GLE Y1 7/0) massive dacite, nonvesicular, phenocryst-poor, clinopyroxene-phyric, aphanitic groundmass.</p> <p>735-740 ft WR/+10F: 100% angular chips of massive dacite, phenocrysts (&lt;1% by volume) small (&lt;1 mm in diameter) black opaque, commonly euhedral cpx and greenish amber opx(?); groundmass fresh grading to weakly altered downward in the interval.</p> <p>740-755 ft WR/+10F: similar composition to 735-740 ft; weak, Mn-, Fe-oxide staining on fracture surfaces.</p>	Tt2	
755-780	<p>Dacite lava—light gray (GLE Y1 7/0) massive dacite, nonvesicular, phenocryst-poor, clinopyroxene-phyric, aphanitic groundmass; strongly fractured interval.</p> <p>755-770 ft WR/+10F: 100% angular chips, massive dacite lava, phenocrysts (&lt;1% by volume) of small (&lt;1 mm in diameter) black opaque cpx commonly intergrown in small clusters with greenish-amber translucent opx(?); weak Mn-, Fe-oxides and/or white clay on fracture surfaces.</p> <p>770-780 ft WR/+10F: compositionally similar to 755-760 ft; more abundant fractures with weak Mn-, Fe-oxide precipitation.</p>	Tt2	
780-800	<p>Dacite lava—light gray (GLE Y1 7/0) massive dacite, phenocryst-poor, clinopyroxene-phyric, aphanitic groundmass; moderately fractured interval.</p> <p>780-800 ft WR/+10F: 100% angular massive dacite chips, phenocrysts (&lt;1% by volume) of small black opaque commonly euhedral cpx that are intergrown in small clusters with greenish-amber translucent opx(?) and fine white plagioclase; weak Mn-, Fe-oxide precipitation on fracture/joint surfaces; groundmass weakly altered.</p>	Tt2	
800-840	<p>Dacite lava—light gray (GLE Y1 7/0) massive dacite, phenocryst-poor, cpx-phyric, aphanitic groundmass; moderately fractured interval.</p> <p>800-840 ft WR/+10F: 99%–100% angular massive dacite chips, phenocrysts (&lt;1% by volume) of small black euhedral cpx intergrown with green-amber opx(?) intergrown in small clusters with greenish amber translucent opx(?) and fine white plagioclase; minor white to pale orange calcite(?) chips; weak Mn-, Fe-oxide precipitation on fracture/joint surfaces; groundmass weakly altered.</p>	Tt2	



## Borehole Lithologic Log (continued)

Borehole ID: R-46		TA: 63	Page: 15 of 25
DEPTH (ft bgs)	Lithology	Lithologic Symbol	Notes
840–865	Dacite lava– light gray (GLE Y1 7/0) massive dacite, phenocryst-poor, cpx-phyric, aphanitic groundmass; moderately fractured interval. 840–865 ft WR/+10F: 100% angular dacite chips, phenocrysts (<1% by volume) of small black opaque cpx intergrown with green-amber opx(?) and fine white plagioclase; weak Mn-, Fe-oxide precipitation on some fracture/joint surfaces.	Tt2	
865–890	Dacite lava–light gray (GLE Y1 6/0) massive dacite, phenocryst-poor with aphanitic groundmass; moderately fractured interval. 865–890 ft WR/+10F: 100% angular dacite chips, phenocrysts (up to 1% by volume) of small black commonly euhedral cpx, green-amber opx(?) and white plagioclase that occur in cumulo-phyric clusters; groundmass appears fresh; weak bleaching/alteration on fracture surfaces.	Tt2	
890–910	Dacite lava– light gray (GLE Y1 6/0) massive dacite, phenocryst-poor with aphanitic groundmass; strongly fractured and/or jointed interval. 890–910 ft WR/+10F: 100% angular dacite chips, phenocrysts (up to 1% by volume) of small black commonly euhedral cpx and green-amber opx(?) that occur as cumulo-phyric clusters; groundmass appears fresh; weak pinkish Mn-, Fe-oxide occurring on numerous joints/fractures.	Tt2	
910–921	Dacite lava–light gray (GLE Y1 6/0) to pink (2.5YR 7/6) massive, phenocryst-poor with aphanitic groundmass, cpx-phyric, strongly fractured and/or jointed interval. 910–921 ft WR/+10F: 100% angular dacite lava chips, phenocrysts (up to 1% by volume) of small (up to 1 mm in diameter) black euhedral cpx and pale green-amber opx(?); groundmass appears fresh to weakly altered; numerous joints/fractures with weak pinkish tan alteration.	Tt2	The base of the dacite lava is placed at 921 ft bgs, based on cuttings and on borehole geophysical and video log data.

## Borehole Lithologic Log (continued)

Borehole ID: R-46		TA: 63	Page: 16 of 25
DEPTH (ft bgs)	Lithology	Lithologic Symbol	Notes
921-935	<p><b>DACITE SCORIA AND BRECCIA:</b> Dacite scoria and breccia—light gray (GLE Y1 7/0) and light red (2.5YR 7/6), mixed gray cpx-phyric dacite and ferruginous, strongly vesicular-altered dacite.</p> <p>921-935 ft WR/+10F: 40% angular phenocryst-poor, cpx-phyric dacite lava chips exhibiting Mn-, Fe-oxide alteration on frequent fractures; 60% reddish brown ferruginous dacite that is partly glassy, vesicular to scoriaceous; strong pale tan clay on fracture surfaces and clasts.</p>	Tt2	The dacitic scoria and breccia, from 921 to 955 ft bgs, is estimated to be 34 ft thick.
935-940	<p>Dacite scoria and breccia—varicolored, light gray (GLE Y1 6/0) and reddish brown (2.5YR 7/6), mixed gray massive and reddish glassy dacite chips.</p> <p>935-940 ft WR/+10F: angular chips composed of 20%–30% light gray cpx-phyric dacite; 20%–25% dark gray, weakly vesicular, vitric dacite; 50%–60% light red vesicular to scoriaceous glassy dacite fragments that are commonly coated with white to yellowish clay.</p> <p>940-945 ft +10F: similar to 935-940 ft, trace white hornblende-dacite with abundant acicular hbn phenocrysts.</p>	Tt2	
940-955	<p>Dacite scoria and breccia—varicolored, light gray (GLE Y1 6/0), white (5YR 8/1) and light red (2.5YR 7/6), mixed massive, vitric and scoriaceous dacite chips.</p> <p>940-955 ft WR/+10F: 10%–20% light gray massive cpx-phyric dacite chips; 10%–20% dark gray porphyritic vitrophyre; 60%–80% light red-brown glassy, vesicular to scoriaceous, cpx-dacite commonly coated with white clay.</p>	Tt2	
955-960	<p><b>PUYE FORMATION:</b> Volcaniclastic sediments —varicolored, light gray (GLE Y1 6/0), pale tan (5YR 6/4), mixed angular dacite chips (lava) and detrital dacite clasts.</p> <p>955-965 ft WR/+10F: 50%–60% angular gray, glassy, scoriaceous and massive cpx-dacite chips; 40%–50% subrounded detrital clasts (up to 12 mm) white-cpx- and hbn-phyric dacites; all chips clay coated.</p> <p>965-970 ft WR/+10F: clasts composed of various gray dacites, red to black ferruginous vitrophyre, fragments of indurated silt, fine-grained sandstone, fragments of light tan clay.</p>	Tpf	<p>The contact between dacite scoria and breccia and underlying Puye Formation is placed at 955 ft bgs, at the first appearance of subrounded detrital clasts,</p> <p>The Puye Formation, from 955 to 1405 ft bgs, is estimated to be 450 ft thick.</p>

## Borehole Lithologic Log (continued)

Borehole ID: R-46		TA: 63	Page: 17 of 25	
DEPTH (ft bgs)	Lithology	Lithologic Symbol	Notes	
960–985	<p>Volcaniclastic sediments– varicolored, light gray (GLE Y1 7/0), reddish brown (2.5YR 7/6) and white (5YR 8/1), silty fine to medium gravel and fine- to coarse-grained sandstone; mixed angular dacite chips (lava) and detrital dacite clasts.</p> <p>970–985 ft WR/+10F: broken and subrounded clasts (up to 20 mm in diameter) composed of various gray dacites, red to black ferruginous vitrophyre, fragments of indurated silty fine-grained sandstone, fragments of light tan clay.</p>	Tpf		
985–1000	<p>Volcaniclastic sediments–varicolored, medium gray (GLE Y1 6/0) to white (5YR 8/1), pebble-size and coarser gravels with fine- to coarse-grained sandstone; detrital clasts, predominantly of dacite.</p> <p>985–1000 ft WR/+10F: broken chips and subangular to subrounded clasts (up to 10 mm in diameter) of various volcanic lithologies: abundant gray cpx- and hbn-phyric dacites that commonly have a glassy matrix, white dacite with acicular hornblende phenocrysts, dark gray porphyritic vitrophyre; local trace abundances of light pinkish tan clay.</p>	Tpf		
1000–1020	<p>Volcaniclastic sediments–varicolored, light gray (GLE Y1 7/0) to pink (2.5YR 7/6), pebble-size and coarser gravels with fine- to coarse-grained sandstone; clayey matrix, detritus predominantly dacitic.</p> <p>1000–1010 ft WR/+10F: broken chips and subangular clasts (up to 10 mm in diameter) mostly gray to pink cpx-dacite, minor white biotite-dacite; some clasts clay coated. +35F: minor pale tan clay shards.</p> <p>1010–1020 ft +10F: coarser gravels present; broken chips and subangular clasts (up to 15 mm in diameter) predominantly cpx-dacite, minor biotite-dacite; local fragments of fine-grained silty sandstone.</p>	Tpf		

## Borehole Lithologic Log (continued)

Borehole ID: R-46		TA: 63	Page: 18 of 25	
DEPTH (ft bgs)	Lithology	Lithologic Symbol	Notes	
1020–1045	<p>Volcaniclastic sediments—varicolored, light gray (GLE Y1 7/0) coarse gravels with fine- to coarse-grained sandstone; detritus predominantly dacitic.</p> <p>1020–1025 ft WR/+10F: broken chips (up to 25 mm in diameter) and subangular to subrounded clasts of light to medium gray cpx-dacites, minor white biotite-rhyodacite.</p> <p>1025–1030 ft WR/+10F: clasts composed of gray and orange brown cpx- and hbn-dacites, minor coarsely porphyritic black vitrophyre.</p> <p>1030–1040 ft WR/+10F: broken and subrounded clasts (up to 10 mm in diameter) composed of gray and reddish brown cpx-dacite and lesser hbn-dacite.</p> <p>1040–1045 ft WR/+10F: compositionally similar to 1030–1040 ft; also fragments of indurated fine-grained sandstone.</p>	Tpf		
1045–1060	<p>Volcaniclastic sediments—light gray (GLE Y1 7/0) to varicolored, fine gravels with fine- to coarse-grained sandstone; detritus predominantly gray porphyritic dacitic.</p> <p>1045–1050 ft WR/+10F: broken chips and subrounded pebble clasts (up to 10 mm in diameter) composed mostly of gray and reddish cpx-dacites, minor white hbn-dacites.</p> <p>1050–1060 ft WR/+10F: subrounded clasts (up to 25 mm in diameter) composed predominantly of gray cpx-dacite, lesser dark gray coarsely porphyritic andesite.</p>	Tpf		
1060–1065	<p>Volcaniclastic sediments—light gray (GLE Y1 7/0) to varicolored, coarse to medium gravels with fine- to coarse-grained sandstone with silt; detritus predominantly gray porphyritic dacitic.</p> <p>1060–1065 ft WR/+10F: abundant large broken chips (up to 30 mm in diameter) and subrounded clay/silt-coated clasts of diverse volcanic lithologies: gray cpx-dacites, black to reddish (altered) coarsely porphyritic vitrophyre, pale pink biotite-phyric dacite/rhyodacite.</p>	Tpf		
1065–1075	<p>Volcaniclastic sediments—light gray (GLE Y1 7/0) to varicolored, fine gravels with fine to coarse sand; detritus predominantly dacitic.</p> <p>1065–1075 ft WR/+10F: broken chips subrounded clasts mainly of gray cpx-dacite, black porphyritic vitrophyre, pale pink quartz-phyric rhyodacite.</p>	Tpf		

## Borehole Lithologic Log (continued)

Borehole ID: R-46		TA: 63	Page: 19 of 25
DEPTH (ft. bgs)	Lithology	Lithologic Symbol	Notes
1075–1090	<p>Volcaniclastic sediments— light gray (GLE Y1 7/0) fine to coarse silty gravels with fine to coarse sand; clasts and detrital grains predominantly porphyritic dacites.</p> <p>1075–1085 ft WR/+10F: subangular to subrounded pebbles and large broken chips (up to 25 mm in diameter) composed of gray cpx- and hbn-dacite with abundant fine acicular hornblendes; clasts commonly with rinds of fine-grained silty sandstone.</p> <p>1085–1090 ft WR/+10F: compositionally similar to 1075–1085 ft also presents silty fine-grained sandstone matrix rinds on many clasts and fragments of indurated silty sandstone.</p>	Tpf	
1090–1105	<p>Volcaniclastic sediments—light gray (GLE Y1 7/0) fine (i.e., pebble) gravels with fine- to coarse-grained sandstone; detritus composed predominantly of various dacites.</p> <p>1090–1095 ft WR/+10F: abundant subrounded pebble clasts composed of light gray and pink cpx-dacites, minor black porphyritic vitrophyre.</p> <p>1095–1100 ft WR/+10F: similar to 1090–1095 ft; coarser clasts present, commonly with silty rinds.</p> <p>1100–1005 ft WR/+10F: clasts predominantly of cpx- and hbn-phyric dacites; note also abundant fragments of indurated silty very fine-grained sandstone.</p>	Tpf	
1105–1115	<p>Volcaniclastic sediments—light brown (2.5YR 6/2) silty to fine- to coarse-grained sandstone with fine gravel, predominantly dacitic detritus.</p> <p>1105–1115 ft WR: abundant silt matrix. +10F: broken chips and subangular small pebbles (up to 8 mm in diameter) of light gray dacite, lesser black to reddish; fragments of indurated silty very fine-grained sandstone.</p>	Tpf	
1115–1125	<p>Volcaniclastic sediments— pale yellowish brown (10YR 8/4) to light gray (GLE Y1 7/0) fine gravel with coarse- to fine-grained sandstone, predominantly dacitic detritus.</p> <p>1115–1125 ft WR: abundant silt in matrix. +10F: broken chips and subangular clasts composed of light gray and pink, hbn- and biotite-phyric dacites; clasts coated with yellowish tan silt.</p>	Tpf	

## Borehole Lithologic Log (continued)

Borehole ID: R-46		TA: 63	Page: 20 of 25
DEPTH (ft bgs)	Lithology	Lithologic Symbol	Notes
1125–1140	<p>Volcaniclastic sediments— varicolored, pale yellowish tan (10YR 8/4) to light gray (GLE Y1 7/0) silty fine gravel with coarse- to fine-grained sandstone, predominantly dacitic detritus.</p> <p>1125–1130 ft WR/+10F: silt-coated subangular to subrounded granules and small pebbles (up to 8 mm in diameter) made up of light gray, pink and white, hbn- and biotite-phyric dacites; minor black porphyritic vitrophyre.</p> <p>1130–1135 ft WR: abundant silt-coated granules. +10F: compositionally similar to 1130–1135 ft; also present small percentage of large (up to 23 mm), distinctively well-rounded dacite pebbles.</p> <p>1135–1140 ft WR: abundant yellowish silt matrix. +10F: similar to 1125–1130 ft.</p>	Tpf	
1140–1165	<p>Volcaniclastic sediments—light gray (GLE Y1 7/0) silty fine, medium and locally coarse gravels with coarse- to fine-grained sandstone, detrital clasts predominantly dacitic.</p> <p>1140–1145 ft WR/ +10F: broken chips (up to 30 mm in diameter) and subangular clasts made up of light gray, pink and white, hbn- and bt-phyric dacites.</p> <p>1145–1150 ft +10F: subangular to subrounded dacitic pebbles and granules (up to 10 mm in diameter).</p> <p>1150–1165 ft +10F: silt-coated clasts; matrix becoming more silt-rich downward in this interval.</p>	Tpf	
1165–1185	<p>Volcaniclastic sediments—pale yellowish tan (10YR 8/4) to light gray (GLE Y1 7/0) fine, medium and coarse gravels with fine- to coarse-grained sandstone, detritus predominantly dacitic.</p> <p>1165–1175 ft WR/ +10F: broken chips (up to 25 mm in diameter) and subangular pebble-size clasts compose of light gray, pink and white, hbn- and bt-phyric dacites; trace black porphyritic vitrophyre.</p> <p>1175–1185 ft WR/ +10F: compositionally similar to 1165–1170; clasts coated with yellowish silt.</p>	Tpf	
1185–1195	<p>Volcaniclastic sediments—pale yellowish tan (10YR 8/4) to light gray (GLE Y1 7/0) silty coarse to fine gravels with medium- to coarse-grained sandstone, detritus predominantly dacitic.</p> <p>1185–1195 ft WR/ +10F: broken chips (up to 20 mm in diameter) and subangular clasts of light gray, pink and white dacites; minor porphyritic vitrophyre; clasts coated with light yellowish tan silt.</p>	Tpf	

## Borehole Lithologic Log (continued)

Borehole ID: R-46		TA: 63	Page: 21 of 25	
DEPTH (ft bgs)	Lithology	Lithologic Symbol	Notes	
1195–1235	<p>Volcaniclastic sediments—pale yellowish tan (10YR 8/4) to light gray (GLE Y1 7/0) fine gravel with fine- to coarse-grained sandstone and silt, detritus predominantly dacitic.</p> <p>1195–1215 ft WR/ +10F: broken chips and subangular granules to small pebbles composed of white, light gray and pink, bt- and hbn-phyric dacites; minor black phenocryst-rich vitrophyre; fragments of indurated silty very fine-grained sandstone; detrital clasts typically coated with yellowish tan silt.</p> <p>1195–1235 ft No cuttings available; lost circulation.</p>	Tpf		
1235–1255	<p>Volcaniclastic sediments—reddish brown (5YR 6/6) silty fine gravel and coarse- to medium-grained sandstone; detritus of dacite and pumice.</p> <p>1235–1250 ft WR/ +10F: clasts strongly coated with reddish silt (fines estimate 10%–15% by volume); angular to subangular clasts (up to 18 mm in diameter) composed of gray bt- and hbn-phyric dacites; and (up to 10% by volume) glassy white pumice fragments.</p> <p>1250–1255 ft WR: similar to 1235–1240 ft. +10F: clasts predominantly pinkish gray dacites; trace pumice.</p>	Tpf		
1255–1280	<p>Volcaniclastic sediments—pale yellowish brown (10YR 8/3) silty fine gravel and coarse- to fine-grained sandstone; detritus predominantly dacite and minor pumice.</p> <p>1255–1270 ft WR: very silty matrix (fines estimated 20%–25% by volume) +10F: subangular to rarely well-rounded granules and pebbles composed of white, gray and pink bt- and hbn-phyric dacites, black vitrophyre trace glassy white pumice fragments.</p> <p>1270–1280 ft WR: moderately abundant silt matrix (fines estimated 15%–20% by volume). +10F: compositionally similar to 1255–1260 ft.</p>	Tpf		

## Borehole Lithologic Log (continued)

Borehole ID: R-46		TA: 63	Page: 22 of 25
DEPTH (ft bgs)	Lithology	Lithologic Symbol	Notes
1280–1295	<p>Volcaniclastic sediments—light pinkish gray (5YR 7/2) medium to fine gravel with silt and sand to silty medium to fine gravels with sand; detritus predominantly dacite.</p> <p>1280–1290 ft WR: moderately abundant silt matrix (fines estimated 15%–20% by volume) +10F: broken and subangular volcanic detrital clasts (up to 15 mm in diameter) including pink, white, and light gray bt- and hbn-phyric dacites, dark gray phenocryst-rich vitrophyre.</p> <p>1290–1295 ft WR: very silty matrix (fines 20%–25% by volume). +10F: compositionally similar to 1280–1285 ft.</p>	Tpf	
1295–1300	<p>Volcaniclastic sediments—light pinkish gray (5YR 7/2) fine gravel with fine to coarse sand and silt; detritus predominantly dacite.</p> <p>1280–1290 ft+10F: subangular granules and small pebbles (up to 15 mm in diameter) composed of light and dark gray dacites, white cpx-dacite(?) and black porphyritic vitrophyre. +35F: abundant white glassy pumice fragments.</p>	Tpf	
1300–1320	<p>Volcaniclastic sediments—pale yellowish brown (10YR 8/2) medium to fine gravel with fine to coarse sand and silt; detritus predominantly dacite.</p> <p>1300–1315 ft WR: silt-coated clasts (fines estimated 10%–15% by volume) +10F: subangular granules and small pebbles (up to 17 mm in diameter) predominantly light gray to pinkish bt- and hbn-phyric dacites, moderately abundances of glassy pumice.</p> <p>1315–1320 ft WR: more abundant silt matrix (fines 15%–20% by volume). +10F: subangular clasts (up to 22 mm in diameter) made up of varieties of dacite, black porphyritic and amber brown vitrophyres, white glassy pumices.</p>	Tpf	



## Borehole Lithologic Log (continued)

Borehole ID: R-46		TA: 63	Page: 23 of 25
DEPTH (ft bgs)	Lithology	Lithologic Symbol	Notes
1320–1340	<p>Volcaniclastic sediments—pale yellowish brown (10YR 8/2) coarse sand with fine gravel and silt; detritus predominantly dacite, some local pumice.</p> <p>1320–1330 ft WR: moderately silty matrix (fines 10%–15% by volume). +10F: subangular granules made up of light gray bt- and hbn-phyric dacites, black porphyritic vitrophyre, white glassy granular pumices.</p> <p>1330–1335 ft WR: somewhat coarser sediments; medium to fine gravels with silt.</p> <p>1335–1340 ft WR: coarse sand with fine gravel and less silt (fines estimated 5%–10% by volume).</p>	Tpf	
1340–1375	<p>Volcaniclastic sediments—pale yellowish tan (10YR 8/3) silty medium to fine gravel and fine to coarse sand; detritus predominantly dacite, some local pumice.</p> <p>1340–1350 ft WR: abundant silt matrix (fines estimated 15%–20% by volume) +10F: broken to subangular clasts (up to 20 mm in diameter) composed predominantly of light gray bt- and hbn-phyric dacites, minor black porphyritic vitrophyre, minor glassy white pumices.</p> <p>1350–1375 ft WR/+10F: silty fine gravels with sand; silt-coated subangular granules and small pebbles; compositionally similar to 1340–1345 ft.</p>	Tpf	
1375–1395	<p>Volcaniclastic sediments—pale yellowish tan (10YR 8/3) silty medium to fine gravel and fine to coarse sand; detritus predominantly dacite, some local pumice.</p> <p>1375–1380 ft WR: clasts strongly coated with silt (fines estimated 10%–15% by volume) +10F: subangular to locally very well-rounded granules and pebbles clasts (up to 20 mm in diameter) composed entirely of light gray bt- and/or hbn-phyric dacites.</p> <p>1380–1395 ft WR: similar to 1375–1380 ft. +10F: subangular to subrounded granules and pebbles (up to 14 mm in diameter) composed exclusively of light gray and white bt- and/or hbn-dacites.</p>	Tpf	

## Borehole Lithologic Log (continued)

Borehole ID: R-46		TA: 63	Page: 24 of 25
DEPTH (ft bgs)	Lithology	Lithologic Symbol	Notes
1395–1405	<p>Volcaniclastic sediments—pale yellowish brown (10YR 8/3) to light gray (GLE Y1 7/0) fine to medium gravel and fine to coarse sand; detritus predominantly dacite.</p> <p>1395–14054 ft WR/10F: angular to subangular granules and pebbles (up to 15 mm in diameter) composed of light gray bt- and /or hbn-phyric dacites, white dacite with abundant fine acicular hornblende phenocrysts, minor black fine-grained vitrophyre.</p>	Tpf	The contact between Puye volcaniclastic sediments and underlying Miocene pumiceous sediments is placed at 1405 ft bgs, as interpreted from cuttings, as well as from natural gamma log geophysical and video log data.
1405–1415	<p><b>MIOCENE PUMICEOUS SEDIMENTS:</b></p> <p>Pumiceous volcaniclastic sediments—varicolored, light gray (GLE Y1 7/0) to white (10YR 8/1) coarse sand with fine gravel; detritus composed of mixed dacite and pumices.</p> <p>1405–1410 ft WR/+10F: angular to subangular granules and small pebbles (up to 10 mm in diameter) composed predominantly of gray, white and reddish dacites (bt- and or hbn-phyric) and lesser (up to 10%–15% by volume) white glassy pumices that are weakly bt-phyric.</p> <p>1410–1415 ft WR/+10F: compositionally similar to 1401–1410 ft, more abundant pumices (20%–25% by volume).</p>	N/S	Miocene pumiceous deposits were encountered from 1405 to the borehole TD at 1415 ft bgs.

ABBREVIATIONS

5YR 8/1 = Munsell soil color notation where hue (e.g., 5YR), value (e.g., 8), and chroma (e.g., 1) are expressed. Hue indicates soil color's relation to red, yellow, green, blue, and purple. Value indicates soil color's lightness. Chroma indicates soil color's strength.

% = Estimated percent by volume of a given sample constituent.

bt = Biotite.

cpx = Clinopyroxene

GM = Groundmass.

hbn = Hornblende

ol = Olivine.

Qal = Quaternary alluvium.

Qct = Cerro Toledo interval.

Qbo = Otowi Member of Bandelier Tuff.

Qbog = Guaje Pumice Bed.

Tb4 = Cerros del Rio basalt.

Tpf = Puye Formation.

N/S = No assigned symbol for geologic unit.

Y = Yellow.

YR = Yellow red.

+10F = Plus No.10 sieve sample fraction.

+35F = plus No. 35 sieve sample fraction.



## **Appendix B**

---

### *Groundwater and Sediment Analytical Results*

## B-1.0 SAMPLING AND ANALYSIS OF GROUNDWATER AT R-46

A total of 22 groundwater-screening samples were collected from R-46 as part of the facility-wide groundwater-monitoring program at Los Alamos National Laboratory (the Laboratory). These screening samples were analyzed for inorganic and organic chemicals. Eight groundwater samples were collected from the vadose zone during drilling at depths ranging from 1115 to 1230 ft below ground surface (bgs), generally at 20-ft-depth intervals. These samples primarily consist of municipal water and AQF-2 foam used during drilling, and they do not contain a significant component of vadose zone groundwater (see discussion in section 3.2). Four groundwater-screening samples were collected at borehole R-46 during drilling within the regional aquifer from 1340 to 1415 ft bgs (Puye Formation). Four groundwater-screening samples were from the screen interval of 1340.0 to 1360.7 ft bgs during well development. The filtered samples were analyzed for cations, anions, and metals. A total of 9498 gal. of groundwater was pumped from well R-46 during well development. Six groundwater-screening samples were collected from the screen interval of 1340.0 to 1360.7 ft bgs during aquifer testing. The nonfiltered samples were analyzed for cations, anions, metals, and total organic carbon (TOC). Approximately 12,168 gal. of groundwater was pumped from well R-46 during aquifer performance testing.

An additional 10 groundwater-screening samples were collected from depths ranging from 1220 to 1415 ft bgs to evaluate the potential presence of organic contamination, as a result of slight organic odors detected during drilling. The nonfiltered samples were analyzed for volatile organic compounds (VOCs), semivolatile organic compounds (SVOCs), and/or tritium. Two sediment samples were also collected from depths of 1210 to 1215 ft bgs and analyzed for VOCs. Analytical results for these samples will be reported in detail in the Material Disposal Area C investigation report.

### B-1.1 Field Preparation and Analytical Techniques

Chemical analyses of groundwater-screening samples were performed at the Laboratory's Earth and Environmental Sciences Group (EES-14). Groundwater samples were filtered (0.45- $\mu$ m membranes) before preservation and chemical analyses. Samples were acidified at the EES-14 wet chemistry laboratory with analytical grade nitric acid to a pH of 2.0 or less for metal and major cation analyses.

Groundwater samples were analyzed using techniques specified in the U.S. Environmental Protection Agency SW-846 manual. Ion chromatography was the analytical method for bromide, chloride, fluoride, nitrate, nitrite, oxalate, perchlorate, phosphate, and sulfate. Analytical results for perchlorate are pending, with anticipated instrument detection limits ranging from 0.002 to 0.005 ppm for this oxyanion. Inductively coupled (argon) plasma optical emission spectroscopy (ICPOES) was used for analyses of dissolved aluminum, barium, boron, calcium, total chromium, iron, lithium, magnesium, manganese, potassium, silica, sodium, strontium, titanium, and zinc. Dissolved aluminum, antimony, arsenic, barium, beryllium, boron, cadmium, cesium, chromium, cobalt, copper, iron, lead, lithium, manganese, mercury, molybdenum, nickel, rubidium, selenium, silver, thallium, thorium, tin, vanadium, uranium, and zinc were analyzed by inductively coupled (argon) plasma mass spectrometry (ICPMS). The precision limits (analytical error) for major ions and trace elements were generally less than  $\pm 7\%$  using ICPOES and ICPMS. Concentrations of TOC in nonfiltered groundwater samples collected during well development were determined by using an organic carbon analyzer. Charge balance errors for total cations and anions were generally less than  $\pm 8\%$  for complete analyses of the above inorganic chemicals. The negative cation-anion charge balance values indicate excess anions for the filtered samples. Total carbonate alkalinity was measured using standard titration techniques.

### B-1.2 Field Parameters

Results of field parameters, consisting of pH, temperature, dissolved oxygen (DO), specific conductance, and turbidity measured during well development, are provided in Table B-1.2-1. Measurements of pH and temperature varied from 8.0 to 8.07 and from 11.16°C to 18.54°C, respectively, at well R-46. Several of the low temperature measurements for groundwater samples were probably influenced by land surface-atmosphere conditions during sampling. Concentrations of DO varied from 10.99 to 12.30 mg/L. The maximum concentrations of DO are calculated at 8.87 and 7.29 mg/L at 11°C and 20°C, respectively, at 6000 ft, based on solubility calculations. Oxidation-reduction potential (ORP) was not recorded at R-46 during well development because a groundwater flow-through cell was not used during sampling. Specific conductance ranged from 130 to 135 microsiemens per centimeter ( $\mu\text{S}/\text{cm}$ ). Values of turbidity measured at R-46 ranged from 4.5 to 5.2 nephelometric turbidity units (NTUs) for the nonfiltered groundwater samples. Two of the 10 turbidity measurements recorded during well development exceeded 5 NTUs (Table B-1.2-1).

Field parameters were measured during aquifer performance testing at well R-46 (Table B-1.2-1) by collecting aliquots from the discharge port of the submersible development pump, allowing the samples to be exposed to the atmosphere. This condition probably resulted in a slight variation of field parameters during well development, most notably, temperature, pH, ORP, and DO. Measurements of pH and temperature varied from 7.94 to 8.29 and from 17.13°C to 23.31°C, respectively, at well R-46. Concentrations of DO varied from 5.62 to 9.59 mg/L. ORP ranged from 27.7 to 76.7 millivolt (mV). Specific conductance ranged from 104 to 124  $\mu\text{S}/\text{cm}$ . Values of turbidity measured at well R-46 ranged from 3.6 to 11.6 NTUs for the nonfiltered groundwater samples. Seventeen of the 20 turbidity measurements recorded during the aquifer performance testing exceeded 5 NTUs (Table B-1.2-1).

### B-1.3 Analytical Results for Groundwater- and Sediment-Screening Samples

Analytical results for groundwater-screening samples collected at well R-46 during drilling and aquifer performance testing are provided in Table B-1.3-1. Calcium and sodium are the dominant cations in groundwater pumped from well R-46. During well development, dissolved concentrations of calcium and sodium ranged from 10.26 to 11.17 ppm (10.26 to 11.17 mg/L) and from 9.10 to 10.98 ppm, respectively. Dissolved concentrations of chloride and fluoride slightly varied from 2.48 to 2.92 ppm and from 0.15 to 0.17 ppm, respectively, during development of well R-46. Dissolved concentrations of nitrate(N) and sulfate ranged from 0.40 to 0.51 ppm and from 2.56 to 3.08 ppm, respectively, at the well. Dissolved concentrations of chloride, nitrate(N), and sulfate at well R-46 do not exceed Laboratory background within the regional aquifer (LANL 2007, 095817). Maximum background concentrations for dissolved chloride, nitrate plus nitrite(N), and sulfate in the regional aquifer are 5.95 mg/L, 1.05 mg/L, and 8.63 mg/L, respectively (LANL 2007, 095817). Concentrations of TOC ranged from 0.29 to 0.47 mgC/L at well R-46 (Table B-1.3-1). During well development, detectable concentrations of dissolved phosphate ranged from 0.08 to 0.75 ppm (as phosphorus, 0.03 to 0.25 ppm). The median, mean, and maximum background concentrations for dissolved phosphorus are 0.02 mg/L, 0.04 mg/L, and 0.34 mg/L, respectively (LANL 2007, 095817).

During development, dissolved concentrations of iron and manganese ranged from 0.037 to 0.318 ppm (37 to 318  $\mu\text{g}/\text{L}$  or 37 to 318 ppb) and from 0.007 to 0.012 ppm, respectively, in groundwater-screening samples collected at well R-46 (Table B-1.3-1). Dissolved concentrations of iron exceed the maximum background value of 0.147 mg/L in the regional aquifer (LANL 2007, 095817). A corroded carbon-steel discharge pipe was used during development at well R-46, resulting in elevated above-background concentrations of dissolved iron during sampling. Dissolved concentrations of manganese are less than the maximum background value 0.124 mg/L (LANL 2007, 095817). Dissolved concentrations of boron ranged from 0.013 to 0.034 ppm (Table B-1.3-1) at well R-46, which is below the maximum background

value of 51.6 µg/L for the regional aquifer. Dissolved concentrations of zinc ranged from 0.004 to 0.031 ppm in groundwater-screening samples collected at R-46 (Table B-1.3-1). Background mean, median, and maximum concentrations of zinc in filtered samples are 3.08 µg/L, 1.45 µg/L, and 32.0 µg/L, respectively, for the regional aquifer (LANL 2007, 095817). Total dissolved concentrations of chromium ranged from 0.005 to 0.007 ppm at well R-46 (Table B-1.3-1), analyzed by ICPMS. Background mean, median, and maximum concentrations of total dissolved chromium are 3.07 µg/L, 3.05 µg/L, and 7.20 µg/L, respectively, for the regional aquifer (LANL 2007, 095817). The carbon-steel discharge pipe is a potential source of chromium and zinc contributing to the measured concentrations of these two trace metals during development at well R-46.

Eight additional groundwater-screening samples were collected from R-46 for tritium analyses during drilling, and these results are pending from an analytical laboratory external to the Laboratory (see Table 4.2-1). Seven groundwater-screening samples and two solid-cuttings samples were collected during drilling and analyzed for VOCs and SVOCs, with results for two samples (GW46-09-2847 and GW46-09-2848) provided in Table B-1.3-2. Acetone (7.23 µg/L), 2-butanone (3.28 µg/L), toluene (0.251 µg/L), 1,2,4-trimethylbenzene (0.293 µg/L), bis(2-ethylhexyl)phthalate (43.2 µg/L, 342 µg/L, and 43 µg/L) were detected in the two borehole water samples. Analytical results for quality assurance samples are also provided in Table B-1.3-2.

## B-2.0 REFERENCES

*The following list includes all documents cited in this appendix. Parenthetical information following each reference provides the author(s), publication date, and ER ID number. This information is also included in text citations. ER ID numbers are assigned by the Environmental Programs Directorate's Records Processing Facility (RPF) and are used to locate the document at the RPF and, where applicable, in the master reference set.*

*Copies of the master reference set are maintained at the NMED Hazardous Waste Bureau and the Directorate. The set was developed to ensure that the administrative authority has all material needed to review this document, and it is updated with every document submitted to the administrative authority. Documents previously submitted to the administrative authority are not included.*

LANL (Los Alamos National Laboratory), May 2007. "Groundwater Background Investigation Report, Revision 3," Los Alamos National Laboratory document LA-UR-07-2853, Los Alamos, New Mexico. (LANL 2007, 095817)





**Table B-1.2-1  
Well Development Volumes, Aquifer Testing Volumes,  
and Associated Field Water-Quality Parameters for R-46**

Date	pH	Temp (°C)	DO (mg/L)	ORP (mV)	Specific Conductivity (µS/cm)	Turbidity (NTU)	Purge Volume between Samples (gal.)	Cumulative Purge Volume (gal.)
<b>Well Development</b>								
02/26/09	n/r*; bailing						625	625
02/28/09	n/r; pumping with swabbing						300	925
03/02/09	n/r; pumping with swabbing						478	1403
03/03/09	n/r; pumping with swabbing						3536	4939
03/03/09	8.02	17.20	11.41	n/r	135	5.2	1483	6422
03/04/09	8.00	14.09	11.03	n/r	133	4.7	296	6718
	8.00	13.60	11.60	n/r	134	4.6	296	7014
	8.06	14.37	11.40	n/r	131	5.2	296	7310
	8.02	11.16	12.10	n/r	132	4.5	296	7606
	8.07	14.50	11.12	n/r	130	4.8	296	7902
	8.06	12.45	12.87	n/r	131	4.4	149	8051
	8.04	14.35	10.99	n/r	130	4.7	149	8200
	8.01	18.54	12.30	n/r	131	4.8	149	8349
03/04/09	8.01	15.89	11.60	n/r	131	4.5	149	8498
03/04/09	n/r; pumping						1000	9498
<b>Aquifer Testing</b>								
3/8/2009	Mini-tests #1 and #2; parameters not collected						690	690
3/10/2009	parameters not collected						576	1266
3/10/2009	8.29	nr	7.23	40	113	11.6	570	1836
	8.04	19.82	6.84	27.7	111	10.6	564	2400
	8.04	20.59	7.27	29.5	112	10	558	2958
	7.99	22.41	6.72	60.1	118	5.9	492	3450
	7.98	22.24	7.17	58.2	117	7.8	474	3924
	7.98	23.21	7.48	37.3	121	6.7	468	4392
	7.98	23.31	8.09	69.3	120	3.6	462	4854
	7.97	22.71	7.31	67.2	124	6.7	552	5406
	7.98	23.21	8.52	76.1	124	6.7	564	5970
	7.94	20.37	7.03	76.7	115	7.4	564	6534
	8.03	20.1	8.48	51.5	119	9.3	564	7098
	8.05	17.13	7.38	53	120	4.9	564	7662
	8.04	20.11	5.62	41.3	107	4.6	564	8226
	8.05	19.25	7.79	42.5	105	5.6	564	8790
	8.03	19.08	7.29	35.9	117	7.9	558	9348
8.01	20.24	7.73	37.5	107	7.1	564	9912	

Table B-1.2-1 (continued)

Date	pH	Temp (°C)	DO (mg/L)	ORP (mV)	Specific Conductivity (µS/cm)	Turbidity (NTU)	Purge Volume between Samples (gal.)	Cumulative Purge Volume (gal.)
3/10/2009	8.03	19.57	9.59	50	107	5.6	564	10476
(cont)	8.04	19.17	7.51	47.8	105	6.6	564	11040
	8.03	19.05	7.21	43.3	104	5.6	564	11604
	8.02	19.42	7.1	45.2	105	6.1	564	12168

Notes: Cumulative purge volumes calculated for well development using average pump discharge rate of 4.94 gpm. Pump discharge rates ranged from 7.7 to 9.6 gpm for aquifer testing.

\* n/r = Not recorded.

**Table B-1.3-1**  
**Analytical Results for Groundwater-Screening Samples Collected from R-46, Pajarito Mesa**

Sample ID	Date Received	ER/RRES-WQH	Sample Type	Depth (feet)	Ag rslt (ppm)	stdev (Ag)	Al rslt (ppm)	stdev (Al)	As rslt (ppm)	stdev (As)	B rslt (ppm)	stdev (B)	Ba rslt (ppm)	stdev (Ba)	Be rslt (ppm)	stdev (Be)	Br(-) ppm	TOC rslt (ppm)	Ca rslt (ppm)
GW46-09-1847	1/26/2009	09-718	Borehole	1115	0.001	U	0.18	0.00	0.0005	0.0000	0.039	0.000	0.098	0.001	0.001	U	0.25	Not analyzed	9.85
GW46-09-1848	1/26/2009	09-718	Borehole	1134	0.001	U	0.37	0.00	0.0005	0.0000	0.036	0.000	0.031	0.000	0.001	U	0.07	Not analyzed	7.30
GW46-09-1849	1/26/2009	09-718	Borehole	1155	0.001	U	0.56	0.02	0.0004	0.0000	0.047	0.001	0.021	0.000	0.001	U	0.07	Not analyzed	4.55
GW46-09-1850	1/26/2009	09-718	Borehole	1175	0.001	U	0.16	0.00	0.0003	0.0000	0.034	0.001	0.016	0.000	0.001	U	0.08	Not analyzed	4.70
GW46-09-1851	1/26/2009	09-718	Borehole	1195	0.001	U	0.57	0.00	0.0006	0.0000	0.021	0.001	0.037	0.000	0.001	U	0.06	Not analyzed	8.46
GW46-09-1852	1/26/2009	09-718	Borehole	1215	0.001	U	0.12	0.00	0.0002	U	0.017	0.000	0.059	0.000	0.001	U	0.07	Not analyzed	16.29
GW46-09-1853	1/26/2009	09-718	Borehole	1230	0.001	U	0.31	0.00	0.0002	U	0.028	0.000	0.027	0.000	0.001	U	0.03	Not analyzed	10.82
GW46-09-1854	1/26/2009	09-735	Borehole	1220	0.001	U	0.51	0.00	0.0002	0.0000	0.031	0.001	0.050	0.000	0.001	U	0.02	Not analyzed	12.69
GW46-09-1855	2/5/2009	09-816	Borehole	1340	0.001	U	0.12	0.00	0.0003	0.0000	0.029	0.000	0.017	0.000	0.001	U	0.02	Not analyzed	6.04
GW46-09-1856	2/5/2009	09-816	Borehole	1360	0.001	U	0.17	0.00	0.0003	0.0000	0.018	0.000	0.026	0.000	0.001	U	0.04	Not analyzed	10.24
GW46-09-1857	2/5/2009	09-816	Borehole	1395	0.001	U	2.94	0.13	0.0003	0.0000	0.016	0.001	0.028	0.001	0.001	U	0.03	Not analyzed	4.96
GW46-09-1858	2/5/2009	09-816	Borehole	1415	0.001	U	3.94	0.25	0.0003	0.0000	0.014	0.001	0.030	0.000	0.001	U	0.02	Not analyzed	8.92
GW46-09-1867	3/5/2009	09-1112	Well, development	1340.0-1360.7	0.001	U	0.007	0.000	0.0008	0.0000	0.023	0.000	0.020	0.000	0.001	U	0.02	0.33	11.07
GW46-09-1868	3/5/2009	09-1112	Well, development	1340.0-1360.7	0.001	U	0.005	0.000	0.0008	0.0000	0.020	0.001	0.019	0.001	0.001	U	0.02	0.32	11.03
GW46-09-1869	3/5/2009	09-1112	Well, development	1340.0-1360.7	0.001	U	0.004	0.000	0.0007	0.0000	0.019	0.001	0.019	0.000	0.001	U	0.02	0.29	11.08
GW46-09-1870	3/5/2009	09-1112	Well, development	1340.0-1360.7	0.001	U	0.007	0.000	0.0008	0.0000	0.018	0.001	0.020	0.000	0.001	U	0.02	0.37	11.17
GW46-09-1871	3/11/2009	09-1165	Well, aquifer testing	1340.0-1360.7	0.001	U	0.004	0.000	0.0008	0.0000	0.034	0.000	0.020	0.002	0.001	U	0.04	0.47	10.26
GW46-09-1872	3/11/2009	09-1165	Well, aquifer testing	1340.0-1360.7	0.001	U	0.003	0.000	0.0007	0.0000	0.030	0.000	0.019	0.000	0.001	U	0.04	0.40	10.34
GW46-09-1873	3/11/2009	09-1165	Well, aquifer testing	1340.0-1360.7	0.001	U	0.004	0.000	0.0007	0.0000	0.018	0.000	0.019	0.000	0.001	U	0.04	0.40	10.66
GW46-09-1874	3/11/2009	09-1165	Well, aquifer testing	1340.0-1360.7	0.001	U	0.004	0.000	0.0007	0.0000	0.016	0.000	0.019	0.000	0.001	U	0.04	0.38	10.70
GW46-09-1875	3/11/2009	09-1165	Well, aquifer testing	1340.0-1360.7	0.001	U	0.005	0.000	0.0007	0.0000	0.013	0.001	0.019	0.000	0.001	U	0.04	0.43	10.79
GW46-09-1876	3/11/2009	09-1165	Well, aquifer testing	1340.0-1360.7	0.001	U	0.005	0.001	0.0007	0.0000	0.015	0.000	0.019	0.001	0.001	U	0.04	0.47	10.85

Table B-1.3-1 (continued)

Sample ID	Date Received	ER/RRES-WQH	Sample Type	stdev (Ca)	Cd rslt (ppm)	stdev (Cd)	Cl(-) ppm	ClO4(-) ppm	ClO4(-) (U)	Co rslt (ppm)	stdev (Co)	Alk-CO3 rslt (ppm)	ALK-CO3 (U)	Cr rslt (ppm)	stdev (Cr)	Cs rslt (ppm)	stdev (Cs)	Cu rslt (ppm)
GW46-09-1847	1/26/2009	09-718	Borehole	0.08	0.001	U	40.4	Pending		0.001	U	0.8	U	0.002	0.000	0.001	U	0.005
GW46-09-1848	1/26/2009	09-718	Borehole	0.04	0.001	U	15.2	Pending		0.001	U	0.8	U	0.001	U	0.001	U	0.004
GW46-09-1849	1/26/2009	09-718	Borehole	0.04	0.001	U	14.6	Pending		0.001	U	0.8	U	0.001	0.000	0.001	U	0.007
GW46-09-1850	1/26/2009	09-718	Borehole	0.02	0.001	U	16.4	Pending		0.001	U	0.8	U	0.001	0.000	0.001	U	0.005
GW46-09-1851	1/26/2009	09-718	Borehole	0.15	0.001	U	12.0	Pending		0.001	U	0.8	U	0.001	U	0.001	U	0.003
GW46-09-1852	1/26/2009	09-718	Borehole	0.05	0.001	U	12.4	Pending	Pending	0.001	U	0.8	U	0.002	0.000	0.001	U	0.025
GW46-09-1853	1/26/2009	09-718	Borehole	0.07	0.001	U	8.88	Pending	Pending	0.001	U	0.8	U	0.001	0.000	0.001	U	0.001
GW46-09-1854	1/26/2009	09-735	Borehole	0.09	0.001	U	9.13	Pending	Pending	0.001	0.000	0.8	U	0.003	0.000	0.001	U	0.003
GW46-09-1855	2/5/2009	09-816	Borehole	0.04	0.001	U	6.69	Pending	Pending	0.001	U	0.8	U	0.001	U	0.001	U	0.001
GW46-09-1856	2/5/2009	09-816	Borehole	0.08	0.001	U	11.3	Pending	Pending	0.001	0.000	0.8	U	0.001	U	0.001	U	0.002
GW46-09-1857	2/5/2009	09-816	Borehole	0.03	0.001	U	4.08	Pending	Pending	0.002	0.000	0.8	U	0.004	0.000	0.001	U	0.006
GW46-09-1858	2/5/2009	09-816	Borehole	0.03	0.001	U	1.92	Pending	Pending	0.001	U	0.8	U	0.003	0.001	0.001	U	0.001
GW46-09-1867	3/5/2009	09-1112	Well, development	0.04	0.001	U	2.89	Pending	Pending	0.001	U	0.8	U	0.007	0.000	0.001	U	0.001
GW46-09-1868	3/5/2009	09-1112	Well, development	0.08	0.001	U	2.56	Pending	Pending	0.001	U	0.8	U	0.005	0.000	0.001	U	0.001
GW46-09-1869	3/5/2009	09-1112	Well, development	0.10	0.001	U	2.51	Pending	Pending	0.001	0.000	0.8	U	0.005	0.000	0.001	U	0.001
GW46-09-1870	3/5/2009	09-1112	Well, development	0.06	0.001	U	2.48	Pending	Pending	0.001	U	0.8	U	0.005	0.000	0.001	U	0.001
GW46-09-1871	3/11/2009	09-1165	Well, aquifer testing	0.06	0.001	U	2.92	Pending	Pending	0.001	U	0.8	U	0.007	0.001	0.001	U	0.001
GW46-09-1872	3/11/2009	09-1165	Well, aquifer testing	0.02	0.001	U	2.87	Pending	Pending	0.001	U	0.8	U	0.007	0.001	0.001	U	0.001
GW46-09-1873	3/11/2009	09-1165	Well, aquifer testing	0.08	0.001	U	2.85	Pending	Pending	0.001	U	0.8	U	0.007	0.001	0.001	U	0.001
GW46-09-1874	3/11/2009	09-1165	Well, aquifer testing	0.06	0.001	U	2.80	Pending	Pending	0.001	U	0.8	U	0.007	0.000	0.001	U	0.001
GW46-09-1875	3/11/2009	09-1165	Well, aquifer testing	0.03	0.001	U	2.83	Pending	Pending	0.001	U	0.8	U	0.007	0.000	0.001	U	0.001
GW46-09-1876	3/11/2009	09-1165	Well, aquifer testing	0.14	0.001	U	2.82	Pending	Pending	0.001	U	0.8	U	0.007	0.000	0.001	U	0.001

Table B-1.3-1 (continued)

Sample ID	Date Received	ER/RRES-WQH	Sample Type	stdev (Cu)	F(-) ppm	Fe rslt (ppm)	stdev (Fe)	Alk-CO3+HCO3 rslt (ppm)	Hg rslt (ppm)	stdev (Hg)	K rslt (ppm)	stdev (K)	Li rslt (ppm)	stdev (Li)	Mg rslt (ppm)	stdev (Mg)	Mn rslt (ppm)	stdev (Mn)
GW46-09-1847	1/26/2009	09-718	Borehole	0.000	3.08	0.067	0.000	231	0.00012	0.00000	6.34	0.06	0.187	0.002	2.27	0.02	0.215	0.001
GW46-09-1848	1/26/2009	09-718	Borehole	0.000	0.91	0.071	0.000	155	0.00007	0.00000	5.63	0.01	0.053	0.000	1.56	0.00	0.059	0.000
GW46-09-1849	1/26/2009	09-718	Borehole	0.000	1.07	0.234	0.002	217	0.00008	0.00000	3.73	0.01	0.046	0.000	0.85	0.00	0.041	0.000
GW46-09-1850	1/26/2009	09-718	Borehole	0.000	1.00	0.043	0.001	177	0.00005	U	3.30	0.01	0.041	0.000	0.79	0.01	0.055	0.000
GW46-09-1851	1/26/2009	09-718	Borehole	0.000	0.69	0.138	0.001	123	0.00005	0.00000	4.90	0.02	0.039	0.000	1.98	0.01	0.089	0.001
GW46-09-1852	1/26/2009	09-718	Borehole	0.001	0.78	0.061	0.000	132	0.00008	0.00000	5.33	0.03	0.050	0.000	4.71	0.04	0.334	0.003
GW46-09-1853	1/26/2009	09-718	Borehole	0.000	0.46	0.144	0.002	110	0.00022	0.00002	5.38	0.04	0.039	0.000	3.75	0.02	0.106	0.001
GW46-09-1854	1/26/2009	09-735	Borehole	0.000	0.50	0.360	0.002	120	0.00032	0.00001	6.00	0.05	0.041	0.000	4.49	0.02	0.254	0.000
GW46-09-1855	2/5/2009	09-816	Borehole	0.000	0.58	0.059	0.000	102	0.00005	U	3.12	0.02	0.045	0.000	2.06	0.02	0.109	0.000
GW46-09-1856	2/5/2009	09-816	Borehole	0.000	0.52	0.323	0.001	117	0.00005	U	4.26	0.01	0.048	0.000	3.66	0.02	0.312	0.001
GW46-09-1857	2/5/2009	09-816	Borehole	0.001	0.32	4.054	1.147	80	0.00005	U	4.48	0.01	0.028	0.000	2.45	0.01	0.260	0.002
GW46-09-1858	2/5/2009	09-816	Borehole	0.000	0.26	1.632	0.038	75	0.00018	0.00000	3.37	0.01	0.037	0.000	4.22	0.04	0.061	0.001
GW46-09-1867	3/5/2009	09-1112	Well, development	U	0.17	0.045	0.000	77	0.00005	U	2.07	0.00	0.021	0.000	3.29	0.01	0.011	0.000
GW46-09-1868	3/5/2009	09-1112	Well, development	U	0.15	0.043	0.000	76	0.00005	U	2.06	0.02	0.020	0.001	3.30	0.03	0.009	0.000
GW46-09-1869	3/5/2009	09-1112	Well, development	U	0.15	0.037	0.001	76	0.00005	U	2.06	0.01	0.020	0.001	3.34	0.05	0.009	0.000
GW46-09-1870	3/5/2009	09-1112	Well, development	0.000	0.15	0.041	0.000	75	0.00005	U	2.03	0.01	0.021	0.001	3.29	0.02	0.009	0.000
GW46-09-1871	3/11/2009	09-1165	Well, aquifer testing	U	0.17	0.315	0.001	79	0.00005	U	2.01	0.01	0.020	0.000	3.13	0.02	0.012	0.001
GW46-09-1872	3/11/2009	09-1165	Well, aquifer testing	U	0.17	0.318	0.001	73	0.00005	U	1.99	0.00	0.020	0.000	3.19	0.03	0.010	0.000
GW46-09-1873	3/11/2009	09-1165	Well, aquifer testing	U	0.16	0.229	0.002	73	0.00005	U	1.97	0.01	0.019	0.000	3.22	0.02	0.008	0.000
GW46-09-1874	3/11/2009	09-1165	Well, aquifer testing	U	0.16	0.219	0.001	72	0.00005	U	1.98	0.01	0.019	0.000	3.26	0.00	0.007	0.000
GW46-09-1875	3/11/2009	09-1165	Well, aquifer testing	U	0.16	0.204	0.001	72	0.00005	U	1.92	0.01	0.019	0.000	3.19	0.02	0.007	0.000
GW46-09-1876	3/11/2009	09-1165	Well, aquifer testing	U	0.16	0.206	0.002	72	0.00005	U	2.08	0.02	0.020	0.000	3.42	0.05	0.007	0.000

Table B-1.3-1 (continued)

Sample ID	Date Received	ER/RRES-WQH	Sample Type	Mo rslt (ppm)	stdev (Mo)	Na rslt (ppm)	stdev (Na)	Ni rslt (ppm)	stdev (Ni)	NO2(ppm)	NO2-N rslt	NO2-N (U)	NO3 ppm	NO3-N rslt	C2O4 rslt (ppm)	C2O4 (U)	Pb rslt (ppm)	stdev (Pb)	Lab pH	PO4(-3) rslt (ppm)
GW46-09-1847	1/26/2009	09-718	Borehole	0.390	0.000	175.06	1.96	0.004	0.000	0.010	0.003	U	0.03	0.01	1.07	0.05	0.0002	U	8.11	0.01
GW46-09-1848	1/26/2009	09-718	Borehole	0.368	0.004	81.24	0.31	0.001	0.000	0.010	0.003	U	3.14	0.71	0.26	0.03	0.0002	U	8.06	0.01
GW46-09-1849	1/26/2009	09-718	Borehole	0.216	0.003	121.59	0.85	0.001	U	0.142	0.043	0.02	0.23	0.05	0.25	0.02	0.0002	U	8.23	0.01
GW46-09-1850	1/26/2009	09-718	Borehole	0.222	0.001	118.58	1.32	0.001	U	0.130	0.040	0.02	2.49	0.56	0.24	0.02	0.0002	U	8.19	0.01
GW46-09-1851	1/26/2009	09-718	Borehole	0.286	0.001	52.07	0.54	0.001	U	0.010	0.003	U	2.33	0.53	0.25	0.02	0.0002	U	7.91	0.01
GW46-09-1852	1/26/2009	09-718	Borehole	0.269	0.003	39.31	0.13	0.003	0.000	0.01	0.00	U	2.33	0.53	0.18	0.02	0.0002	U	7.90	0.01
GW46-09-1853	1/26/2009	09-718	Borehole	0.042	0.001	23.53	0.19	0.001	0.000	0.01	0.00	U	2.26	0.51	0.06	0.01	0.0002	U	7.96	0.01
GW46-09-1854	1/26/2009	09-735	Borehole	0.035	0.000	24.01	0.09	0.003	0.000	0.01	0.00	U	1.81	0.41	0.06	0.01	0.0002	0.0000	7.90	0.01
GW46-09-1855	2/5/2009	09-816	Borehole	0.117	0.001	23.02	0.16	0.001	0.000	0.01	0.00	U	1.05	0.24	0.09	0.01	0.0002	U	7.78	0.01
GW46-09-1856	2/5/2009	09-816	Borehole	0.075	0.001	27.27	0.05	0.004	0.000	0.01	0.00	U	0.68	0.15	0.20	0.02	0.0002	U	7.88	0.01
GW46-09-1857	2/5/2009	09-816	Borehole	0.153	0.000	14.97	0.04	0.003	0.000	0.01	0.00	U	1.52	0.34	0.14	0.01	0.0008	0.0000	7.54	0.01
GW46-09-1858	2/5/2009	09-816	Borehole	0.046	0.000	10.77	0.04	0.002	0.000	0.01	0.00	U	1.91	0.43	0.01	U	0.0009	0.0000	7.60	0.01
GW46-09-1867	3/5/2009	09-1112	Well, development	0.001	U	10.98	0.05	0.001	0.000	0.01	0.00	U	1.82	0.41	0.02	U	0.0002	U	7.79	0.01
GW46-09-1868	3/5/2009	09-1112	Well, development	0.001	U	10.78	0.10	0.001	U	0.01	0.00	U	1.79	0.40	0.02	U	0.0002	U	7.78	0.75
GW46-09-1869	3/5/2009	09-1112	Well, development	0.001	U	10.68	0.07	0.001	U	0.01	0.00	U	1.80	0.41	0.02	U	0.0002	U	7.86	0.73
GW46-09-1870	3/5/2009	09-1112	Well, development	0.001	U	10.45	0.05	0.001	U	0.01	0.00	U	1.82	0.41	0.02	U	0.0002	U	7.86	0.08
GW46-09-1871	3/11/2009	09-1165	Well, aquifer testing	0.001	U	9.90	0.04	0.002	0.000	0.01	0.00	U	2.25	0.51	0.02	U	0.0002	U	7.71	0.10
GW46-09-1872	3/11/2009	09-1165	Well, aquifer testing	0.001	U	9.69	0.04	0.001	0.000	0.01	0.00	U	2.24	0.51	0.02	U	0.0002	U	7.77	0.09
GW46-09-1873	3/11/2009	09-1165	Well, aquifer testing	0.001	U	9.45	0.07	0.002	0.000	0.01	0.00	U	2.26	0.51	0.02	U	0.0002	U	7.74	0.11
GW46-09-1874	3/11/2009	09-1165	Well, aquifer testing	0.001	U	9.35	0.02	0.002	0.000	0.01	0.00	U	2.25	0.51	0.02	U	0.0002	U	7.75	0.11
GW46-09-1875	3/11/2009	09-1165	Well, aquifer testing	0.001	U	9.10	0.02	0.001	0.000	0.01	0.00	U	2.26	0.51	0.02	U	0.0002	U	7.73	0.11
GW46-09-1876	3/11/2009	09-1165	Well, aquifer testing	0.001	U	9.71	0.05	0.002	0.000	0.01	0.00	U	2.27	0.51	0.02	U	0.0002	U	7.86	0.11

Table B-1.3-1 (continued)

Sample ID	Date Received	ER/RRES-WQH	Sample Type	PO4(-3) (U)	Rb rslt (ppm)	stdev (Rb)	Sb rslt (ppm)	stdev (Sb)	Se rslt (ppm)	stdev (Se)	Si rslt (ppm)	stdev (Si)	SiO2 rslt (ppm)	stdev (SiO2)	Sn rslt (ppm)	stdev (Sn)	SO4(-2) rslt (ppm)	Sr rslt (ppm)	stdev (Sr)	Th rslt (ppm)
GW46-09-1847	1/26/2009	09-718	Borehole	U	0.008	0.000	0.001	U	0.001	U	5.1	0.0	10.8	0.1	0.001	U	141	0.087	0.001	0.001
GW46-09-1848	1/26/2009	09-718	Borehole	U	0.007	0.000	0.001	U	0.001	U	7.4	0.0	15.9	0.0	0.001	U	66	0.085	0.001	0.001
GW46-09-1849	1/26/2009	09-718	Borehole	U	0.005	0.000	0.001	U	0.001	U	7.6	0.1	16.2	0.2	0.001	U	96	0.051	0.000	0.001
GW46-09-1850	1/26/2009	09-718	Borehole	U	0.004	0.000	0.001	U	0.001	U	3.9	0.0	8.5	0.1	0.001	U	100	0.046	0.001	0.001
GW46-09-1851	1/26/2009	09-718	Borehole	U	0.007	0.000	0.001	U	0.001	U	9.2	0.0	19.6	0.1	0.001	U	37	0.060	0.000	0.001
GW46-09-1852	1/26/2009	09-718	Borehole	U	0.008	0.000	0.001	U	0.001	U	8.5	0.0	18.1	0.1	0.001	U	33	0.079	0.001	0.001
GW46-09-1853	1/26/2009	09-718	Borehole	U	0.009	0.000	0.001	U	0.001	U	10.2	0.0	21.9	0.1	0.001	U	5.6	0.046	0.000	0.001
GW46-09-1854	1/26/2009	09-735	Borehole	U	0.010	0.000	0.001	U	0.001	U	14.3	0.0	30.7	0.1	0.001	U	7.3	0.062	0.000	0.001
GW46-09-1855	2/5/2009	09-816	Borehole	U	0.007	0.000	0.001	U	0.001	U	5.9	0.1	12.7	0.1	0.001	U	4.8	0.026	0.000	0.001
GW46-09-1856	2/5/2009	09-816	Borehole	U	0.009	0.000	0.001	U	0.001	U	6.5	0.0	14.0	0.0	0.001	U	9.8	0.043	0.000	0.001
GW46-09-1857	2/5/2009	09-816	Borehole	U	0.011	0.000	0.001	U	0.001	U	18.4	0.2	39.3	0.4	0.001	U	3.0	0.023	0.000	0.001
GW46-09-1858	2/5/2009	09-816	Borehole	U	0.010	0.000	0.001	U	0.001	U	30.5	0.3	65.2	0.6	0.001	U	1.9	0.038	0.000	0.001
GW46-09-1867	3/5/2009	09-1112	Well, development	U	0.005	0.000	0.001	U	0.001	U	35.8	0.2	76.5	0.5	0.001	U	3.01	0.047	0.000	0.001
GW46-09-1868	3/5/2009	09-1112	Well, development	0.07	0.005	0.000	0.001	U	0.001	U	35.8	0.3	76.6	0.7	0.001	U	2.67	0.046	0.001	0.001
GW46-09-1869	3/5/2009	09-1112	Well, development	0.07	0.005	0.000	0.001	U	0.001	U	36.2	0.2	77.5	0.4	0.001	U	2.63	0.047	0.000	0.001
GW46-09-1870	3/5/2009	09-1112	Well, development	0.01	0.005	0.000	0.001	U	0.001	U	35.8	0.2	76.6	0.4	0.001	U	2.56	0.047	0.000	0.001
GW46-09-1871	3/11/2009	09-1165	Well, aquifer testing	0.01	0.006	0.000	0.001	U	0.001	U	35.2	0.2	75.3	0.4	0.001	U	3.05	0.051	0.004	0.001
GW46-09-1872	3/11/2009	09-1165	Well, aquifer testing	0.01	0.006	0.000	0.001	U	0.001	U	35.3	0.4	75.5	0.9	0.001	U	3.08	0.047	0.001	0.001
GW46-09-1873	3/11/2009	09-1165	Well, aquifer testing	0.01	0.006	0.000	0.001	U	0.001	U	35.8	0.0	76.7	0.1	0.001	U	2.90	0.045	0.000	0.001
GW46-09-1874	3/11/2009	09-1165	Well, aquifer testing	0.01	0.006	0.000	0.001	U	0.001	U	36.1	0.1	77.3	0.3	0.001	U	2.85	0.046	0.001	0.001
GW46-09-1875	3/11/2009	09-1165	Well, aquifer testing	0.01	0.005	0.000	0.001	U	0.001	U	35.4	0.2	75.7	0.4	0.001	U	2.87	0.043	0.000	0.001
GW46-09-1876	3/11/2009	09-1165	Well, aquifer testing	0.01	0.006	0.000	0.001	U	0.001	U	37.5	0.4	80.3	0.8	0.001	U	2.83	0.045	0.000	0.001



Table B-1.3-1 (continued)

Sample ID	Date Received	ER/RRES-WQH	Sample Type	stdev (Th)	Ti rslt (ppm)	stdev (Ti)	Tl rslt (ppm)	stdev (Tl)	U rslt (ppm)	stdev (U)	V rslt (ppm)	stdev (V)	Zn rslt (ppm)	stdev (Zn)	TDS (ppm)	Cations	Anions	Balance
GW46-09-1847	1/26/2009	09-718	Borehole	U	0.003	0.000	0.001	U	0.0019	0.0000	0.002	0.000	0.007	0.002	622	8.49	8.10	0.02
GW46-09-1848	1/26/2009	09-718	Borehole	U	0.006	0.000	0.001	U	0.0009	0.0000	0.002	0.000	0.006	0.001	353	4.18	4.47	-0.03
GW46-09-1849	1/26/2009	09-718	Borehole	U	0.008	0.000	0.001	U	0.0034	0.0002	0.003	0.000	0.007	0.002	478	5.69	6.07	-0.03
GW46-09-1850	1/26/2009	09-718	Borehole	U	0.002	0.000	0.001	U	0.0011	0.0000	0.002	0.000	0.005	0.002	435	5.55	5.58	0.00
GW46-09-1851	1/26/2009	09-718	Borehole	U	0.011	0.000	0.001	U	0.0005	0.0000	0.001	0.000	0.007	0.001	264	2.99	3.22	-0.04
GW46-09-1852	1/26/2009	09-718	Borehole	U	0.004	0.000	0.001	U	0.0006	0.0000	0.002	0.000	0.007	0.003	267	3.07	3.32	-0.04
GW46-09-1853	1/26/2009	09-718	Borehole	U	0.007	0.000	0.001	U	0.0008	0.0000	0.002	0.000	0.007	0.002	194	2.02	2.26	-0.06
GW46-09-1854	1/26/2009	09-735	Borehole	U	0.014	0.000	0.001	U	0.0007	0.0000	0.002	0.000	0.009	0.000	219	2.22	2.48	-0.05
GW46-09-1855	2/5/2009	09-816	Borehole	U	0.003	0.000	0.001	U	0.0002	U	0.001	U	0.004	0.001	163	1.56	2.04	-0.13
GW46-09-1856	2/5/2009	09-816	Borehole	U	0.008	0.000	0.001	U	0.0002	U	0.001	0.000	0.008	0.001	200	2.13	2.51	-0.08
GW46-09-1857	2/5/2009	09-816	Borehole	U	0.127	0.005	0.001	U	0.0003	0.0000	0.001	U	0.016	0.002	163	1.23	1.60	-0.13
GW46-09-1858	2/5/2009	09-816	Borehole	U	0.075	0.002	0.001	U	0.0012	0.0000	0.002	0.000	0.012	0.000	180	1.36	1.50	-0.05
GW46-09-1867	3/5/2009	09-1112	Well, development	U	0.002	U	0.001	U	0.0007	0.0000	0.008	0.000	0.031	0.000	190	1.40	1.50	-0.04
GW46-09-1868	3/5/2009	09-1112	Well, development	U	0.002	U	0.001	U	0.0006	0.0000	0.008	0.000	0.035	0.001	188	1.30	1.40	-0.03
GW46-09-1869	3/5/2009	09-1112	Well, development	U	0.002	U	0.001	U	0.0006	0.0000	0.008	0.000	0.024	0.000	189	1.40	1.40	-0.03
GW46-09-1870	3/5/2009	09-1112	Well, development	U	0.002	U	0.001	U	0.0006	0.0000	0.008	0.000	0.025	0.000	188	1.30	1.40	-0.03
GW46-09-1871	3/11/2009	09-1165	Well, aquifer testing	U	0.002	U	0.001	U	0.0006	0.0000	0.009	0.001	0.005	0.000	189	1.30	1.50	-0.09
GW46-09-1872	3/11/2009	09-1165	Well, aquifer testing	U	0.002	U	0.001	U	0.0006	0.0000	0.008	0.000	0.005	0.000	184	1.30	1.40	-0.06
GW46-09-1873	3/11/2009	09-1165	Well, aquifer testing	U	0.002	U	0.001	U	0.0005	0.0000	0.008	0.000	0.005	0.000	184	1.30	1.40	-0.05
GW46-09-1874	3/11/2009	09-1165	Well, aquifer testing	U	0.002	U	0.001	U	0.0005	0.0000	0.008	0.000	0.004	0.000	184	1.30	1.40	-0.05
GW46-09-1875	3/11/2009	09-1165	Well, aquifer testing	U	0.002	U	0.001	U	0.0005	0.0000	0.008	0.000	0.004	0.000	182	1.30	1.40	-0.05
GW46-09-1876	3/11/2009	09-1165	Well, aquifer testing	U	0.002	U	0.001	U	0.0005	0.0000	0.008	0.000	0.004	0.000	188	1.30	1.40	-0.04











**Table B-1.3-2  
Organic Analytical Results for Groundwater-Screening Samples Collected from Borehole R-46**

Location	Depth (ft)	Request	Sample	Date	Fld Prep	Field Matrix	Field QC Type	Lab Sample Type	Method	CAS	Analyte	Sym	Result	Units	Lab Qual	MDL	Quant Limit	Lab	DF	2nd Qual	2nd Reason	Reporting Flag	Sample Tech	Sample Usage	URI	USI	ULI
R-46	1220	09-761	GW46-09-2848	1/26/2009	UF	W	NA	CS	SW-846:8270C	99-09-2	Nitroaniline[3-]	<	10.5	ug/L	U	2.1	11	GELC	1	U	U_LAB	Y	BA	INV	57278102	871922	2459492
R-46	1220	09-761	GW46-09-2848	1/26/2009	UF	W	NA	CS	SW-846:8270C	100-01-6	Nitroaniline[4-]	<	10.5	ug/L	U	3.2	11	GELC	1	UJ	SV7a	Y	BA	INV	57277462	871922	2459492
R-46	1220	09-761	GW46-09-2848	1/26/2009	UF	W	NA	DL	SW-846:8270C	100-01-6	Nitroaniline[4-]	<	104	ug/L	U	31	100	GELC	10	UJ	SV88	Y	BA	INV	57277952	871922	2459492
R-46	1220	09-761	GW46-09-2848	1/26/2009	UF	W	NA	CS	SW-846:8270C	98-95-3	Nitrobenzene	<	10.5	ug/L	U	3.2	11	GELC	1	U	U_LAB	Y	BA	INV	57278812	871922	2459492
R-46	1220	09-761	GW46-09-2848	1/26/2009	UF	W	NA	DL	SW-846:8270C	98-95-3	Nitrobenzene	<	104	ug/L	U	31	100	GELC	10	UJ	SV88	Y	BA	INV	57278902	871922	2459492
R-46	1220	09-761	GW46-09-2848	1/26/2009	UF	W	NA	CS	SW-846:8270C	88-75-5	Nitrophenol[2-]	<	10.5	ug/L	U	2.1	11	GELC	1	R	SV3	Y	BA	INV	57276942	871922	2459492
R-46	1220	09-761	GW46-09-2848	1/26/2009	UF	W	NA	DL	SW-846:8270C	88-75-5	Nitrophenol[2-]	<	104	ug/L	U	21	100	GELC	10	UJ	SV88	Y	BA	INV	57277892	871922	2459492
R-46	1220	09-761	GW46-09-2848	1/26/2009	UF	W	NA	DL	SW-846:8270C	100-02-7	Nitrophenol[4-]	<	104	ug/L	U	21	100	GELC	10	UJ	SV88	Y	BA	INV	57278252	871922	2459492
R-46	1220	09-761	GW46-09-2848	1/26/2009	UF	W	NA	CS	SW-846:8270C	100-02-7	Nitrophenol[4-]	<	10.5	ug/L	U	2.1	11	GELC	1	R	SV3	Y	BA	INV	57279032	871922	2459492
R-46	1220	09-761	GW46-09-2848	1/26/2009	UF	W	NA	CS	SW-846:8270C	62-75-9	Nitrosodimethylamine[N-]	<	10.5	ug/L	U	2.1	11	GELC	1	U	U_LAB	Y	BA	INV	57277972	871922	2459492
R-46	1220	09-761	GW46-09-2848	1/26/2009	UF	W	NA	DL	SW-846:8270C	62-75-9	Nitrosodimethylamine[N-]	<	104	ug/L	U	21	100	GELC	10	UJ	SV88	Y	BA	INV	57278932	871922	2459492
R-46	1220	09-761	GW46-09-2848	1/26/2009	UF	W	NA	CS	SW-846:8270C	621-64-7	Nitroso-di-n-propylamine[N-]	<	10.5	ug/L	U	2.1	11	GELC	1	U	U_LAB	Y	BA	INV	57278422	871922	2459492
R-46	1220	09-761	GW46-09-2848	1/26/2009	UF	W	NA	DL	SW-846:8270C	621-64-7	Nitroso-di-n-propylamine[N-]	<	104	ug/L	U	21	100	GELC	10	UJ	SV88	Y	BA	INV	57279072	871922	2459492
R-46	1220	09-761	GW46-09-2848	1/26/2009	UF	W	NA	CS	SW-846:8270C	108-60-1	Oxybis(1-chloropropane)[2,2'-]	<	10.5	ug/L	U	2.1	11	GELC	1	U	U_LAB	Y	BA	INV	57277782	871922	2459492
R-46	1220	09-761	GW46-09-2848	1/26/2009	UF	W	NA	DL	SW-846:8270C	108-60-1	Oxybis(1-chloropropane)[2,2'-]	<	104	ug/L	U	21	100	GELC	10	UJ	SV88	Y	BA	INV	57278112	871922	2459492
R-46	1220	09-761	GW46-09-2848	1/26/2009	UF	W	NA	DL	SW-846:8270C	87-86-5	Pentachlorophenol	<	104	ug/L	U	21	100	GELC	10	UJ	SV88	Y	BA	INV	57276882	871922	2459492
R-46	1220	09-761	GW46-09-2848	1/26/2009	UF	W	NA	CS	SW-846:8270C	87-86-5	Pentachlorophenol	<	10.5	ug/L	U	2.1	11	GELC	1	R	SV3	Y	BA	INV	57278842	871922	2459492
R-46	1220	09-761	GW46-09-2848	1/26/2009	UF	W	NA	CS	SW-846:8270C	85-01-8	Phenanthrene	<	1.05	ug/L	U	0.21	1.1	GELC	1	U	U_LAB	Y	BA	INV	57279132	871922	2459492
R-46	1220	09-761	GW46-09-2848	1/26/2009	UF	W	NA	DL	SW-846:8270C	85-01-8	Phenanthrene	<	10.4	ug/L	U	2.1	10	GELC	10	UJ	SV88	Y	BA	INV	57279392	871922	2459492
R-46	1220	09-761	GW46-09-2848	1/26/2009	UF	W	NA	DL	SW-846:8270C	108-95-2	Phenol	<	104	ug/L	U	10	100	GELC	10	UJ	SV88	Y	BA	INV	57278472	871922	2459492
R-46	1220	09-761	GW46-09-2848	1/26/2009	UF	W	NA	CS	SW-846:8270C	108-95-2	Phenol	<	10.5	ug/L	U	1.1	11	GELC	1	R	SV3	Y	BA	INV	57279052	871922	2459492
R-46	1220	09-761	GW46-09-2848	1/26/2009	UF	W	NA	CS	SW-846:8270C	129-00-0	Pyrene	<	1.05	ug/L	U	0.32	1.1	GELC	1	U	U_LAB	Y	BA	INV	57277072	871922	2459492
R-46	1220	09-761	GW46-09-2848	1/26/2009	UF	W	NA	DL	SW-846:8270C	129-00-0	Pyrene	<	10.4	ug/L	U	3.1	10	GELC	10	UJ	SV88	Y	BA	INV	57279112	871922	2459492
R-46	1220	09-761	GW46-09-2848	1/26/2009	UF	W	NA	CS	SW-846:8270C	110-86-1	Pyridine	<	10.5	ug/L	U	1.1	11	GELC	1	U	U_LAB	Y	BA	INV	57278992	871922	2459492
R-46	1220	09-761	GW46-09-2848	1/26/2009	UF	W	NA	DL	SW-846:8270C	110-86-1	Pyridine	<	104	ug/L	U	10	100	GELC	10	UJ	SV88	Y	BA	INV	57279672	871922	2459492
R-46	1220	09-761	GW46-09-2848	1/26/2009	UF	W	NA	DL	SW-846:8270C	120-82-1	Trichlorobenzene[1,2,4-]	<	104	ug/L	U	21	100	GELC	10	UJ	SV88	Y	BA	INV	57278772	871922	2459492
R-46	1220	09-761	GW46-09-2848	1/26/2009	UF	W	NA	CS	SW-846:8270C	120-82-1	Trichlorobenzene[1,2,4-]	<	10.5	ug/L	U	2.1	11	GELC	1	U	U_LAB	Y	BA	INV	57279172	871922	2459492
R-46	1220	09-761	GW46-09-2848	1/26/2009	UF	W	NA	DL	SW-846:8270C	95-95-4	Trichlorophenol[2,4,5-]	<	104	ug/L	U	10	100	GELC	10	UJ	SV88	Y	BA	INV	57278312	871922	2459492
R-46	1220	09-761	GW46-09-2848	1/26/2009	UF	W	NA	CS	SW-846:8270C	95-95-4	Trichlorophenol[2,4,5-]	<	10.5	ug/L	U	1.1	11	GELC	1	R	SV3	Y	BA	INV	57279702	871922	2459492
R-46	1220	09-761	GW46-09-2848	1/26/2009	UF	W	NA	DL	SW-846:8270C	88-06-2	Trichlorophenol[2,4,6-]	<	104	ug/L	U	21	100	GELC	10	UJ	SV88	Y	BA	INV	57279042	871922	2459492
R-46	1220	09-761	GW46-09-2848	1/26/2009	UF	W	NA	CS	SW-846:8270C	88-06-2	Trichlorophenol[2,4,6-]	<	10.5	ug/L	U	2.1	11	GELC	1	R	SV3	Y	BA	INV	57279222	871922	2459492

Note: Rows highlighted in yellow, blue, and red indicate detections of organic chemicals, quality assurance samples, and rejected samples, respectively.

# **Appendix C**

---

## *Aquifer Testing Report*



## C-1.0 INTRODUCTION

This appendix describes the hydraulic analysis of pumping tests at well R-46 located at Technical Area 63 (TA-63) on an unnamed mesa between Mortandad and Pajarito Canyons. The tests were conducted to establish well performance parameters and determine the hydraulic properties of the formation screened by R-46.

Testing consisted primarily of constant-rate pumping tests. During the tests, water levels were monitored only in the pumped well. The nearest wells in the area (R-14 and R-17) were about a half mile away and were not expected to show a response to pumping R-46.

Consistent with most of the R-well pumping tests conducted on the plateau, an inflatable packer system was used in R-46 to attempt to eliminate the effects of casing storage on the test data. However, as described below, there appeared to be a significant storage effect in the pumping response, likely caused by air in the filter pack behind the blank casing above the well screen. This could have been simple dewatering of the filter pack during operation or permanently trapped air in the filter pack opposite tight formation sediments above the screen. The storage phenomenon somewhat limited the analysis of the pumping test data.

### Conceptual Hydrogeology

R-46 is completed at the top of the regional aquifer within the Puye Formation. It is a single-screen completion with 20.7 ft of screen between 1340.0 and 1360.7 ft below ground surface (bgs). The static water level measured at the onset of testing was 12 ft above the top of the screen and 4 ft above the top of the filter pack, at 1328.0 ft bgs. The ground-surface elevation at R-46 was 7213 ft above mean sea level (amsl), putting the groundwater elevation at about 5885 feet amsl.

### R-46 Testing

R-46 was tested from March 7 to 12, 2009. Testing consisted of brief pumping on March 7 to fill the drop pipe and verify the flow rate and operation of the pumping equipment: two trial tests on March 8—background data collection and a 24-h constant-rate pumping test that was begun on March 10.

After brief pumping on March 7 to fill the drop pipe, identify the discharge rate, and evaluate the performance of the pumping equipment, two trial tests were conducted on March 8. Trial 1 was conducted at a discharge rate of 10.0 gpm for 59 min from 9:01 to 10:00 a.m. and was followed by 60 min of recovery until 11:00 a.m. Trial 2 was conducted at a flow rate of 9.5 gpm for 60 min until 12:00 p.m. Following shutdown, recovery data were recorded for 44 h, until 8:00 a.m. on March 10.

At 8:00 a.m. on March 10, the 24-h pumping test was begun at a rate a little over 10 gpm. During the test, the discharge rate declined somewhat. In addition, manual adjustments to the pumping rate were made for a period during the middle of the test as described below. Pumping continued until 8:00 a.m. on March 11. Following shutdown, recovery measurements were recorded for 1487 min until 8:47 a.m. on March 12.

### Aerated Water

During testing, small air bubbles were observed in the discharge water, indicating that the pumped water was slightly aerated. It is possible that air was forced into the aquifer during drilling and lodged in the formation pore spaces around the well and/or dissolved in the aquifer water. Pressure reduction during pumping may have allowed liberation of dissolved gasses or release of trapped air. It is also possible that the observed aeration may have been attributable to natural dissolved gas in the groundwater.

The gas content in the water had two apparent effects during the testing. First, the efficiency of the screened interval diminished slightly over time, likely a response to partial clogging of the pore spaces near the well bore with released gas. Second, the efficiency of the pump seemed to fluctuate (both up and down), likely as a function of the amount of gas pulled through the submersible pump. Running gas along with the water through a submersible pump can cause cavitation and affect the hydraulic performance of the pump in a chaotic way.

## C-2.0 BACKGROUND DATA

The background water-level data collected in conjunction with running the pumping tests allow the analyst to see what water-level fluctuations occur naturally in the aquifer and help distinguish between water-level changes caused by conducting the pumping test and changes associated with other causes.

Background water-level fluctuations have several causes, among them barometric pressure changes, operation of other wells in the aquifer, earth tides, and long-term trends related to weather patterns. The background data hydrographs from the monitored wells were compared with barometric pressure data from the area to determine if a correlation existed.

Previous pumping tests on the plateau have demonstrated a barometric efficiency for most wells between 90% and 100%. Barometric efficiency is defined as the ratio of water-level change divided by barometric pressure change, expressed as a percentage. In the initial pumping tests conducted on the early R-wells, downhole pressure was monitored using a *vented* pressure transducer. This equipment measures the difference between the total pressure applied to the transducer and the barometric pressure, this difference being the true height of water above the transducer.

Subsequent pumping tests, including R-46, have utilized *nonvented* pressure transducers. These devices simply record the total pressure on the transducer, that is, the sum of the water height plus the barometric pressure. This results in an attenuated "apparent" hydrograph in a barometrically efficient well. Take as an example a 90% barometrically efficient well. When monitored using a vented transducer, an *increase* in barometric pressure of 1 unit causes a *decrease* in recorded downhole pressure of 0.9 unit because the water level is forced downward 0.9 unit by the barometric pressure change. However, using a nonvented transducer, the total measured pressure *increases* by 0.1 unit (the combination of the barometric pressure increase and the water-level decrease). Thus, the resulting apparent hydrograph changes by a factor of 100 minus the barometric efficiency and in the same direction as the barometric pressure change, rather than in the opposite direction.

Barometric pressure data were obtained from TA-54 tower site from the Environmental Division—Meteorology and Air Quality Group (ENV-MAQ). The TA-54 measurement location is at an elevation of 6548 ft amsl, whereas the wellhead elevation is approximately 7213 ft amsl. The static water level was 1328 ft below land surface, making the water-table elevation roughly 5885 ft amsl. Therefore, the measured barometric pressure data from TA-54 had to be adjusted to reflect the pressure at the elevation of the water table within R-46.

The following formula was used to adjust the measured barometric pressure data:

$$P_{WT} = P_{TA54} \exp \left[ - \frac{g}{3.281R} \left( \frac{E_{R42} - E_{TA54}}{T_{TA54}} + \frac{E_{WT} - E_{R46}}{T_{WELL}} \right) \right]$$

Equation C-1

Where,  $P_{WT}$  = barometric pressure at the water table inside R-46,

$P_{TA54}$  = barometric pressure measured at TA-54,

$g$  = acceleration of gravity, in  $m/sec^2$  (9.80665  $m/sec^2$ ),

$R$  = gas constant, in  $J/Kg/degree$  Kelvin (287.04  $J/Kg/degree$  Kelvin),

$E_{R46}$  = land surface elevation at R-46 site, in feet (7213 ft),

$E_{TA54}$  = elevation of barometric pressure measuring point at TA-54, in feet (6548 ft),

$E_{WT}$  = elevation of the water level in R-46, in feet (approximately 5885 ft),

$T_{TA54}$  = air temperature near TA-54, in degrees Kelvin (assigned a value of 37.1 degrees Fahrenheit, or 276.0 degrees Kelvin), and

$T_{WELL}$  = air temperature inside R-46, in degrees Kelvin (assigned a value of 65.8 degrees Fahrenheit, or 291.9 degrees Kelvin).

This formula is an adaptation of an equation that ENV-MAQ provided. It can be derived from the ideal gas law and standard physics principles. An inherent assumption in the derivation of the equation is that the air temperature between TA-54 and the well is temporally and spatially constant and that the temperature of the air column in the well is similarly constant.

The corrected barometric pressure data reflecting pressure conditions at the water table were compared with the water-level hydrographs to discern the correlation between the two.

### C-3.0 IMPORTANCE OF EARLY DATA

When pumping or recovery first begins, the vertical extent of the cone of depression is limited to approximately the well screen length, the filter pack length, or the aquifer thickness in relatively thin permeable strata. For many pumping tests on the plateau, the early pumping period is the only time that the effective height of the cone of depression is known with certainty. Thus, the early data often offer the best opportunity to obtain hydraulic conductivity information because conductivity would equal the earliest-time transmissivity divided by the well screen length.

Unfortunately, in many pumping tests, casing storage effects dominate the early-time data, hindering the effort to determine the transmissivity of the screened interval. The duration of casing-storage effects can be estimated using the following equation (Schafer 1978, 098240).

$$t_c = \frac{0.6(D^2 - d^2)}{\frac{Q}{s}}$$

Equation C-2

Where,  $t_c$  = duration of casing storage effect, in minutes,

$D$  = inside diameter of well casing, in inches,

$d$  = outside diameter of column pipe, in inches,

$Q$  = discharge rate, in gallons per minute, and

$s$  = drawdown observed in pumped well at time  $t_c$ , in feet.

In some instances, it is possible to eliminate casing-storage effects by setting an inflatable packer above the tested screen interval before conducting the test. Therefore, this option has been implemented for the R-well testing program, including the R-46 pumping tests. As described below, however, antecedent drainage of a portion of the filter pack or simple dewatering and resaturation of the pack during pumping and recovery may have left air pockets in places that contributed to a casing-storage-like effect. This limited the range of analysis that could be applied and conclusions that could be drawn from the R-46 pumping test data.

#### C-4.0 TIME-DRAWDOWN METHODS

Time-drawdown data can be analyzed using a variety of methods. Among them is the Theis method (1934-1935, 098241). The Theis equation describes drawdown around a well as follows:

$$s = \frac{114.6Q}{T} W(u) \quad \text{Equation C-3}$$

Where,

$$W(u) = \int_u^{\infty} \frac{e^{-x}}{x} dx \quad \text{Equation C-4}$$

and

$$u = \frac{1.87r^2S}{Tt} \quad \text{Equation C-5}$$

and where,  $s$  = drawdown, in feet,

$Q$  = discharge rate, in gallons per minute,

$T$  = transmissivity, in gallons per day per foot,

$S$  = storage coefficient (dimensionless),

$t$  = pumping time, in days, and

$r$  = distance from center of pumpage, in feet.

To use the Theis method of analysis, the time-drawdown data are plotted on log-log graph paper. Then, Theis curve matching is performed using the Theis type curve—a plot of the Theis well function  $W(u)$  versus  $1/u$ . Curve matching is accomplished by overlaying the type curve on the data plot and, while keeping the coordinate axes of the two plots parallel, shifting the data plot to align with the type curve, effecting a match position. An arbitrary point, referred to as the match point, is selected from the overlapping parts of the plots. Match-point coordinates are recorded from the two graphs, yielding four values:  $W(u)$ ,  $1/u$ ,  $s$ , and  $t$ . Using these match-point values, transmissivity and storage coefficient are computed as follows:

$$T = \frac{114.6Q}{s} W(u) \quad \text{Equation C-6}$$

$$S = \frac{Tut}{2693r^2}$$

Equation C-7

Where,  $T$  = transmissivity, in gallons per day per foot,

$S$  = storage coefficient,

$Q$  = discharge rate, in gallons per minute,

$W(u)$  = match-point value,

$s$  = match-point value, in feet,

$u$  = match-point value, and

$t$  = match-point value, in minutes.

An alternative solution method applicable to time-drawdown data is the Cooper–Jacob method (1946, 098236), a simplification of the Theis equation that is mathematically equivalent to the Theis equation for most pumped well data. The Cooper–Jacob equation describes drawdown around a pumping well as follows:

$$s = \frac{264Q}{T} \log \frac{0.3Tt}{r^2S}$$

Equation C-8

The Cooper–Jacob equation is a simplified approximation of the Theis equation and is valid whenever the  $u$  value is less than about 0.05. For small radius values (e.g., corresponding to borehole radii),  $u$  is less than 0.05 at very early pumping times and therefore is less than 0.05 for most or all measured drawdown values. Thus, for the pumped well, the Cooper–Jacob equation usually can be considered a valid approximation of the Theis equation.

According to the Cooper–Jacob method, the time-drawdown data are plotted on a semilog graph, with time plotted on the logarithmic scale. Then a straight line of best fit is constructed through the data points and transmissivity is calculated using

$$T = \frac{264Q}{\Delta s}$$

Equation C-9

Where,  $T$  = transmissivity, in gallons per day per foot,

$Q$  = discharge rate, in gallons per minute, and

$\Delta s$  = change in head over one log cycle of the graph, in feet.

### C-5.0 RECOVERY METHODS

Recovery data were analyzed using the Theis recovery method. This is a semilog analysis method similar to the Cooper–Jacob procedure.

In this method, residual drawdown is plotted on a semilog graph versus the ratio  $t/t'$ , where  $t$  is the time since pumping began and  $t'$  is the time since pumping stopped. A straight line of best fit is constructed through the data points and  $T$  is calculated from the slope of the line as follows:

$$T = \frac{264Q}{\Delta s}$$

Equation C-10

The recovery data are particularly useful compared with time-drawdown data. Because the pump is not running, spurious data responses associated with dynamic discharge rate fluctuations are eliminated. The result is that the data set is generally "smoother" and easier to analyze.

### C-6.0 SPECIFIC CAPACITY METHOD

The specific capacity of the pumped well can be used to obtain a lower-bound value of hydraulic conductivity. The hydraulic conductivity is computed using formulas that are based on the assumption that the pumped well is 100% efficient. The resulting hydraulic conductivity is the value required to sustain the observed specific capacity. If the actual well is less than 100% efficient, it follows that the actual hydraulic conductivity would have to be greater than calculated to compensate for well inefficiency. Thus, because the efficiency is unknown, the computed hydraulic conductivity value represents a lower bound. The actual conductivity is known to be greater than or equal to the computed value.

For fully penetrating wells, the Cooper-Jacob equation can be iterated to solve for the lower-bound hydraulic conductivity. However, the Cooper-Jacob equation (assuming full penetration) ignores the contribution to well yield from permeable sediments above and below the screened interval. To account for this contribution, it is necessary to use a computation algorithm that includes the effects of partial penetration. One such approach was introduced by Brons and Marting (1961, 098235) and augmented by Bradbury and Rothchild (1985, 098234).

Brons and Marting introduced a dimensionless drawdown correction factor,  $s_p$ , approximated by Bradbury and Rothschild as follows:

$$s_p = \frac{1 - \frac{L}{b}}{\frac{L}{b}} \left[ \ln \frac{b}{r_w} - 2.948 + 7.363 \frac{L}{b} - 11.447 \left( \frac{L}{b} \right)^2 + 4.675 \left( \frac{L}{b} \right)^3 \right]$$

Equation C-11

Where,  $s_p$  = partial penetration correction, dimensionless,

$L$  = well screen length, in feet,

$b$  = aquifer thickness, in feet, and

$r_w$  = radius of the pumping well, in feet.

In this equation,  $L$  is the well screen length in feet. Incorporating the dimensionless drawdown parameter, the conductivity is obtained by iterating the following formula:

$$K = \frac{264Q}{sb} \left( \log \frac{0.3Tt}{r_w^2 S} + \frac{2s_p}{\ln 10} \right)$$

Equation C-12

Where,  $K$  = hydraulic conductivity, in feet per day,

$Q$  = flow rate, in gallons per minute,

$T$  = transmissivity, in gallons per day per foot,

$t$  = time, in minutes,

$Sp$  = partial penetration correction, dimensionless,

$s$  = drawdown, in feet,

$b$  = aquifer thickness, in feet,

$r_w$  = radius of the pumping well, in feet, and

$S$  = storage coefficient, dimensionless.

To apply this procedure, a storage coefficient value must be assigned. Unconfined conditions were assumed for R-46 with the static water level passing through the Puye sediments just above the screen. Storage coefficient values for unconfined conditions can be expected to range from about 0.01 to 0.25, depending on sediment makeup (Driscoll 1986, 104226). The calculation result is not particularly sensitive to the choice of storage coefficient value, so a rough estimate of the storage coefficient is generally adequate to support the calculations. An assumed value of 0.1 was used for R-46.

The analysis also requires assigning a value for the saturated aquifer thickness,  $b$ . For calculation purposes, the aquifer thickness of 100 ft was used. The computed result is not particularly sensitive to the exact aquifer thickness because sediments far above or below the screen have little effect on yield and drawdown response. Therefore, the calculation based on the assumed aquifer thickness value was deemed to be adequate.

Computing the lower-bound estimate of hydraulic conductivity can provide a useful frame of reference for evaluating the other pumping test calculations.

### C-7.0 BACKGROUND DATA ANALYSIS

Background aquifer pressure data collected during the R-46 tests were plotted along with barometric pressure to determine the barometric effect on water levels.

Figure C-7.0-1 shows aquifer pressure data from R-46 along with barometric pressure data from TA-54 that have been corrected to equivalent barometric pressure at the water table in feet of water. The R-46 data are referred to in the figure as the "apparent hydrograph" because the measurements reflect the sum of water pressure and barometric pressure, having been recorded using a nonvented pressure transducer. The times of the pumping periods for the R-46 pumping tests are included on the figure for reference.

From Figure C-7.0-1 it can be seen that the fluctuation in the apparent hydrograph was substantially less than the barometric pressure change, implying a high barometric efficiency. The most prominent feature of the apparent hydrograph was the steady diurnal signal having a magnitude of a few hundredths of a foot. This is typical of the response to earth tides commonly seen in regional wells on the plateau.

The barometric pressure curve also showed a diurnal effect as evidenced by the appearance of two relative peaks in the observed pressure each day. They were more erratic, however, than the regular-appearing hydrograph signal. Because of the diurnal barometric pressure pattern, there was some uncertainty regarding the true cause of the hydrograph signal.

The barometric pressure curve was corrected for barometric efficiency and lag time in an attempt to better correlate it to the hydrograph. Figures C-7.0-2 and C-7.0-3 show the results obtained for a barometric efficiency of 75% and a time lag of 9 h, for both nonsmoothed and smoothed data, respectively. The smoothed data in Figure C-7.0-3 were based on a 6-h rolling average of the barometric pressure measurements.

In Figures C-7.0-2 and C-7.0-3, the correlation between barometric pressure and the apparent hydrograph was inconsistent. For example, the sinusoidal responses on March 11 and 12 were in phase, showing good correlation. On the other hand, much of the sinusoidal hydrograph response was absent from the barometric pressure curve on March 8 and 9, and portions of those signals appeared to be out of phase. This observation limited the confidence that could be placed in the attempted correlations shown in Figures C-7.0-2 and C-7.0-3. Once R-46 is put online and monitored continually, the additional water-level data collected should be used to better define the effect of atmospheric pressure and earth tides on aquifer pressure.

Note that there was an offset between the hydrograph and modified barometric pressure curve from March 7 to early March 8. This may have been related to inflation of the packer that occurred late morning on March 8. It is not uncommon for the packer inflation procedure to cause an offset in the resulting hydrograph data set, perhaps because of stretching or compression of the drop pipe that may occur as the packer grips the inner sidewall of the well casing and continues to expand against the overlying pipe string.

The run times for PM-5, the municipal production well nearest R-46, were included in Figure C-7.0-3 to check for drawdown effects in R-46 caused by operation of PM-5. Quite clearly, pumping PM-5 did not affect water levels in R-46. Water levels *rose* in R-46 during a few of the PM-5 operating cycles. At other times, the same fluctuations were observed in R-46 when PM-5 was idle.

The questionable correlation implied by Figures C-7.0-2 and C-7.0-3 lent credibility to the idea that earth tides were key in affecting the hydrograph data. No correction for earth tides was made to the data. As discussed below, this did not affect interpretation of the pumping test data.

## **C-8.0 R-46 DATA ANALYSIS**

This section presents the data obtained from the R-46 pumping tests and the results of the analytical interpretations. Data are presented for drawdown and recovery for trials 1 and 2 as well as the 24-h constant-rate pumping test.

### **Specific Capacity Data**

Specific capacity data were used along with well geometry to estimate a lower-bound conductivity value for R-46 for comparison to the pumping test values. This helped provide a frame of reference for guiding and evaluating the subsequent calculations.

As described below, the efficiency of R-46 seemed to decline with increased pumping. Therefore, early data offered the best estimate of a lower-bound hydraulic conductivity value before subsequent efficiency reduction further biased the resulting value downward. Therefore, data from trial 1 were used to estimate the lower-bound hydraulic conductivity value. Further, data from early in the pumping period were utilized, as some efficiency reduction occurred during the latter stages of trial 1.



In addition to specific capacity, other input values used in the calculations included the aquifer thickness, arbitrarily assigned a value of 100 ft, a storage coefficient estimated at 0.1, and a borehole radius of 0.51 ft. The calculations are somewhat insensitive to the assigned aquifer thickness, as long as the selected value is substantially greater than the screen length. Also, the choice of storage coefficient can be somewhat arbitrary, having only a minor effect on the calculated result.

Early in trial 1, R-46 produced 10.05 gpm with a drawdown of 9.25 ft after 20 min of pumping for a specific capacity of 1.09 gpm/ft. Applying the Brons and Marting method to these inputs yielded a lower-bound hydraulic conductivity value for the screened interval of 40.6 gpd/ft<sup>2</sup>, or 5.4 ft/d. This value was used in assessing the subsequent computations of aquifer parameters.

### **Trial 1**

Trial 1 was conducted at a discharge rate of 10.0 gpm for 59 min. Figure C-8.0-1 shows a semilog plot of the trial 1 drawdown data. The transmissivity computed from the early data was 1010 gpd/ft. Assuming that this value corresponded to a sediment thickness roughly equal to the screen length of 20.7 ft, this corresponded to a hydraulic conductivity 48.8 gpd/ft<sup>2</sup>, or 6.5 ft/d, consistent with the lower-bound hydraulic conductivity value obtained from the specific capacity of the well.

Within a minute of starting the pump, the slope of the data trace steepened, consistent with what would be expected when storage effects are present. Expansion of trapped air in the filter pack could have caused the observed response. If this were the cause of the increase in slope of the drawdown graph, it would have rendered the transmissivity calculation invalid. Under such circumstances, any correspondence between the resulting hydraulic conductivity value and that obtained from the specific capacity of the well would be coincidental.

After a minute and a half, the drawdown curve began flattening, consistent with both casing-storage response and vertical expansion of the cone of depression through the underlying Puye sediments. Indeed, the drawdown level appeared to stabilize about 15 min into the test. Such stabilization is common in many of the R-wells completed in thick, permeable sediments of the Puye Formation.

After 15 min, however, the slope of the drawdown curve began increasing again. Subsequent recovery data, described next, showed that continued stabilization (curve flattening) should have occurred, rather than ongoing steepening of the curve. The actual drawdown response implied a loss of well efficiency at extended pumping time, most likely related to numerous tiny air bubbles observed in the discharge water. It was likely that some of the air was accumulating in the pore spaces around the well bore, reducing the permeability of the near-well sediments.

Figure C-8.0-2 shows the recovery response recorded following the trial 1 pump shutoff. The data showed a pronounced storage effect greater than that observed in the drawdown data. The transition from the early flat slope (right side of graph) to the steep intermediate slope was characteristic of storage effects—presumably related to compression of air that was trapped in the filter pack or simple refilling of a portion of the filter pack that had become dewatered during pumping. The transmissivity shown on the graph is not a true value and is clearly erroneous. It has been included just to emphasize and confirm that storage has affected the data. Any valid analysis would have to be restricted to the late data, discussed below.

According to the well completion information, the top of the permeable transition sand above the filter pack was at a level 1332 ft bgs, just 4 ft below the static water level. Thus, depending on the permeability of the sediments above the well screen, it was possible that pulling down the water level several feet during pumping could have drawn air from the vadose zone into the filter pack. The presence of air in the

filter pack would have caused a significant storagelike effect in the subsequent recovery data, as suggested by Figure C-8.0-2.

Figure C-8.0-3 shows a comparison of time-drawdown and time-recovery data from trial 1. Normally, the two curves should be similar and, at early time, identical. Actually, the two curves were different.

The early-recovery data showed a more sluggish response than the early-drawdown data, that is, a more pronounced storage effect. There was less recovery at early time than there had been drawdown at a comparable pumping time. This response was consistent with the idea of additional air being drawn into the filter pack during pumping.

However, it also was consistent with the presence of a fixed volume of air in the filter pack that may have expanded during pumping and contracted during recovery. In this latter scenario, a given impetus (water-level change) would be applied to a smaller, higher-pressure air volume during the pumping phase and thus the storage effect would be relatively less. During recovery, on the other hand, the starting air volume would have been greater (caused by the air expanding during antecedent pumping) and its pressure would have been less. Therefore, a given impetus would have caused a greater air volume change at early-recovery time than was seen at early pumping time.

From the available data, it was not possible to determine whether air was drawn into the filter pack during pumping and expelled, to some extent, during recovery, or simply expanded and contracted in response to pumping and recovery.

The late-recovery data in Figures C-8.0-2 and C-8.0-3 showed a steady, continuous flattening of the response curves in contrast to the slope increase observed in the drawdown data. This suggested that there may have been efficiency degradation during the pumping period.

The area of the graph where the recovery magnitude exceeded the drawdown magnitude could have had a hysteresis component also. In unconfined aquifers, rate of recovery can be more rapid than that of drawdown because of a smaller effective storage coefficient during recovery. During pumping, the capillary fringe above the water table increases in thickness, while during recovery it gets thinner (Bevan et al. 2005, 105186). If the rate of thinning during recovery exceeds the rate of growth during pumping, the effective storage coefficient during recovery will be less than that during pumping, resulting in a more rapid recovery rate than drawdown rate. Additionally, as the water table rebounds during recovery, it can trap air in the previously dewatered pore spaces, further decreasing the effective recovery storage coefficient.

Figure C-8.0-4 shows an expanded-scale graph of the late-recovery data. It was clear that the slope of the curve continued to decrease over time, as the cone of impression expanded vertically beyond the screened interval. The late data in Figure C-8.0-4, extending to an hour after pump shutoff, revealed a transmissivity of 6320 gpd/ft. There was no way to determine the corresponding height of the cone of impression to allow calculating a hydraulic conductivity value.

### **Trial 2**

Trial 2 was conducted at a discharge rate of 9.5 gpm for 60 min. Figure C-8.0-5 shows a semilog plot of the trial 2 drawdown data. The usual storage effect was present as the overall s-shaped curve, with the late data showing flattening associated with the cessation of storage and vertical expansion of the cone of depression.

An attempt was made to use the very early drawdown data to compute a transmissivity value. It was hoped that the first few data points might support a valid analysis because of a possible delay in draining the filter pack. The storage phenomenon in this case depended on the expansion of the trapped air in the

filter pack, which in turn depended on physical drainage of the water in the filter pack beneath the trapped air. It was suspected that a slight delay in the drainage due to inertial effects might produce a few valid data points that could be analyzed.

Examination of Figure C-8.0-5 showed initial drawdown (before 1 s), followed by a brief transient flattening. It was hypothesized that the flattening was associated with delayed drainage of the filter pack and that the preceding data might support a valid analysis.

As shown in Figure C-8.0-5, the transmissivity value determined from the early data points was 1910 gpd/ft. However, the low drawdown magnitude of the first data point suggested the possibility that the  $u$ -value condition of the Cooper–Jacob equation might be violated, invalidating the semilog analysis. To account for this possibility, a Theis analysis was performed on the early data. Figure C-8.0-6 shows the resulting data plot.

The transmissivity computed from the early data in Figure C-8.0-6 was 1350 gpd/ft. This value differed from that in Figure C-8.0-5, confirming that the semilog analysis was not valid. Assuming that the resulting transmissivity value corresponded to a sediment thickness roughly equal to the screen length of 20.7 ft, the hydraulic conductivity was 65.2 gpd/ft<sup>2</sup>, or 8.7 ft/d, roughly consistent with the lower-bound hydraulic conductivity value obtained from the specific capacity of the well (5.4 ft/d).

The final drawdown at the end of trial 2 shown in Figure C-8.0-5 was 9.94 ft at the indicated pumping rate of 9.5 gpm. During trial 1, the well was pumped at 10.0 gpm with the same 9.94 ft of drawdown. Thus, the specific capacity of the well declined about 5% during trial 2. Recall also that it already had declined by some amount during the latter stages of the trial 1 test. Both episodes of yield and efficiency reduction were likely related to clogging of the pore spaces around the well bore with the gas that was observed being produced with the groundwater.

Figure C-8.0-7 shows the recovery data obtained after shutdown of trial 2. The s-shaped response curve showed a pronounced storage effect yielding the erroneous transmissivity value shown on the graph. As pointed out previously for the trial 1 test, the transmissivity shown on the graph is not a true value and is clearly erroneous. It has been included just to emphasize and confirm that storage has affected the data. Any valid analysis would have to be restricted to the late data, discussed below.

At an early time, the "ripple" that had been evident in the drawdown graph, apparently associated with inertial effects (delayed drainage of the water in the filter pack), was not present. The reason for this was not known, although it may have been related to the much shorter water column above the screen at the time of pump shutoff as opposed to start-up. The early-recovery data were not used to support a determination of transmissivity.

As shown in Figure C-8.0-7, the late-recovery data showed a steady flattening over time, consistent with ongoing vertical expansion of the cone of impression into sediments beneath the well.

Figure C-8.0-8 shows a comparison of the time-drawdown and time-recovery data from trial 2. As was the case with trial 1, the storage effect was greater in the recovery data (more sluggish response) as the relatively greater air volume and lower air pressure were more effective at absorbing hydraulic head changes in the well at the onset of pumping. The relatively flatter slope of the middle data in the time-drawdown plot was attributable to the gradual efficiency reduction with time. Finally, at late time the recovery data showed continued flattening associated with vertical expansion of the cone of impression. The drawdown data showed a steeper late-time slope because of ongoing efficiency reduction.

As described previously, the area of the graph where the recovery magnitude exceeded the drawdown magnitude could have had a hysteresis component also. The reduced storage coefficient associated with hysteresis and possible trapping of air in the formation pores during water-table rebound could have contributed to the relatively more rapid recovery response as compared with the drawdown response.

Figure C-8.0-9 shows an expanded-scale plot of the late-recovery data. The line of fit corresponding to the first hour of recovery revealed a transmissivity of 6270 gpd/ft, similar to what was obtained from trial 1. Subsequent data, covering several hours of recovery, showed a transmissivity value of 13,900 gpd/ft, representing an even greater, yet still unknown, sediment thickness.

After several hours of recovery, any subtle change in residual drawdown was obscured by background effect—earth tides and barometric pressure changes. A cursory examination of the data indicated that the ongoing residual drawdown change was only on the order of a hundredth of a foot or less—a small fraction of the magnitude of the background noise in the data set. This implied a large transmissivity for the Puye sediments beneath R-46 and precluded a rigorous analysis of the late data because errors resulting from data corrections likely would have exceeded the sought change in residual drawdown. The complete recovery implied a good connection between the R-46 sediments and the greater regional aquifer. Also of note was the possibility that full recovery was achieved quickly because of a reduced storage coefficient during recovery associated with hysteresis and trapped air in the former cone of depression during water-table rebound.

#### **C-8.1 R-46 24-H Constant-Rate Pumping Test**

Figure C-8.1-1 shows a semilog plot of the drawdown data recorded during the 24-h constant-rate pumping test conducted at R-46. There are a number of important features of the graph that require explanation.

The very early data showed the ripple effect seen in trial 2 presumably associated with brief delay in water draining from the filter pack. It was hoped that the earliest data would support a valid determination of the transmissivity of the screen zone, similar to the analysis performed for trial 2.

After a few minutes of pumping, the drawdown curve began leveling off in response to cessation of storage effects and vertical growth of the cone of depression.

About 40 min into the test, a slight offset appeared in the drawdown data. This corresponded to a minor pumping rate reduction that occurred when the discharge hose was elevated an additional 12 ft to reach the entry port on the frac tank used to store the pumped water.

Between about 40 and 300 min, the measured discharge rate declined gradually from 9.7 to 9.2 gpm. At the time, the steady decline in flow rate suggested the possibility that the pumping water level had reached the pump intake and that cavitation was occurring (possibly damaging to the pump). Because of this possibility, the discharge rate was cut back to below 8 gpm in hopes of alleviating this condition. However, after partially closing the valve, the discharge rate still continued to decline slowly. It was concluded that the pump had not been breaking suction previously and that there must have been another cause of the observed performance. Therefore, the discharge valve was reopened so that the maximum discharge rate could be obtained. The “square wave” on the drawdown graph indicates the time period when the pumping rate was temporarily cut back.

Between 40 and 300 min, the increase in drawdown and pumping water level was not sufficient to cause the flow rate reductions measured at the well head. Therefore, it was possible that the pump efficiency had degraded slowly over time because of air/gas being drawn into the pump, affecting pump operation.

An alternate possibility was that air entrainment (the bubbles observed in the discharge water) was affecting the accuracy of the flow meter. Either explanation meant that a dynamic change in the gas content of the pumped water was occurring.

After the valve was reopened to maximize the discharge rate, the measured pumping rate increased gradually from 8.2 to 9.4 gpm, as shown in Figure C-8.1-1. The substantial increase in drawdown shown on the graph implied the likelihood that the rate actually was increasing and the observation was not an artifact of entrained gas affecting operation of the flow meter. Again, the data revealed a dynamic effect associated with running gas bubbles through the submersible pump.

Taking the discharge rates at face value, the computed specific capacity of R-46 declined steadily during both periods of interest before temporarily closing the discharge valve and after reopening it.

Note that the hydraulic head in the pumped well was pulled below the top of the well screen, estimated to be about 12 ft below the static water level. Curiously, there was no temporary stabilization of the water level as it passed that depth. Normally, if the top of the screen is dewatered and exposed to atmospheric pressure, air will rise into the blank casing, draining the portion of the casing between the packer and the top of the screen. The transient source of suspended water just under the packer looks like a transient recharge source in the data set. This response was not seen. What's more, the pump intake was estimated to be just above the top of the screen, meaning that the pumping water level was pulled about a 1.5 ft below the pump intake. This implied that a vacuum had been maintained inside the casing above the well screen, keeping the true water level from reaching the top of the screen. Apparently, formation water entering the filter pack just above the screen maintained complete saturation in that zone, keeping air in the filter pack from reaching the well screen and breaking the vacuum.

The transmissivity computed from the very early data in Figure C-8.1-1 was 1090 gpd/ft. However, as with trial 2, because of the minimal drawdown and early pumping time, there was doubt that the  $u$ -value condition of the Cooper–Jacob equation was satisfied. To check this, the data were plotted on a log-log graph and analyzed using Theis curve matching.

Figure C-8.1-2 shows the Theis curve match obtained from the early data. The analysis yielded a transmissivity value of 850 gpd/ft. This was different than that obtained from Figure C-8.1-1, confirming that the semilog analysis was not valid and that the log-log plot must be used.

Assuming that the resulting transmissivity value corresponded to a sediment thickness roughly equal to the screen length of 20.7 ft, the hydraulic conductivity was 41.1 gpd/ft<sup>2</sup>, or 5.5 ft/d, consistent with the lower-bound hydraulic conductivity value obtained from the early specific capacity of the well (5.4 ft/d).

Figure C-8.1-3 shows the recovery data obtained after shutdown of the 24-h test. The s-shaped response curve showed a pronounced storage effect yielding the erroneous transmissivity value shown on the graph. As pointed out previously for the trial 1 and 2 tests, the transmissivity shown on the graph is not a true value and is clearly erroneous. It has been included just to emphasize and confirm that storage has affected the data. Any valid analysis would have to be restricted to the late data, discussed below.

At an early time, the ripple that had been evident in the drawdown graph, apparently associated with inertial effects (delayed drainage of the water in the filter pack), was not present, similar to the trial 2 recovery data. The reason for this was not known, although it may have been related to the much shorter water column above the screen at the time of pump shutoff as opposed to start-up. The early-recovery data were not used to support a determination of transmissivity.

As shown in Figure C-8.1-3, the late-recovery data showed a steady flattening over time, consistent with ongoing vertical expansion of the cone of impression into sediments beneath the well.

Figure C-8.1-4 shows a comparison of the time-drawdown and time-recovery data from the 24-h test. As was the case with trials 1 and 2, the storage effect was greater in the recovery data (more sluggish response at early time) as the relatively greater air volume in the filter pack was more effective at absorbing hydraulic head changes. The relatively flatter slope of the middle data in the time-drawdown plot was attributable to the gradual efficiency reduction with time. Finally, at late time the recovery data showed continued flattening associated with vertical expansion of the cone of impression. The drawdown data showed a steeper late-time slope because of ongoing efficiency reduction.

As described previously, the area of the graph where the recovery magnitude exceeded the drawdown magnitude could have had a hysteresis component also. The reduced storage coefficient associated with hysteresis and possible trapping of air in the formation pores during water table rebound could have contributed to the relatively more rapid recovery response as compared with drawdown response.

Figure C-8.1-5 shows an expanded-scale plot of the late-recovery data from the 24-h test. The line of fit corresponding to the first hour of recovery revealed a transmissivity of 6800 gpd/ft, similar to what was obtained from trials 1 and 2. Subsequent data, covering an additional hour of recovery showed a transmissivity value of 15,300 gpd/ft, representing an even greater, yet still unknown, sediment thickness.

After 2 to 3 h of recovery, any subtle change in residual drawdown was obscured by background effects—earth tides and barometric pressure changes. A cursory examination of the data suggested that the ongoing residual drawdown change was only on the order of a hundredth of a foot or less, a small fraction of the magnitude of the background noise in the data set. This implied a large transmissivity for the Puye sediments beneath R-46 and precluded a rigorous analysis of the late data because errors resulting from data corrections would have exceeded the sought change in residual drawdown. Again of note was the possibility that full recovery was achieved quickly because of a reduced storage coefficient during recovery associated with hysteresis and trapped air in the former cone of depression during water table rebound.

Figure C-8.1-6 shows a plot of the recovery data from all three pumping tests: trial 1, trial 2, and the 24-h test. In theory, if the discharge rates were equal, all three curves should coincide. The slight differences in the actual flow rates (10.0, 9.5, and 9.2 gpm) meant that the curves should nearly coincide but be separated just slightly.

The recovery curves from trials 1 and 2 actually coincided exactly. Even though the discharge rates were different, the degradation in efficiency in trial 2 produced the same drawdown that had been observed in trial 1. Furthermore, the durations of the tests were nearly the same. Given these conditions, exact coincidence of the recovery curves, as opposed to a slight difference, indicated that the responses were storage-dominated.

Similarly, the 24-h test recovery, which had a different duration and started from a different drawdown level, followed an entirely different trace than the other curves. Again, this was an indication of storage-dominated response. Without storage effects, the 24-h recovery would have mirrored the other recovery curves but with slightly less drawdown (in direct proportion to the test pumping rates).

## C-9.0 SUMMARY

Constant-rate pumping tests were conducted on R-46 at TA-63 on an unnamed mesa between Mortandad and Pajarito Canyons. The tests were conducted to gain an understanding of the hydraulic characteristics of the aquifer and the production parameters of the well. Numerous observations and conclusions were drawn for the tests as summarized below.

- Water-level data from R-46 indicated a barometric efficiency of about 75%. The data also indicated a strong earth-tide response.

- The water produced from R-46 was aerated as gas apparently escaped from solution at surface pressure. The presence of the gas at times affected the production rate of the submersible pump used for testing. The gas also apparently clogged the pore spaces around the well bore, reducing the efficiency of R-46 continuously throughout the test period.
- The source of the gas could have been natural or could have been forced into the aquifer during drilling. It was not related to development operations, as the well was pumped at a modest rate during development, which would not have imparted air to the formation.
- Early on, R-46 produced a specific capacity of more than 1 gpm/ft, implying a lower-bound hydraulic conductivity value of 5.4 ft/d for the screened interval.
- Draining and refilling of the filter pack, or expansion and contraction of air trapped in the filter pack, during pumping and recovery caused the data sets to be dominated by storage effects. This limited the analyses that could be applied to the data.
- Very early pumping data from trials 1 and 2 and the 24-h pumping test indicated a hydraulic conductivity of the screened sediments averaging about 6.9 ft/d, consistent with the computed lower-bound value.
- The cone of depression (and impression) continued to expand vertically throughout pumping (and recovery). Based on recovery data, after about an hour, the cone of impression intercepted sediments having a transmissivity of about 6500 gpd/ft. After a few hours, the height of the cone of impression corresponded to a transmissivity of more than 14,000 gpd/ft. There was no way to know what thickness of sediments corresponded to these transmissivity values. After several hours, the recovery curve flattened almost completely, getting obscured by the background water-level fluctuations. The late data corresponded to a large transmissivity, possibly some tens of thousands of gallons per day per foot at the R-46 location.
- The complete recovery of water levels suggested good connection of the R-46 sediments to the greater regional aquifer.
- The rapid complete recovery may have resulted, in part, to a reduced storage coefficient during recovery compared with drawdown, caused by hysteresis effects associated with changes in the thickness of the capillary fringe as well as incomplete resaturation of the cone of depression (trapping air in the pore spaces) during rebound of the water table.
- Hysteresis effects (the capillary fringe thinning more rapidly during recovery than it thickens during pumping) can result in a reduced storage coefficient during recovery and therefore faster recovery than drawdown. A comparison of drawdown and recovery for the R-46 tests suggested the possibility of a hysteresis component in the response.

#### C-10.0 REFERENCES

*The following list includes all documents cited in this appendix. Parenthetical information following each reference provides the author(s), publication date, and ER ID number. This information is also included in text citations. ER ID numbers are assigned by the Environmental Programs Directorate's Records Processing Facility (RPF) and are used to locate the document at the RPF and, where applicable, in the master reference set.*

*Copies of the master reference set are maintained at the NMED Hazardous Waste Bureau and the Directorate. The set was developed to ensure that the administrative authority has all material needed to review this document, and it is updated with every document submitted to the administrative authority. Documents previously submitted to the administrative authority are not included.*

- Bevan, M.J., A.L. Endres, D.L. Rudolph, and G. Parkin, December 2005. "A Field Scale Study of Pumping-Induced Drainage and Recovery in an Unconfined Aquifer," *Journal of Hydrology*, Vol. 315, No. 1-4, pp. 52-70. (Bevan et al. 2005, 105186)
- Bradbury, K.R., and E.R. Rothschild, March-April 1985. "A Computerized Technique for Estimating the Hydraulic Conductivity of Aquifers from Specific Capacity Data," *Ground Water*, Vol. 23, No. 2, pp. 240-246. (Bradbury and Rothschild 1985, 098234)
- Brons, F., and V.E. Marting, 1961. "The Effect of Restricted Fluid Entry on Well Productivity," *Journal of Petroleum Technology*, Vol. 13, No. 2, pp. 172-174. (Brons and Marting 1961, 098235)
- Cooper, H.H., Jr., and C.E. Jacob, August 1946. "A Generalized Graphical Method for Evaluating Formation Constants and Summarizing Well-Field History," *American Geophysical Union Transactions*, Vol. 27, No. 4, pp. 526-534. (Cooper and Jacob 1946, 098236)
- Driscoll, F.G., 1986. Excerpted pages from *Groundwater and Wells*, 2nd Ed., Johnson Filtration Systems Inc., St. Paul, Minnesota. (Driscoll 1986, 104226)
- Schafer, D.C., January-February 1978. "Casing Storage Can Affect Pumping Test Data," *The Johnson Drillers Journal*, pp. 1-6, Johnson Division, UOP, Inc., St. Paul, Minnesota. (Schafer 1978, 098240)
- Theis, C.V., 1934-1935. "The Relation Between the Lowering of the Piezometric Surface and the Rate and Duration of Discharge of a Well Using Ground-Water Storage," *American Geophysical Union Transactions*, Vol. 15-16, pp. 519-524. (Theis 1934-1935, 098241)



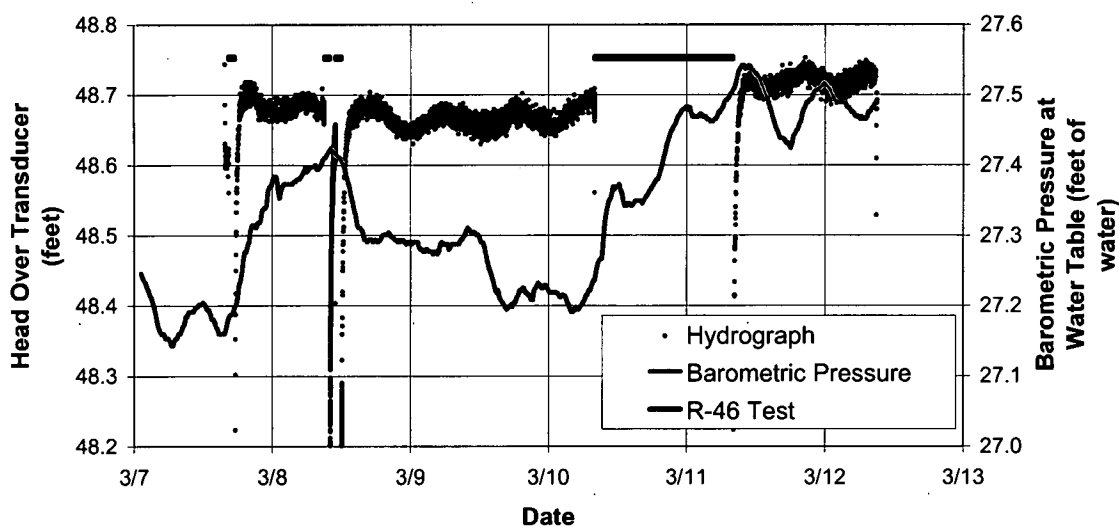


Figure C-7.0-1 Comparison of R-46 apparent hydrograph and adjusted TA-54 barometric pressure

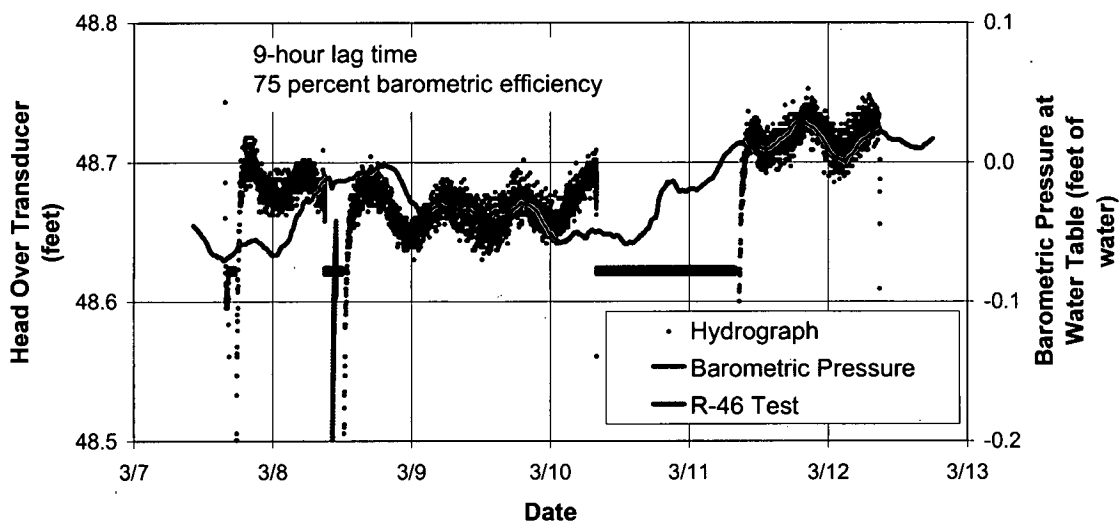


Figure C-7.0-2 Comparison of R-46 apparent hydrograph and adjusted TA-54 barometric pressure change

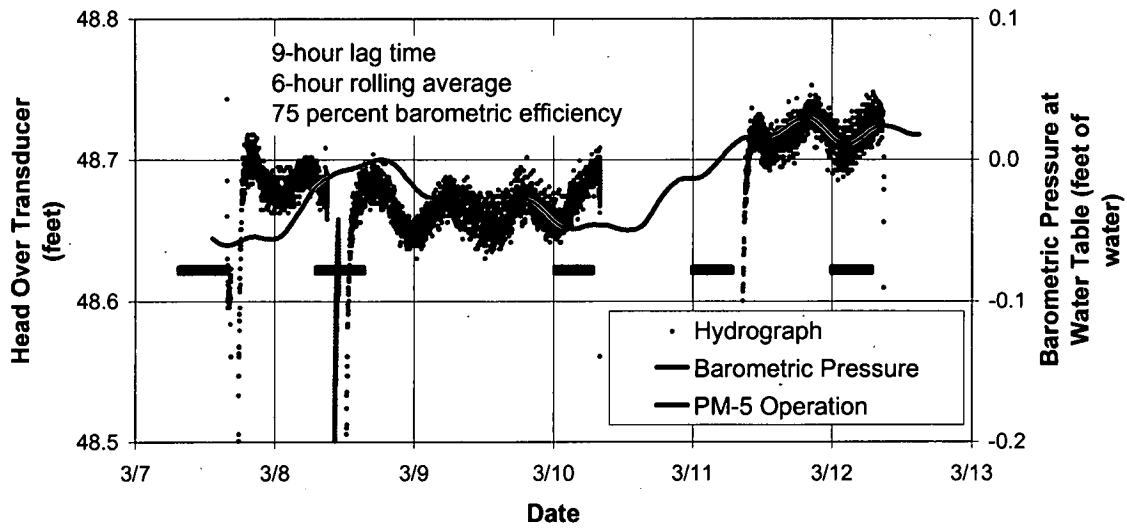


Figure C-7.0-3 Comparison of R-46 apparent hydrograph and rolling average TA-54 barometric pressure change

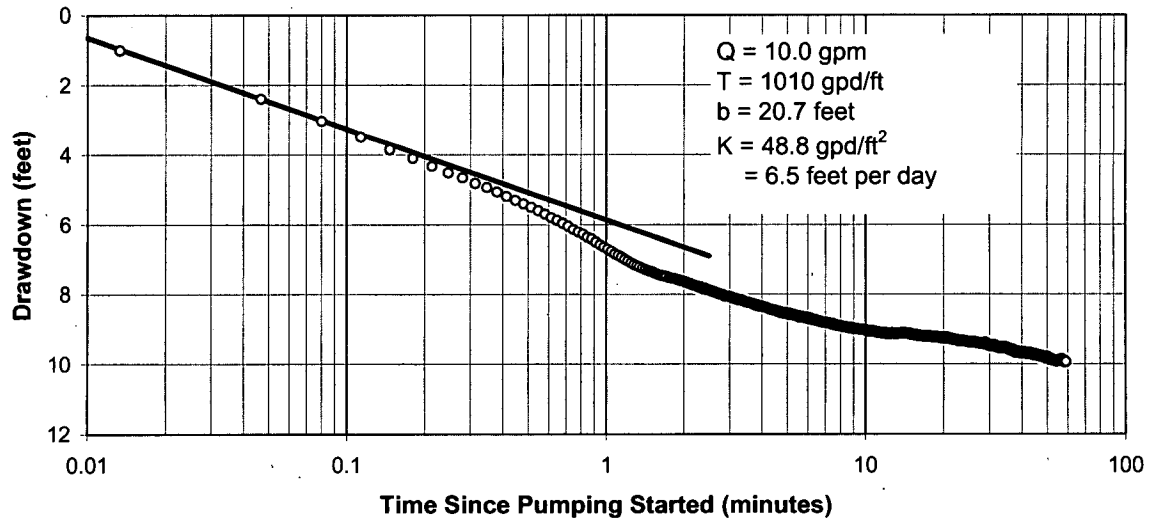


Figure C-8.0-1 Well R-46 trial 1 drawdown

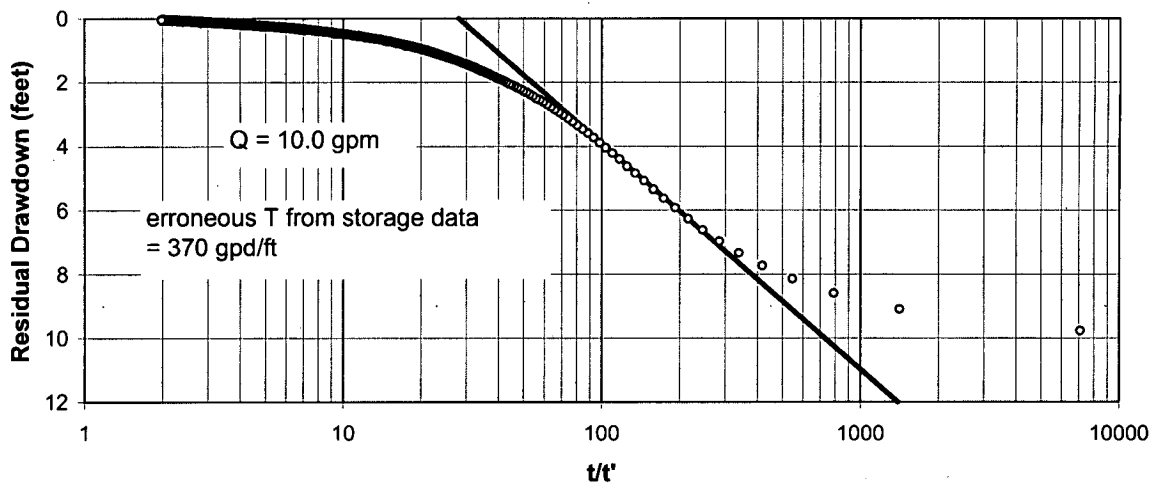


Figure C-8.0-2 Well R-46 trial 1 recovery

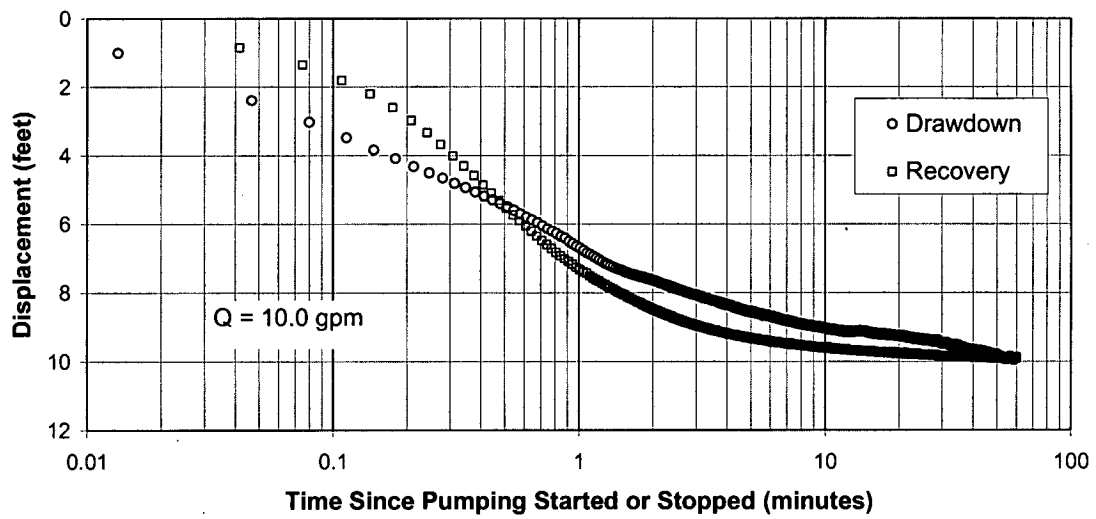


Figure C-8.0-3 Well R-46 trial 1 drawdown and recovery

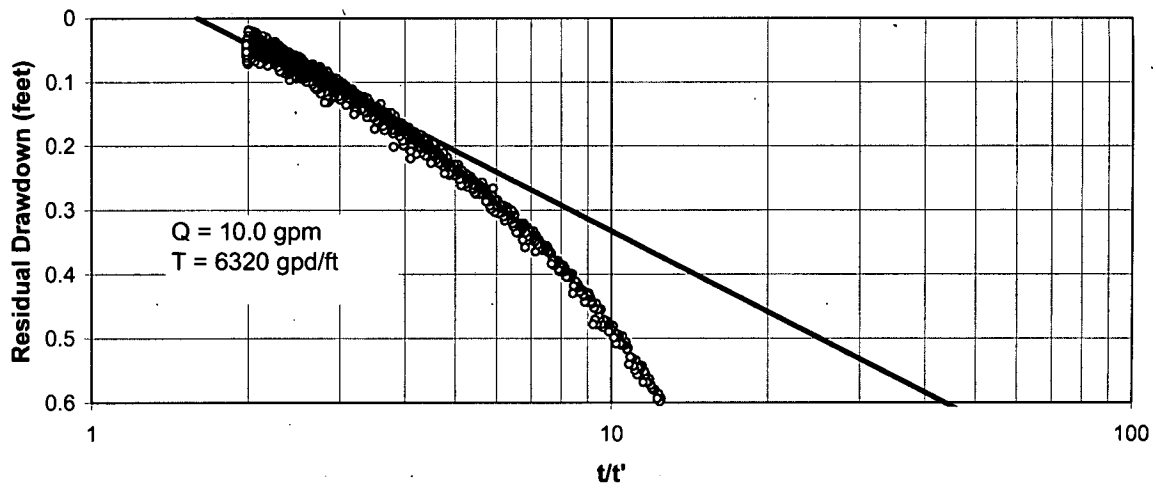


Figure C-8.0-4 Well R-46 trial 1 recovery-expanded scale

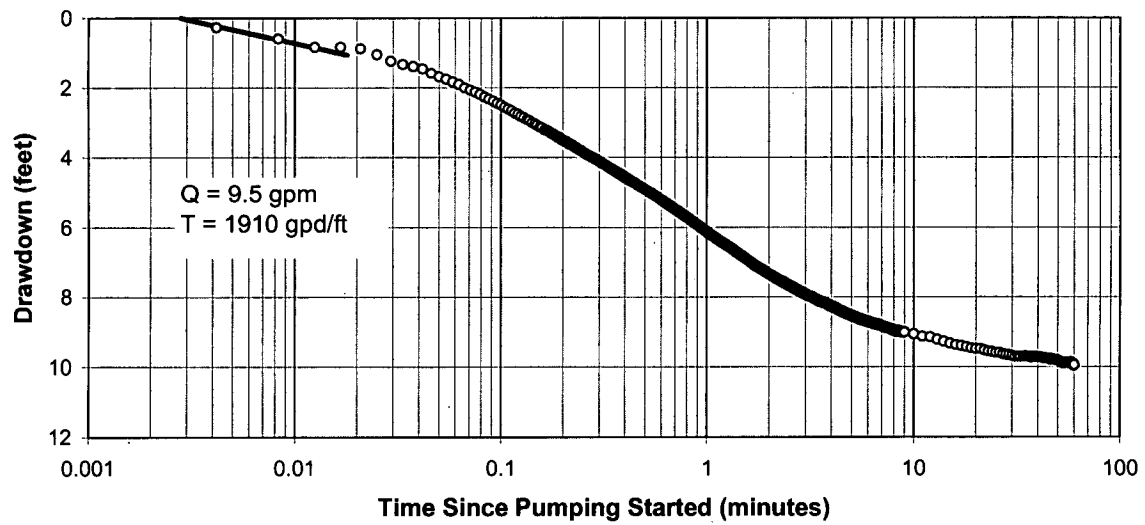


Figure C-8.0-5 Well R-46 trial 2 drawdown

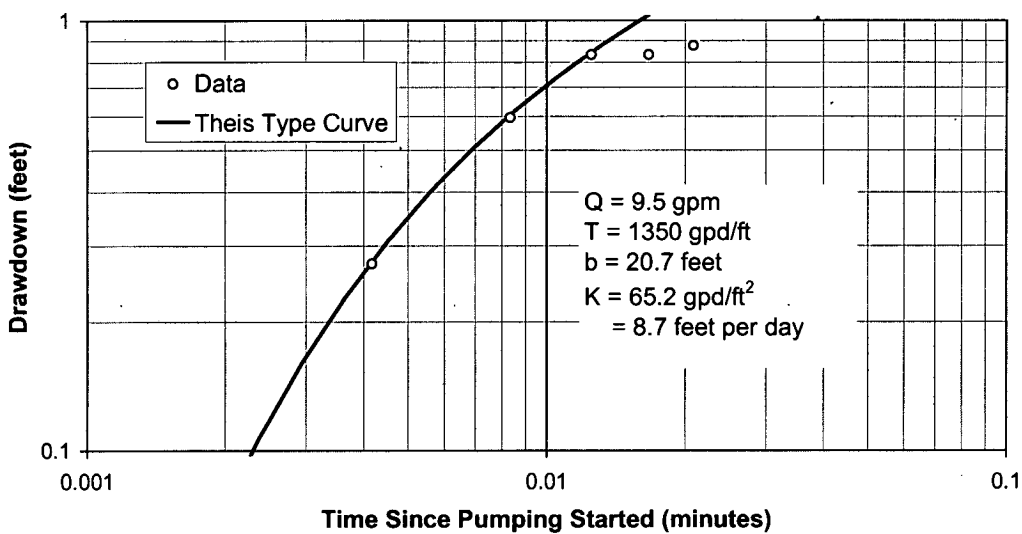


Figure C-8.0-6 Well R-46 trial 2 drawdown—Theis analysis

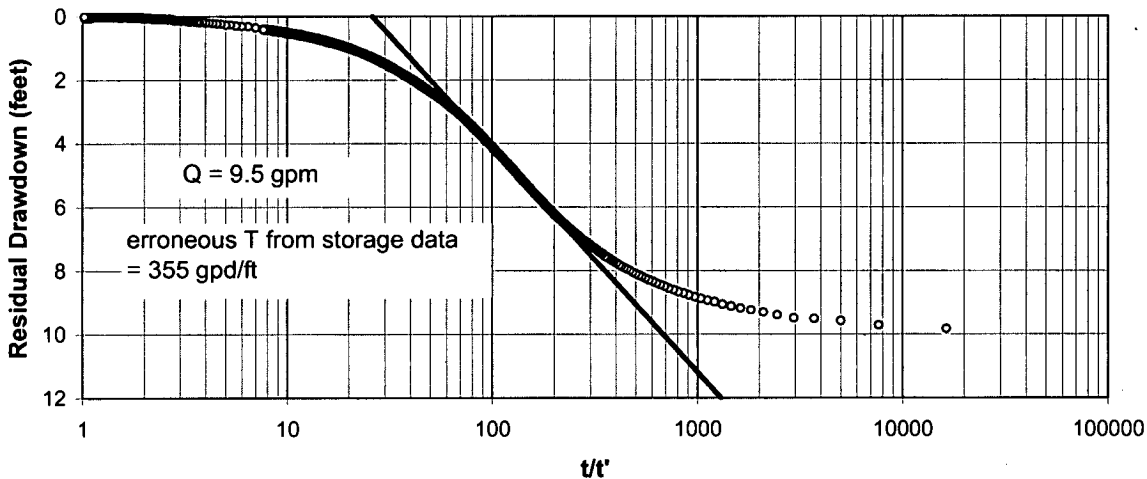


Figure C-8.0-7 Well R-46 trial 2 recovery

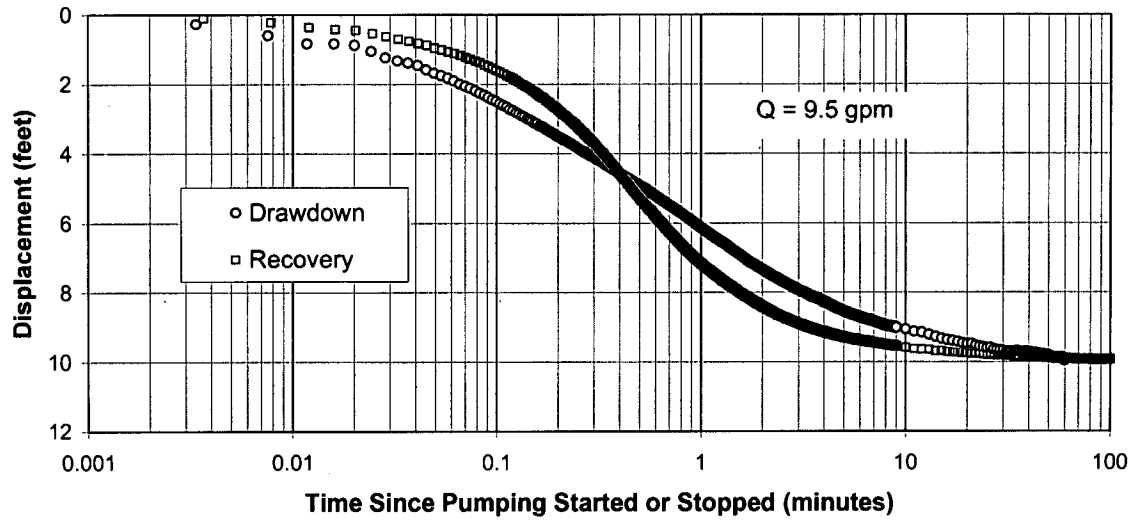


Figure C-8.0-8 Well R-46 trial 2 drawdown and recovery

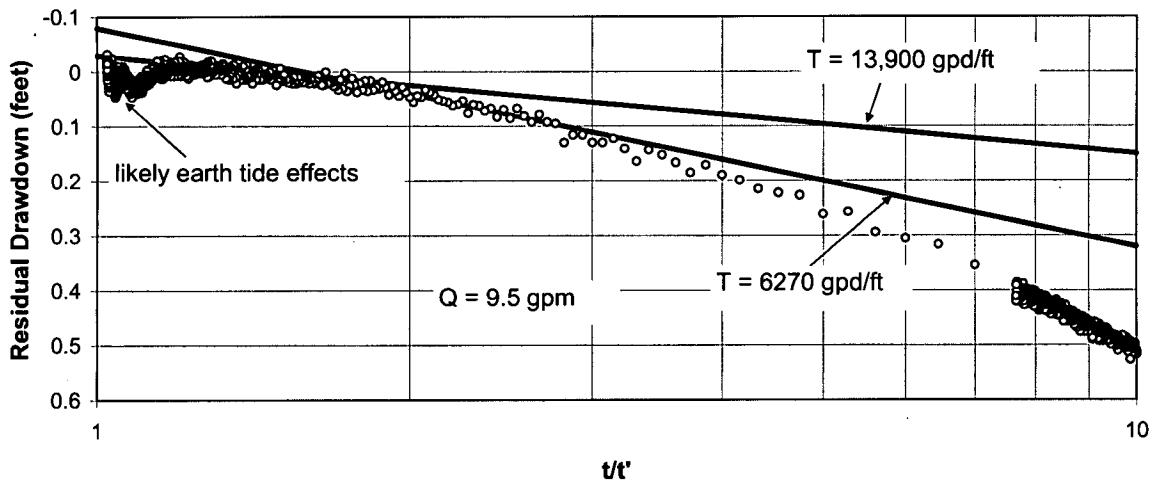


Figure C-8.0-9 Well R-46 trial 2 recovery-expanded scale

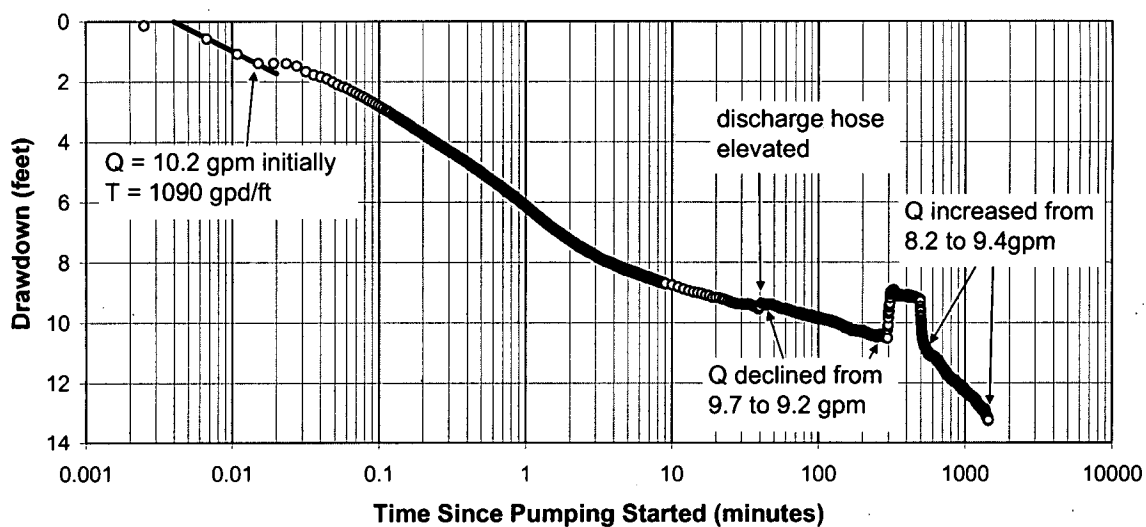


Figure C-8.1-1 Well R-46 drawdown

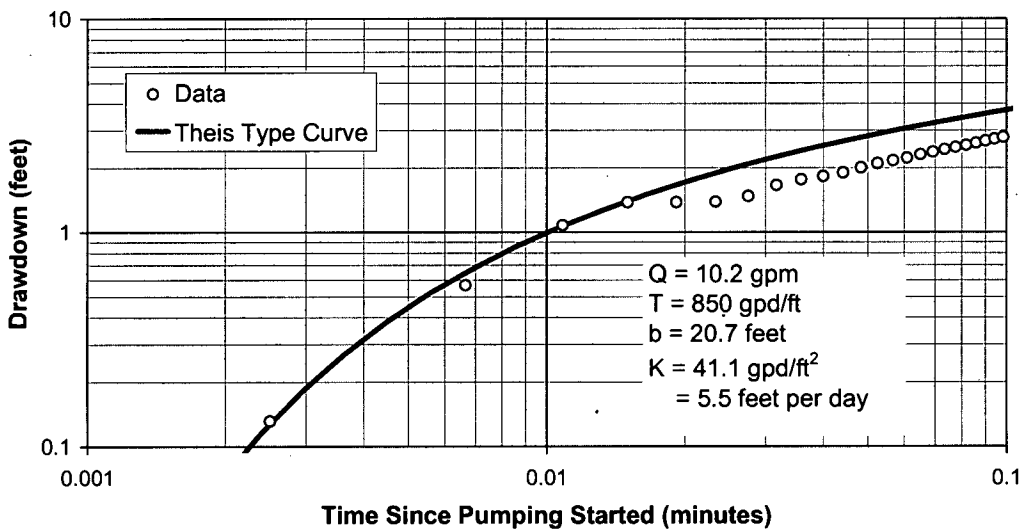


Figure C-8.1-2 Well R-46 drawdown—This analysis

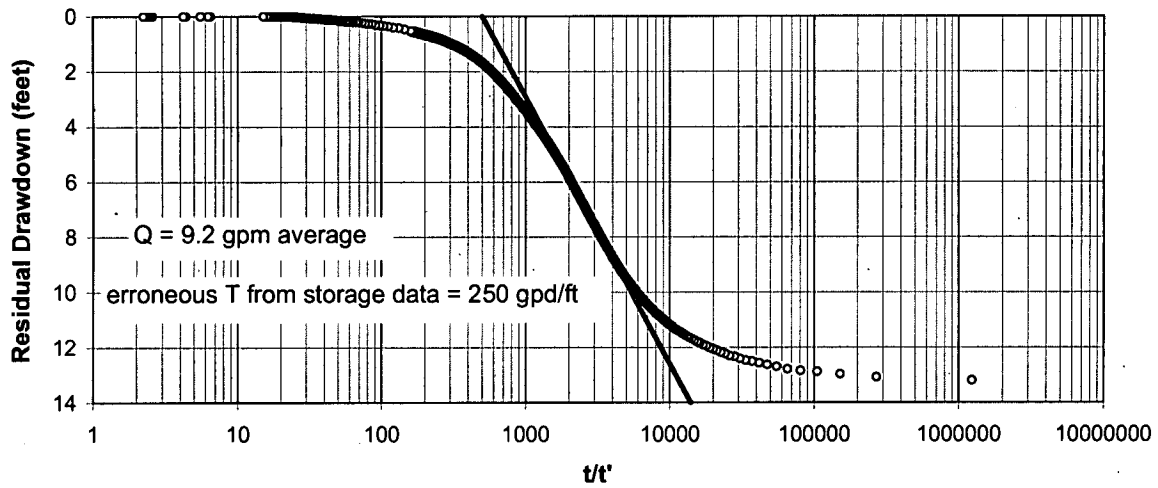


Figure C-8.1-3 Well R-46 recovery

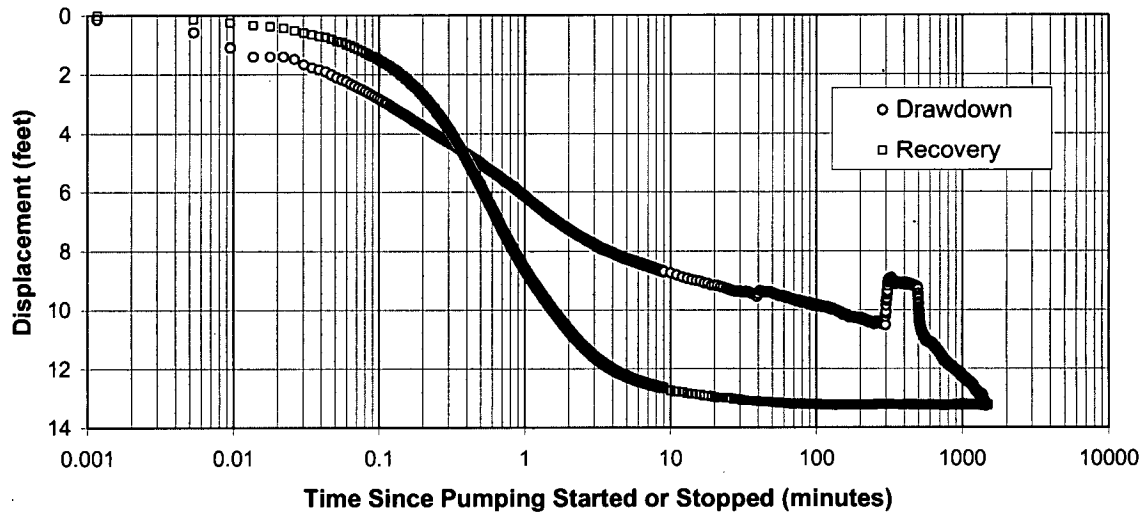


Figure C-8.1-4 Well R-46 drawdown and recovery



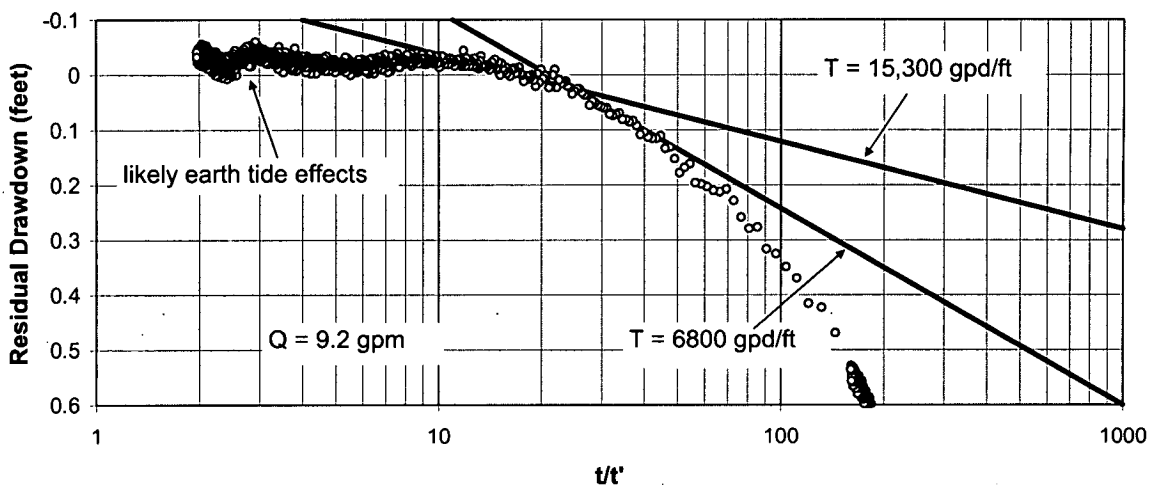


Figure C-8.1-5 Well R-46 recovery-expanded scale

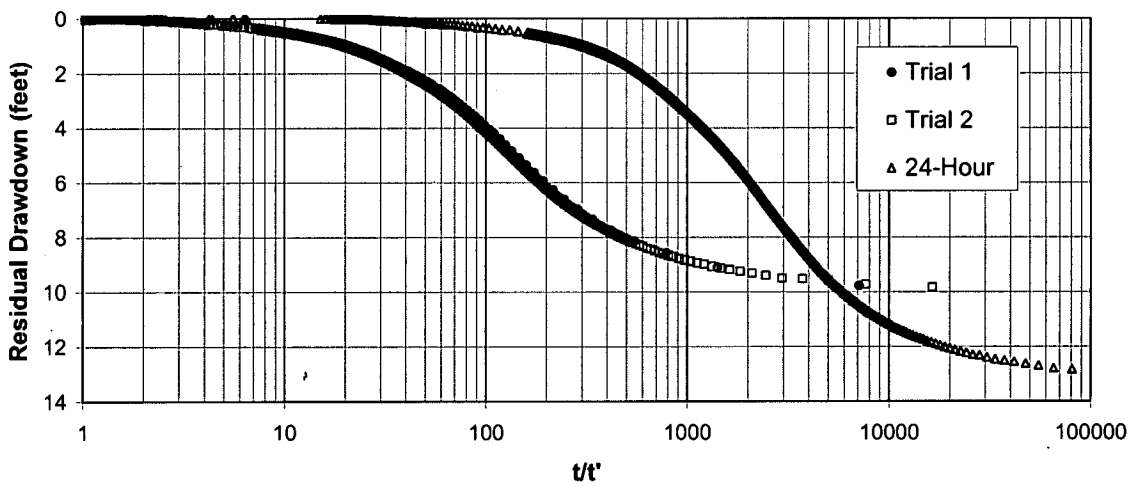


Figure C-8.1-6 Well R-46 recovery for all tests



## **Appendix D**

---

*Borehole Video Logging (on DVDs included with this document)*

## **Appendix E**

---

*Jet West Geophysical Logs and  
Schlumberger Geophysical Logging Report  
(on CD included with this document)*

# **Appendix F**

---

## *Screen-Interval Selection*

### F-1.0 R-46 WELL OBJECTIVES

The principal objective of R-46 is to monitor groundwater at the top of the regional zone of saturation immediately downgradient of Material Disposal Area (MDA) C. R-46 is near the entry point for potential contaminants entering the regional aquifer from the vadose zone. Because the regional aquifer is made up of well-stratified sediments, hydraulic properties are expected to be highly anisotropic, favoring lateral flow within strata near the water table. Water table maps indicate that groundwater flow is toward the east-southeast. The R-46 well objectives are best met by installing a well screen in the uppermost part of the regional aquifer downgradient of MDA C.

### F-2.0 R-46 RECOMMENDED WELL DESIGN

It is recommended that R-46 be installed as a single-screen well with a 20-ft stainless-steel, 20-slot, wire-wrapped well screen extending from 1340 to 1360 ft below ground surface (bgs). The most reliable estimate for the depth of the water table is 1326 ft (see discussion below). The primary filter pack will consist of 10/20 sand extending 5 ft above and 2 ft below the screen openings. A 2-ft secondary filter pack will be placed above the primary filter pack and a 3-ft secondary filter pack will be placed below. The proposed well design is shown in Figure F-2.0-1.

This well design is based on the objectives stated above and on the information summarized below.

### F-3.0 R-46 WELL DESIGN CONSIDERATIONS

The top of the regional zone of saturation was predicted to occur at a depth of about 1322 ft, based on water table maps of the area. Borehole geophysical logs are in close agreement with this prediction, indicating full saturation of rocks below a depth of 1326 ft. The presence of 12-in. drill casing to the total depth (TD) of 1415 ft complicates the direct measurement of water levels in the borehole. During geophysical logging, standing water was detected at a depth of 1362 ft. Twenty-four hours later, the water level had risen to 1343 ft. The water table depth of 1326 ft, based on geophysical logs, is considered reliable and is the basis for the well design.

Preliminary lithologic logs indicate that the geologic units encountered while drilling R-46 are, in descending stratigraphic order, Bandelier Tuff (0–698 ft), dacitic lavas and associated basal sediments (698–980 ft), Puye Formation (980–1405 ft), and Miocene pumiceous sediments (1405–1415 ft TD). The Puye Formation straddles the regional water table and is the primary target for the well screen.

Puye deposits in the regional aquifer are made of coarse-grained dacitic detritus, generally in the form of poorly cemented alluvial boulders, cobbles, and pebbles in a silty and sandy matrix. Despite their coarse-grained nature, these rocks contain ubiquitous silt to depths of about 1395 ft. Water production during drilling was generally about 5 gpm to a depth of 1395 ft and 10+ gpm from 1395 to 1415 ft. Cuttings and geophysical logs indicate that rocks in the 1360–1375-ft interval are particularly silt-rich. Intervals of silt-free gravels and sands occur in the 1335–1340-ft and 1395–1415-ft intervals. A summary of density, neutron, gamma, and Elemental Capture Logs collected by Schlumberger, Inc., is shown in Figures F-3.0-1a and F-3.0-1b.

Based on drill cuttings and the geophysical logs, the rocks above 1360 ft appear to have the best characteristics for water production in the vicinity of the water table. Although water production from this zone is not particularly high, sustained flows of 5 gpm were obtained when attempts were made to evacuate water from the borehole during drilling. Porosities obtained from the density log are about 30%. Rocks above 1360 ft represent the uppermost transmissive strata beneath the regional water table. The top of the proposed well screen (1340 ft) is approximately 14 ft below the water table. Submergence of the well screen will facilitate well development.

#### **F-4.0 OTHER ZONES CONSIDERED FOR THE R-46 WELL SCREEN**

Rocks in the 1360–1380-ft interval are less favorable for monitoring purposes because they contain greater amounts of silt and probably are less transmissive of groundwater. Additionally, there is a concern that the greater silt content might cause sampled waters to be turbid despite proper development. Water was produced and collected at 1339 ft and 1360 ft during drilling but could not be collected at 1380 ft, indicating a significant barrier to flow beginning between 1360 and 1380 ft. This barrier is likely to retard any downward movement of contaminants to the more productive sediments below. The proposed screen depth is above these silt-rich rocks.

Rocks below 1395 ft are silt-free and produce water at a higher rate than the zones above. Based on the density log, the porosity of this zone is 30%–35%. This zone straddles the contact between the lower Puye Formation and underlying Miocene pumiceous sedimentary deposits. Although these rocks have good hydrologic characteristics, they are too deep (>70 ft below the water table) to address the goal defined for R-46 of monitoring for contamination near the top of the regional aquifer in the vicinity of MDA C. As discussed above, groundwater transport of potential contaminants is expected to be dominated by lateral flow within strata closest the water table.

The proposed well design incorporates a 20-ft well screen. A 10-ft well screen from 1340 to 1350 ft was evaluated as a means to monitor a more discrete zone of groundwater near the water table. However, it is believed a longer screen is necessary to ensure a viable well because the aquifer is not very productive at this location. The longer 20-ft screen selected for the well design increases the chances that the well screen will intersect with whatever fast groundwater pathways are present in the upper part of this low-yielding aquifer.

A 40-ft screen from 1340 to 1380 ft was also evaluated as a means to improve water production by increasing the number of thin-producing stringers of water intersected by the well screen. The 40-ft screen was rejected because the additional footage would have extended the well screen into strata with even higher silt contents than in the upper part of the aquifer, and the additional screen length would have provided little additional benefit.

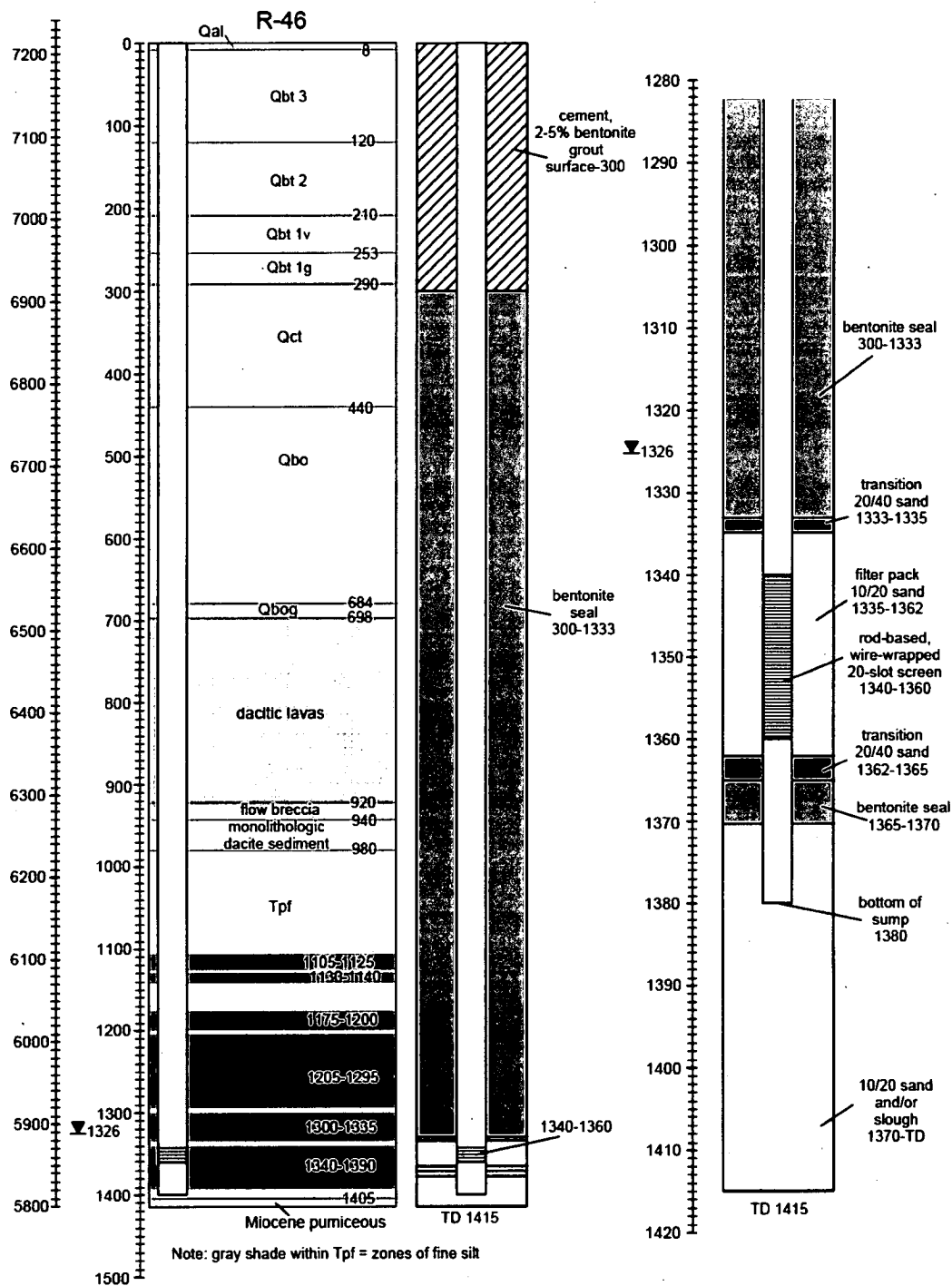


Figure F-2.0-1 Proposed well design for R-46

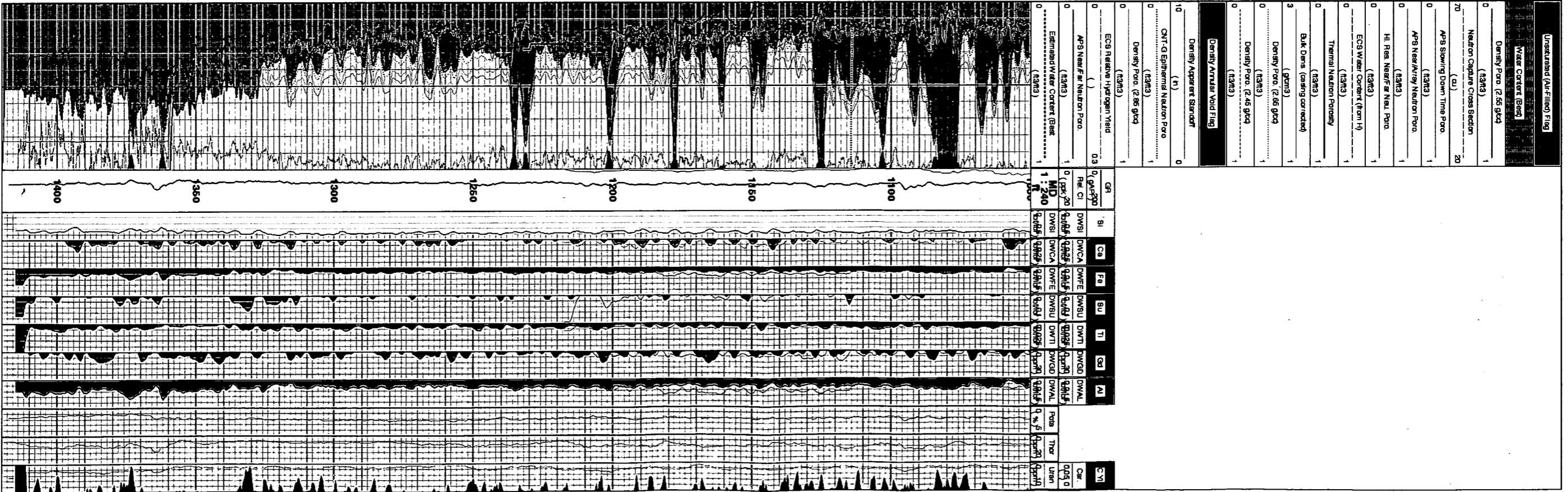






Figure F-3.0-1a Schlumberger combined geophysical logs for R-46

Figure F-3.0-1b Schlumberger combined geophysical logs for R-46



**LANL Environmental Programs (EP) Directorate, Record Transmittal Form**

**PRINT**

To complete this form, see instructions on following pages. Use continuation version of form to list more records. See EP-DIR-SOP-4004 for more information.

Transmittal date: 07/03/2009 Priority Processing? Yes  No  Official Use Only? Yes  No  UCNI? Yes  No  Page 1 of 1

Reference Cited in NMED Deliverables? Yes  No  Receipt Acknowledgement: Do you need this form returned to you? Yes  No

**Transmitter Information**

Z #: 181787 Name: Amanda Martinez E-mail: amandam@lanl.gov Transmitters Organization: WES-DO

**Contamination Potential**

To the best of my knowledge, the record(s) has no radioactive contamination.

Signature: *Amanda Martinez*

Record Type: Individual Record  New package  E-mail  Add to existing package  Resubmitted/superseded record   
(no package) (fill in # and title below) (record #)

Package(s) #: 1729 Package title(s):

**Reference/Retrieval Information**

Organization: EP: LANL Water Stewardship Program (LWSP) – PKG #1729

**Record (Package) Contents**

Record Title	Media Type	Document Date	Author/Originator	Other Doc. # (e.g. Doc. Catalog #)	Page Count	ERID (RPF only)
Completion Report for Regional Aquifer Well R-46	Paper (letter)	03/30/2009	Mark Everett	EP2009-0140 LA-UR-09-1338	62	108592
Cross Ref Info	Paper (letter)	03/30/2009	Mark Everett	EP2009-0140 LA-UR-09-1338	7	108593

RPF Use Only: (names and dates)

Accepted

Entered AM 6-7-09

Scanned

*07/03/09 Presby M. Salas*

QC: PS

[Click here for Continuation Form](#)

# Media Target Page

The original media for this document can be obtained through the Records Processing Facility or requested through rpf\_records@lanl.gov.

ERID # 105592

---

OUO:  Yes  No

UCNI:  Yes  No

Media Type:

LETTER / CD

Date:

Other Document #(s):

Subject: 1) SUBMITTAL OF THE COMPLETION REPORT FOR  
REGIONAL AQUIFER WELL R-46, 2) COMPLETION REPORT, 3)  
CD5 EP 2009-0140, LA-UR-09+1338

Filed in RPF